Role of Six1 in controlling DNA accessibility and epigenetic landscape dynamics in myoblasts

Ramya Balakrishnan

A thesis submitted to the University of Ottawa in partial fulfillment of the requirements for the degree of Master of Science in Biochemistry specialized in Bioinformatics

Department of Biochemistry, Microbiology, and Immunology

Faculty of Medicine

University of Ottawa

ABSTRACT

Owing to the presence of muscle stem cells (MuSC), adult skeletal muscle is capable of regenerating after injury. Quiescent muscle stem cells become activated and proliferate into myoblasts which undergo myogenic differentiation to repair damaged tissue. The transcription factor (TF) Six1 is a known regulator of muscle stem cells which potentially plays a role in the early stages of MuSC activation. When bound to the appropriate cofactor, Six family transcription factors are capable of activating or repressing transcription. Previous work suggests that Six1 establishes the accessibility landscape required for the myogenic regulatory factor (MRF) MyoD to bind to DNA. It was hypothesized that Six1 recruits p300 to acetylate Histone H3 lysine 122 which then renders DNA more accessible and facilitates gene transcription. The objective of this research was to investigate the role of Six1 in regulating the epigenetic and accessibility state of DNA in myoblasts. It was found that Six1 and the histone acetyltransferase p300 coincide at many gene enhancers. In addition, Six1 knock-down is associated with reduced DNA accessibility at a large number of loci in C2C12 myoblasts and with gene downregulation. In this research, we determined that recruitment of p300 by Six1 alters chromatin accessibility and gene expression in proliferating myoblasts, providing evidence of Six1 pioneer factor activity.

ACKNOWLEDGMENTS

I would firstly like to thank my thesis supervisor, Dr. Alexandre Blais for the opportunity to work on this project in his laboratory. His wealth of knowledge, in addition to his encouragement and guidance, was indispensable to the completion of this work.

I would also like to thank my Thesis Advisory Committee, Dr. Jeffrey Dilworth and Dr. Theodore Perkins for their time and valuable input on this project. I would like to extend my gratitude to our lab manager, Dabo Yang, for his positive, can-do attitude and willingness to lend a helping hand.

I would like to thank my mother, Genges and sister, Vyshnavi for all their love and support. I am also incredibly grateful to my late father, Balakrishnan Sivalingam, for his example of integrity, compassion and perseverance. Lastly, I owe a great debt of gratitude to my best friends and support system, Aaron Lemieux, Vanessa Alphons, Sinthea Baral, Glenda Chiu, Shane Simon and Cynthia Leung.

Table of Contents

ABBREVIATIONS

RUVr Remove Unwanted Variation Using Residuals 37,52,53,56,59,62,66,69

SDS Sodium Dodecyl Sulfate 31,35

siRNA Small Interfering RNA 30,31,32,35,42,43,61,68,73,88

TBS Tris Buffered Saline 31

TF Transcription Factor 8,9,11,13,14,18,26,64,74,76,77,78,84,85,86,87

TR-FRET Time-resolved fluorescence resonance energy transfer assay 20

TMM Trimmed means of M values 37,46,47,51,52,53,56,59,61,62,65,66,69

TSS Transcription Start Site 37,68,69,71

1 Introduction

Skeletal Myogenesis

In vertebrates, skeletal muscle of the back, body wall, and limbs derive from spherical, embryonic structures bordering the neural tube called somites (Christ & Ordahl, 1995). Somites delaminate from the hypaxial edge of the dermomyotome, the dorsal region of the somite, in response to signalling by the tyrosine kinase receptor, c-met and SF/HGF genes (Bladt et al., 1995; X. M. Yang et al., 1996).

Two rounds of myogenesis occur during embryonic development of skeletal muscle. The first round of embryonic myogenesis gives rise to primary muscle fibers whereas during the second round, primary myofibers fuse to form secondary myofibers (Duxon et al., 1989). The muscle fiber types present in fast versus slow twitch muscle are distinguished by the presence of differing myosin isoforms during the second round of myogenesis (Lyons et al., 1990). In adult skeletal muscle, muscle precursor cells (MPC) termed satellite cells reside between the basal lamina and plasma membrane where they can become activated in response to muscle injury or growth demands (Mauro, 1961).

1.1 Muscle Disorders

Mutations to genes involved in the regulation of myogenesis have been associated to various muscle disorders. Muscle disorders are typically associated with muscle wasting and can be genetic or nonhereditary. Progressive muscle wasting which occurs during the aging process is termed sarcopenia (Rosenberg, 1997). Elevated levels of apoptotic

proteins found in sarcopenia have been suggested to contribute to protein degradation and muscle fiber loss (Dirks & Leeuwenburgh, 2002; Dupont-Versteegden, 2005).

Muscular dystrophies are group of heritable muscle disorders which akin to sarcopenia are also characterized by progressive muscle wasting (Emery, 2002). Dysregulation of several myogenic regulators including myostatin and mTOR (mammalian target of rapamycin) have been observed in both sarcopenia and muscular dystrophies (Anand et al., 2021; Risson et al., 2009; Siriett et al., 2006; Wagner et al., 2002).

Two of the most common muscular dystrophies, Duchenne Muscular Dystrophy (DMD) and Becker Muscular Dystrophy (BMD) are X-linked recessive diseases caused by loss of function mutations in the DMD gene which encodes for the dystrophin protein (Kunkel, 1986). Dystrophin plays a key role in maintaining myofiber stability during muscle contraction by connecting the intracellular cytoskeleton to the extracellular matrix (Petrof et al., 1993). The absence of dystrophin in MuSCs results in fragile and easily damaged myofibers, ultimately leading to muscle wasting and higher susceptibility to injury.

The incidence rate of BMD is approximately 1 in 18450 male births worldwide (Bushby et al., 1991). BMD is characterized by a deficiency in dystrophin resulting from in-frame exon mutations, which while leaving the reading frame intact, results in a truncated and partially functional dystrophin protein (Malhotra et al., 1988). BMD onset typically occurs during childhood, with loss of ambulation occurring during the third decade (Beggs et al., 1991; Mah et al., 2014). Symptoms of BMD include muscle weakness, cramps, and difficulty walking. Severity of BMD symptoms and disease progression are suggested to be related to the structure of the truncated dystrophin at the deletion site (Nicolas et al.,

2015). The leading cause of death in both Duchenne and Becker Muscle Dystrophy patients is reported to be from cardiac or respiratory complications (Connuck et al., 2008; Nigro et al., 1990).

1.2 Duchenne Muscular Dystrophy

The most common form of muscular dystrophy is Duchenne Muscular Dystrophy. DMD effects approximately 1 in 3500-5000 male births worldwide (Price et al., 2007). DMD is defined by a loss of function mutation DMD gene which encodes the protein dystrophin (Koenig et al., 1987). Although MuSCs can differentiate and replace the damaged myofibers, new muscle tissue continues to retain the mutation. Cycling between degeneration and regeneration results in decline in muscle function and progression of the disease (Haddix et al., 2018). At present, there is no known cure for DMD, and the median life expectancy at birth is 23 years (Landfeldt et al., 2020). Symptoms of DMD are typically more severe than Becker Muscular Dystrophy where onset of symptoms and loss of ambulation typically occurs in the first decade of life (Bello et al., 2016). Current research efforts are being directed towards exploring potential curative treatments for DMD include exon skipping, gene-based and cell-based therapies.

Gene-based therapy includes genome editing using CRISPR/Cas9 to correct the frame-shift mutation in the DMD gene (Young et al., 2016). Young et al. demonstrated the restoration of the DMD reading frame in human induced pluripotent stem cell lines (hiPSCs) through internal deletion of exons 45-55 of the dystrophin protein. The internal deletion was capable of restoring the function of dystrophin in both hiPSC-derived cardiomyocytes and skeletal muscle cells. Deletion of exon 23 was also found to

partially recover dystrophin in cardiac and myofibers in the mdx mouse model of DMD (Nelson et al., 2016). Thousands of mutations to DMD have been identified in patients, as such, development of optimal gene correction strategies for each known mutation poses a logistical challenge for the use of CRISPR technologies for treatment of DMD (Bladen et al., 2015). Double-cutting is a method whereby multiple double-stranded DNA breaks separated by large genomic regions are introduced. Excision of multiple large regions of the DMD gene could allow for the transcription of truncated yet functional dystrophin and serve as a comprehensive correction strategy for multiple common DMD mutations (Olson, 2021). However, double cutting has previously been associated to off-target mutations or genome rearrangements (Nelson et al., 2019).

DMD gene transfer using recombinant adeno-associated virus (rAAV) is another promising approach to treatment of Duchenne Muscular Dystrophy. Truncated dystrophin cDNA (Complementary Deoxyribonucleic Acid) transferred by an AAV vector into dystrophic mdx muscles was shown to improve muscle contraction (Yoshimura et al., 2004). AAV vector transferred micro-dystrophin treatment in female mdx mice reduced myocardial fibrosis and improved ECG results, suggesting its promise for use in Duchenne cardiomyopathy treatment (Bostick et al., 2011). Recombinant AAV serotype 9 (rAAV-9) vectors have been used to create in-frame deletions of exon 23 and is reported to restore dystrophin synthesis in skeletal muscles in the mdx mouse model (Long et al., 2016). A clinical trial by Sarepta Therapeutics (NCT04281485) testing rAAV microdystrophin gene therapy on children aged 3 months to 7 years is ongoing and two additional trials using rAAV-9 (NCT03368742, NCT03375164) are in the recruitment stage. One challenge in realizing the use of rAAV vectors for delivering

DMD cDNA is due to the complex and resource-intensive production (C. Li & Samulski, 2020). In multiple current clinical trials (NCT04468742, NCT03362502), high doses of 10^{14} vector genomes (vg) per kilogram bodyweight are required, as such research efforts are being made into scaling the manufacturing of AAV vectors and exploring strategies for reducing dosage (Colella et al., 2018; Jayandharan et al., 2010; Lock et al., 2010; Tabebordbar et al., 2021).

1.4 Cell Therapy

Cell therapy for treatment of Duchenne Muscular Dystrophy and other muscular degenerative disorders involves injection of MuSCs which possess a functional Dystrophin gene to improve host muscle regeneration (Cossu & Sampaolesi, 2007). For cell therapy to be effective, donor myogenic precursors must be capable of locating to the sublaminar muscle stem cell nice, reconstructing damaged muscle tissue and repopulating the stem cell pool.

Several populations of stem cells from various origins could potentially be used for DMD treatment. Transplantation of a single myofiber into dystrophic mouse muscle was found to be capable of extensive proliferation and retained the capacity for self-renewal (Hall et al., 2010). Multiple studies have explored various stem cell populations for their potential use in cell therapy using mdx dystrophic mice. Injection of muscle derived CD34+ stem cells have previously been found to be capable of dystrophin restoration in mdx mice (Torrente et al., 2001). Additionally, CD133+ mesangioblasts, multipotent stem cells associated with vessels, were also found to be capable of restoring dystrophin in mdx mice (Torrente et al., 2004).

A Phase I clinical trial was previously conducted wherein donor myoblasts were transplanted through injection into DMD patients. While myoblast implantation resulted in a modest increase in dystrophin positive fibers, the levels detected were not clinically significant (Miller et al., 1997). An ongoing Phase I/II clinical trial (NCT02196467) is currently being conducted testing the effectiveness of high-density transplantation of donor myoblasts in DMD patients.

A major challenge in realizing cell therapy as a treatment for DMD is attaining large numbers of engraftable muscle stem cells (MuSCs) which also maintain an undifferentiated state (Muir & Chamberlain, 2009). Furthering the understanding of the molecular mechanisms controlling MuSCs may aid in the realization of cell therapy as a cure for DMD.

1.5 Muscle Stem Cells and Regeneration

Adult skeletal muscle is comprised of either from unipotent, myogenic progenitor cells called satellite cells or multipotent cells which can differentiate into an array of cell types in response to extracellular signalling (Seale et al., 2001). Although unipotent satellite cells only produce myogenic cells (Starkey et al., 2011), satellite cells fall under the stem cell classification as they have the capacity for continual self renewal and differentiation.

Stem cells are contained and regulated within complex microenvironments referred to as “niches” (Scadden, 2006). A key component of the stem cell niche is the extracellular matrix (ECM) which imparts both structural support and mediates regulatory signalling pathways through binding of cellular receptors (Bissel & Barcellos-

Hoff, 1987; Boudreau & Jones, 1999). The basal lamina is a layer of ECM which provides both a scaffold for stem cells to tether and a dynamic microenvironment which regulates proliferation and differentiation within the stem cell niche (Boonen & Post, 2008). The capability of muscle stem cells to continually self-renew is dependent on maintenance of the stem cell niche.

To keep pace with the demands for muscle regeneration in response to growth, muscle injury or disease, a pool of stem cells must be continually maintained within the stem cell niche. Muscle stem cells can undergo symmetric divisions to produce identical daughter cells or asymmetric divisions to produce cells which either differentiate towards the muscle lineage or return to quiescence to maintain the stem cell pool (Feige et al., 2018). The absence of dystrophin in DMD results in a reduction of asymmetric cell divisions, leading to insufficient numbers of muscle precursors available for muscle regeneration (Dumont et al., 2015).

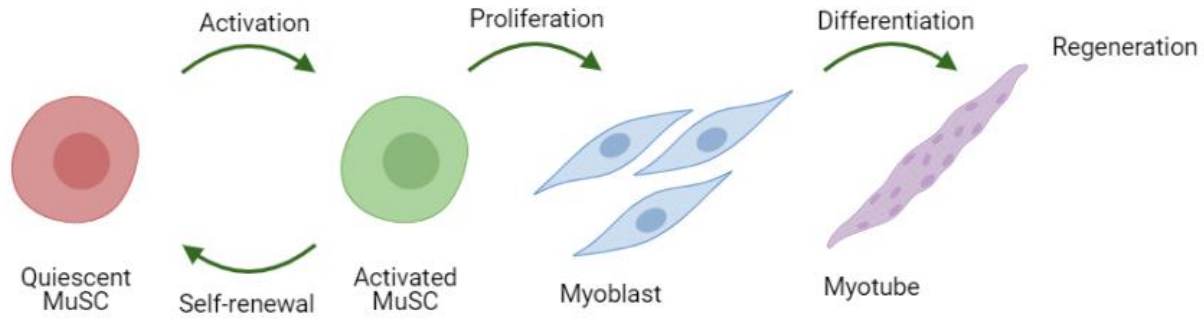

Figure 1 Steps involved in muscle stem cell activation and self-renewal

Following injury in healthy adult muscle, stem cells become activated, re-enter the cell cycle to proliferate, and fuse into myofibers which can repair damaged tissues. In adult

skeletal muscle, the transitions from MuSC to myoblasts which later fuse to form myofibers are orchestrated by numerous transcription factors.

1.6 Transcription Factors

The myogenic regulatory factors, MyoD, Myogenin, MRF4 and Myf5, are basic-helix-loop-helix (bHLH) transcription factors required for both the commitment and regulation of myogenic progenitor cells (MPC), myoblasts poised to proliferate and eventually form muscle tissue (Weintraub et al., 1991). While deletion of either Myf5 or MyoD alone does not affect muscle formation (Braun et al., 1992; Rudnicki et al., 1992), skeletal muscle is eliminated in double knock-out mice (Rudnicki et al., 1993). In Myf5::MyoD double mutant mice, MRF4 was also found to be capable of conferring myogenic identity by substituting for MyoD (Kassar-Duchossoy et al., 2004).

In culture, both MyoD and myogenin are capable of converting non-myogenic cells to the muscle lineage (Sassoon et al., 1989). In contrast to MyoD, Myf5 and MRF4, inactivation of the myogenin gene is lethal in mice, and results in severe reductions to differentiated skeletal muscle (Hasty et al., 1993). Myogenin expression was diminished in double knock-out mouse embryos of MyoD and NFATc3, while unaltered in embryos with single knock-outs of either factor, suggesting the involvement of NFAT in upregulating myogenin (Armand et al., 2008).

Synergistically with the MRFs, MyoD and myogenin, the transcription factor MEF2 (myocyte enhancer factor-2) initiates myogenesis through binding domain interactions (Molkentin et al., 1995). During terminal differentiation, MyoD elicits cell cycle withdrawal through inducing the upregulation of p21 (Halevy et al., 1995). The

transcription factor Runx1 also co-operates with MyoD to regulate myoblast proliferation during muscle regeneration (Umansky et al., 2015). Dystrophic mdx mice which were also Runx1-deleted in the muscle lineage (floxed Runx1 alleles deleted by transgenic Myf5::Cre), were found to have decreased myoblast proliferation, resulting in both disrupted muscle regeneration and decreased lifespan.

Wnt family proteins mediate dorsalizing signals required for both the formation of the epithelial structure of somites and maintenance of the dermomyotome (Ikeya & Takada, 1998; Linker et al., 2005). Wnt and Shh signalling initiates myogenesis through activation of the transcription factors Pax3 and Pax7 (Maroto et al., 1997). Pax3 expression has been found to be sufficient in inducing the expression of both transcription factors MyoD and Myf5 (Maroto et al., 1997).

Following delamination, cells expressing Lbx1 and Pax3 migrate laterally to the limb buds (Gross et al., 2000). Shh initiates proliferation of MPCs in the limb bud (Duprez et al., 1998). During myogenic differentiation, Lbx1 and Pax3 expression is downregulated in the limb, whereas the myogenic regulatory factors, including Myf5, myogenin, MyoD and MRF4 are upregulated (Gross et al., 2000).

In addition to the aforementioned MRFs, which regulate the expression of genes at different stages of myogenesis, the paired-box transcription factor, Pax7, is required for regulating both proliferation and differentiation of activated muscle stem cells (Zammit et al., 2006). To replenish the stem cell pool, a subset of Pax7+MyoD- cells return to quiescence, whereas MyoD+ cells continue onto differentiation into myofibers and a permanent cell cycle withdrawal. Wnt7a and Notch signalling also facilitates stem cell

population maintenance respectively through induction of symmetric or asymmetric cell divisions (Cheng et al., 2018; Le Grand et al., 2009; Mourikis & Tajbakhsh, 2014).

1.7 MyoD

Satellite cells in a quiescent state express Pax7, which inhibits myogenesis through repression of the MRF, MyoD (Olguin et al., 2007). As previously mentioned, MyoD and Myf5 are both required for muscle lineage specification. Transfection of genomic DNA from mouse C2C12 myoblasts treated with 5-azadeoxycytidine, an inhibitor of methyltransferase activity (Jones & Taylor, 1980), was found to be capable of converting 10T1/2 fibroblasts into myoblasts (Lassar et al., 1986). Furthermore, binding of MyoD to two sites of the mouse muscle creatine kinase gene (MCK) enhancer was capable of initiating myogenic commitment (Lassar et al., 1989). The expression of the basic and Myc homologous domains of MyoD in 10T1/2 fibroblasts was sufficient for DNA binding and inducing conversion into the myogenic lineage (R. L. Davis et al., 1987; Tapscott et al., 1988). The MyoD protein regulates transcription of the MyoD gene through a positive autoregulatory loop which potentially contributes to the stability of myogenic commitment, suggesting that MyoD is responsible for stable commitment of undifferentiated cells to the muscle lineage (Thayer et al., 1989).

MyoD-deficient mdx mice were found to have satellite cells with normal levels of differentiation, however, they had poor regenerative potential due to reduced proliferation (Megeney et al., 1996). Montarras et al. presented a mouse model of cell therapy which engrafted donor MuSCs into recipient muscle. MuSCs which became activated and expressed MyoD *in vitro* culture differentiated into myofibers but failed to

repopulate the stem cell pool. Activated myoblasts are capable of escaping differentiation by maintaining Pax7 expression, downregulating MyoD and returning to quiescence (Zammit et al., 2006).

1.8 Epigenetics and DNA Accessibility

As myogenic precursor cells progress through various stages of myogenesis, the activity of numerous transcription factors are dynamically up or downregulated. As such, myogenesis implicates both a stringent temporal and spatial regulation of gene expression. The structural organization of DNA impacts gene expression by controlling the ability of transcription factors to bind to target regions and transcriptional machinery, such as RNA polymerase II (RNAPII), to bind to promoters, initiate transcription and engage in productive elongation.

These relatively stable alterations to DNA accessibility or structure which affect gene expression without affecting the genetic code are termed epigenetic modifications (Creyghton et al., 2010; Handy et al., 2011). Negatively charged DNA is packaged into nuclei around positively charged histone octamers. Post translational modifications (PTMs) on histones including acetylation, phosphorylation, glycosylation, ubiquitination, and methylation can alter the stability of the DNA-histone complex, resulting in DNA compaction or expansion. DNA in an accessible, euchromatic state is generally transcriptionally active (Shahbazian & Grunstein, 2007). While acetylated histones are often associated with transcriptional activation (Hebbes et al., 1988), histone methylation can be activating or repressive depending on the histone or lysine residue targeted for methylation (Carrozza et al., 2003; Hsieh, 1994).

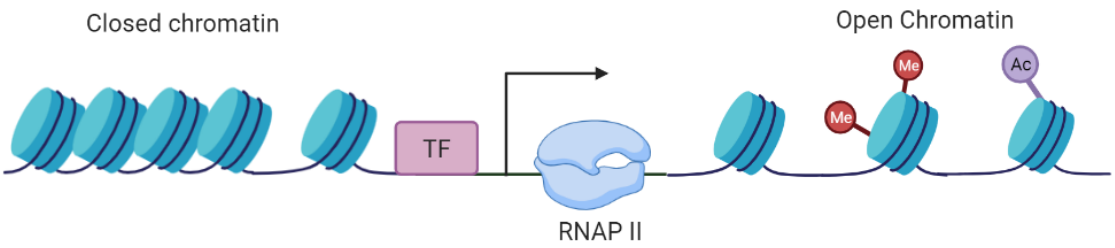

Figure 2 Schematic illustration of epigenetic regulation of gene expression. Histone acetylation and methylation are epigenetic modifications which have the capability of modifying gene expression either by altering chromatin structure or through recruitment of transcription factors.

Epigenetic modifications have been well established to be implicated during myogenesis and muscle stem cell maintenance (Blais, 2015; Dilworth et al., 2004; Dilworth & Blais, 2011; Giordani & Puri, 2013; Puri, Sartorelli, et al., 1997; Puri et al., 2001; Singh et al., 2015). Maintenance of satellite cells in a quiescent state requires repression of genes involved in activation through the formation of heterochromatin. Previous research investigating changes to genome architecture in muscle cells revealed that the MRF, MyoD could regulate gene expression through chromatin remodelling (Megeney et al., 1996).

1.9 Six family of transcription Factors

The homeobox gene *sine oculis* (so) was first identified in the Drosophila melanogaster as an essential regulator of compound eye morphogenesis (Cheyette et al., 1994; Serikaku & O'Tousa, 1994). While there are two transcription factors in drosophila, in mammalian species there are six members of the Six family of transcription factors (SIX1-SIX6) (Figure 3). Homologues to sine oculis, Six family proteins were also identified in a variety of other organisms including mammals, avians, fish, xenopus and nematodes (Bovolenta et al., 1998; Kawakami, 1996; Loosli et al., 1998; Oliver et al.,

1995). Six proteins are present in several tissues and regulate numerous developmental processes in addition to eye formation. In mammals, Six1, Six2, Six4 and Six5 are expressed in adult skeletal muscle or satellite cells (Klesert et al., 2000; Laclef, Hamard, et al., 2003; Ozaki et al., 2001; Relaix et al., 2013).

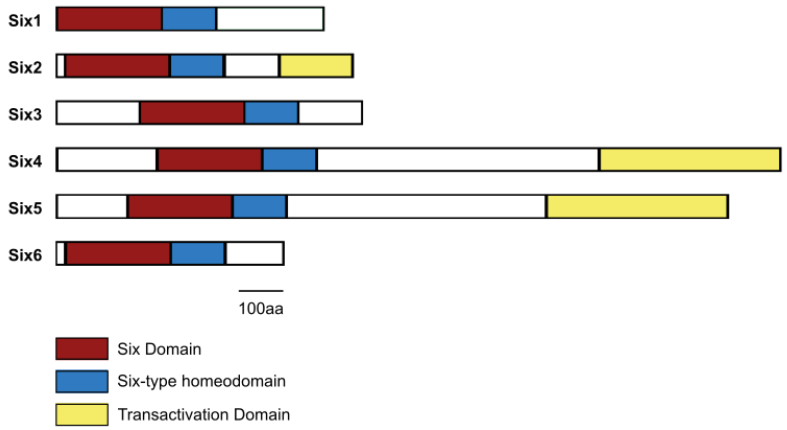

Figure 3 Six family of transcription factors homology and protein domain distribution created with reference to Kawakami et al., 2000.

Triple silencing of Six1/2/4 in chick embryos resulted in anencephaly, suggesting a role for Six1/2/4 expression in both craniofacial development and brain morphogenesis (Garcez et al., 2014). The role of Six2 is well established to control kidney development through regulation of nephron progenitor self renewal (Kirby et al., 2001). Additionally, manipulation of Six3 and Six6 expression using murine models also points to the involvement of these transcription factors in neurogenesis (Appolloni et al., 2008; Pandolfi et al., 2019). UNC-38, a homologue of Six4/5 in *Caenorhabditis elegans*, has been found to regulate cell migration and differentiation (Yanowitz et al., 2004). Overexpression of the Six6 homologue, Optx2, in Xenopus laevis resulted in retina over

proliferation and ectopic eye formation, suggesting a role in retinal cell fate determination (Bernier et al., 2000).

1.10 Six1

In adult skeletal muscle, the homeodomain transcription factor Six1 is required for both the activation and return to quiescence of MuSCs (Le Grand et al., 2012). Six1 null mice die at birth due to severe muscle hypoplasia (Laclef, Hamard, et al., 2003; Laclef, Souil, et al., 2003; X. Li, Oghi, et al., 2003). Conditional Six1 knock-out in murine adult satellite cells has been found to impair myoblast differentiation and self-renewal capability during skeletal muscle regeneration (Le Grand et al., 2012).

Our lab has identified MRF target genes for Six1 in C2C12 myoblasts and demonstrated that Six1/Six4 contributes to skeletal muscle gene induction in cooperation with MyoD (Y. Liu et al., 2010). Six1 has also been found to act as a direct upstream regulator of MyoD (Y. Liu et al., 2013). Double knock-out of Six1 and Six4 in mice has been found to result in muscle hypoplasia as well as rib and craniofacial defects (Grifone et al., 2004). Six family proteins bind DNA through a divergent homeodomain on sequence elements called MEF3 sites (Y. Liu et al., 2012; Spitz et al., 1998). MEF3 DNA elements have been identified within the core enhancer regions (CER) of MyoD (Le Grand et al., 2012; Y. Liu et al., 2013). Through the CER regions, Six1 is able to bind and regulate MyoD expression in cultured primary myoblasts (Y. Liu, 2017; Y. Liu et al., 2013). While loss of Six1 in quiescent cells does not produce any detectable phenotype, Six1 regulates the return to quiescence following regeneration through ERK signalling (Le Grand et al., 2012). Six1 plays a critical role in maintaining homeostasis of the stem cell

pool during skeletal muscle regeneration by regulating the extracellular signal-regulated kinase 1/2 (ERK1/2) pathway.

Although many of the pathways and TFs involved in the transition from satellite cell to myofiber and maintenance of the stem cell pool have been identified, the role and mode of action of Six1 in these processes is not yet fully understood.

1.11 The co-factors of Six1

In Drosophila, the homeobox gene, sine oculis, eyeless (ey), eyes absent (eya) and dachshund (dac) are required for compound eye development (Serikaku & O'Tousa, 1994). In vertebrates, Eya family proteins (Eya1-4) and Dach are respectively homologous to eyes absent and dachshund (R. J. Davis et al., 1999). Six1 lacks an activation domain and requires interactions with Eya for activation of target genes (Fougerousse et al., 2002; Grifone et al., 2004, p. 1; X. Li, Oghi, et al., 2003). The Six domain of Six1 forms an interaction through a single α-helix with the C-terminal Eya domain (Patrick et al., 2013). The interaction between Six1 and Eya forms a bipartite transcriptional complex involved in mammalian development and disease (X. Li, Oghi, et al., 2003). Additional bipartite transcriptional complexes such as beta-catenin with Lef form functional interactions which activate transcription of target genes involved in organogenesis (Behrens et al., 1996; van Genderen et al., 1994). Mutations to either Six1 or Eya result in BOR (branchio-oto-renal) syndrome, an autosomal dominant disorder associated with loss of hearing, kidney malformations, and branchial abnormalities (Patrick et al., 2013).

The Eya domain belongs to the haloacid dehalogenase (HAD) superfamily and has tyrosine phosphatase activity (X. Li, Oghi, et al., 2003). Similarly to Six1, Eya protein phosphatase activity is needed for regulating precursor cell proliferation (X. Li, Oghi, et al., 2003). Double knock-out of Eya and Six1 in developing mouse embryos have been found to result in a reduction in epaxial muscle and elimination of hypaxial muscle. Additionally, Eya4 mutations have been linked to dilated cardiomyopathy and heart failure in humans (Abe et al., 2018).

Dach is homologous in vertebrates to dachshund and is related to the corepressors Ski/Sno (Hammond et al., 1998). The Dach domain can downregulate genes through binding with histone deacetylases (HDAC) (K. Chen et al., 2013). In mice, Six6 and Dach were found to bind to promoter regions to repress renal and pituitary precursor cell proliferation (X. Li et al., 2002). Interestingly, in murine myoblasts Eya phosphatase activity was determined to be capable of converting the function of an interaction between Six1 and Dach1/2 from transcriptional repression to activation by facilitating the interaction with the histone acetyltransferase (HAT) CBP (CREB-binding protein) (X. Li, Oghi, et al., 2003). The molecular details of this mechanism, and whether it is applicable to all of the target genes of Six1, remain uncertain. Dach2, Eya2 and Six1 have also been demonstrated in chick myoblasts precursors to synergistically regulate myogenesis (Heanue et al., 1999).

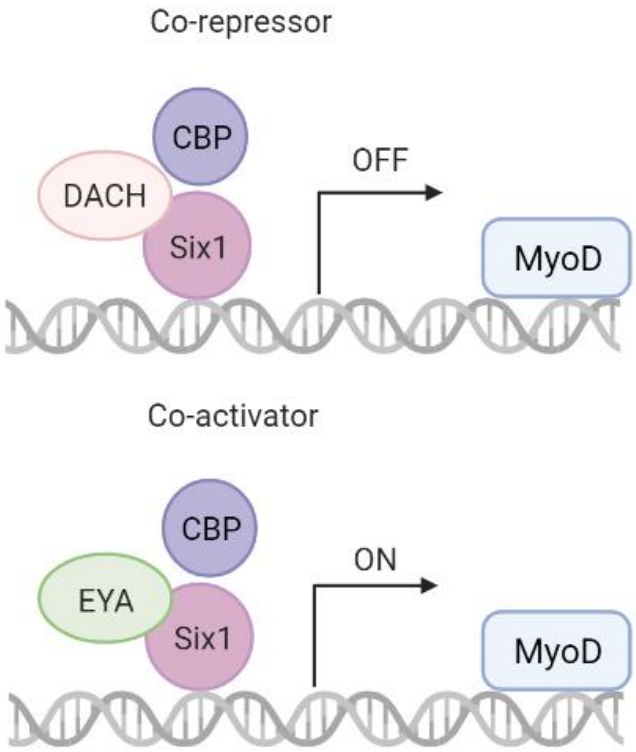

Figure 4 Co-repressor and co-activator activity of Six1 by Dach and Eya.

BRG1 and BRM are ATPase subunits of the chromatin remodelling complex SWI/SNF (Bultman et al., 2000). The activity of Eya and Six1 during neurogenesis are enhanced through ATPase activity of BRG1 (Ahmed et al., 2012). Additionally, BRG1 deficiency in mice results in a reduction in Eya and Six1 expression (Xu et al., 2021). Furthermore, a co-immunoprecipitation (co-IP) revealed a direct physical interaction between BRG1 and Six1-Eya, supporting that the chromatin remodelling properties of BRG1, and likely the entire SWI/SNF complex, may assist transcriptional regulation by Six1. Efforts to identify cofactors of regulatory elements involved during myogenesis could reveal potential therapeutic targets for treatment of muscular degenerative disorders.

1.12 Histone Acetylation by p300

One of the best studied transcriptional co-activators is p300/CBP, which are known to be implicated in possibly all biological processes, including myogenesis (Khilji et al., 2018; Puri, Avantaggiati, et al., 1997). p300 and its related protein, CBP, are transcriptional coactivators known to be involved in developmental processes.

CBP was first identified through interaction with phosphorylated CREB (cAMP-response element binding protein), as a transcriptional coactivator (Chrivia et al., 1993). The CBP paralog, p300, was subsequently isolated as a binding protein of the adenovirus, early region 1A (E1A) (Eckner et al., 1994). CBP and p300 are reported to act as coregulators of numerous transcription factors including MyoD, Myf5, (Roth et al., 2003).

Acetylation of histone octamers by p300 has been determined to be necessary for myogenesis in C2C12 murine cell line of myoblasts (J. Chen et al., 2015). p300/CBP is required for dynamic acetylation of transcription factors and epigenetic enzymes (Carrozza et al., 2003; Imhof et al., 1997). A role for p300 in the initiation of muscle function genes during terminal differentiation has also previously been demonstrated (Pradeepa, 2016).

Although paralogous, p300 and CBP regulate distinct functions. p300 knock-out mouse embryos display more severe abnormalities in heart development in comparison to CBP knock-out (Yao et al., 1998). Conversely, CBP was determined to be required for hematopoietic differentiation whereas no abnormalities were observed in mice with a p300 heterozygous null mutation (Kung et al., 2000). Variations in CBP and p300

coregulation may be attributed to preferential acetylation of different lysine residues. For example, on H4, CBP preferentially acetylates lysine 18 while lysines 5 and 8 are preferential to p300 (Henry et al., 2013; Schiltz et al., 1999).

Through inhibition of either CBP or p300, only the activity of p300 was determined to be necessary for regulation of myogenesis (Puri, Sartorelli, et al., 1997). p300 inhibition resulted in a reduction of expression of Myf5 and MyoD required for muscle cell fate determination, whereas cells with CBP inhibition continue to progress through myogenesis. Artificial recruitment of the HAT domain of p300 is sufficient in inducing enhancer acetylation and promotor proximal transcription of MyoD (Hilton et al., 2015). Knock-down of p300 results in impairment in proliferation, cardiac development, and neurulation, suggesting its significance during embryonic development (Sun et al., 2010).

Both p300 and CBP have a catalytic HAT domain (Bannister & Kouzarides, 1996; Ogryzko et al., 1996). Autoacetylation of an activation loop motif within the p300 HAT domain was found to increase its catalytic activity (Thompson et al., 2004). While p300 is capable of acetylating all four core histones, the ZZ-type zinc finger (ZZ) and bromodomain of p300 modulate the preferential acetylation of H3 (H3K27, H3K18) and H4 (Y. Zhang et al., 2018). The bromodomain and PHD finger of p300 cooperate to stably bind to acetylated lysine residues on histone tails (Manning et al., 2001; Ragvin et al., 2004). Following DNA damage, the bromodomain of p300 binds to p53 which mediates acetylation-dependent coactivator recruitment that is required for cellular stress responses including apoptosis (Mujtaba et al., 2004).

The HAT activity of p300/CBP promotes the assembly of the pre-initiation complex (PIC) through recruitment of TFIID and RNAPII at enhancer regulated genes (Narita et al., 2021). Narita et al. proposed that p300/CBP simultaneously promote the recruitment of RNAPII and recruit BRD4 to coordinate pause release of RNAPII. Time-resolved analysis of p300/CBP acetylated sites on both histones and non-histones using the catalytic p300 inhibitor A-485 revealed a rapid turnover of histone acetylation by p300/CBP (Weinert et al., 2018). The rapid deacetylation observed following A-485 treatment suggests constant antagonism mediated by the activity of HDAC's. As the presence of HDACs collectively outweigh the presence of p300/CBP, it can be implied that deacetylation is favoured over acetylation within the environment of the cell nucleus and that acetylation is likely confined to specific loci where HAT activity is concentrated through TF recruitment (Gillespie et al., 2020).

While certain p300/CBP inhibitors target the bromodomain (Hammitzsch et al., 2015), the catalytic inhibitor A-485 competes with acetyl-CoA to inhibit p300 acetyltransferase activity (Lasko et al., 2017). Prior to the discovery of A-485 as a inhibitor of p300, known alternatives included garcinol, a natural polyisoprenyl benzophenone derivative from the fruit rind of Garcinia indica (Balasubramanyam et al., 2004), the synthetic inhibitor, Lys-CoA (Lau et al., 2000), and the small molecule inhibitor C646 (Bowers et al., 2010). Through time-resolved fluorescence resonance energy transfer assay (TR-FRET) evaluation of acetylation of a biotinylated histone H4 peptide following p300 inhibitor treatment, A-485 was determined to be exceedingly potent and selective in comparison to other known inhibitors of p300 (Lasko et al., 2017). Research efforts are being made into determining the potential use of A-485 as treatment for various diseases including

acute liver injury (ALI), melanoma, and osteoporosis (Huo et al., 2021; Peng et al., 2019; R. Wang et al., 2018).

1.13 Histone Acetyltransferases and Deacetylase Activity

In addition to p300/CBP, there are two additional major HAT families including Gcn5-related *N*-acetyltransferases (GNATs) and MYST (MOZ, YBF2, SAS2 and TIP) (Carrozza et al., 2003). HAT families are defined by structure, binding motifs, and catalytic domains. The GNAT family of acetyltransferases is defined by the presence of a C terminal bromodomain and four conserved motifs (A-D) including motif A which is required for acetyl-CoA binding (Modis & Wierenga, 1998; Sternglanz & Schindelin, 1999; Tercero et al., 1992). The MYST family of HATs is defined by the MYST domain as well as the presence of a zinc finger and acetyl-coA binding site (Borrow et al., 1996).

Bromodomain and Extra Terminal domain (BET) are a family (BRD2, BRD3, BRD5, BRDT) of highly conserved proteins which read acetylated lysine residues (Haynes et al., 1992; Zeng & Zhou, 2002). Bromodomains are named after the related brahma gene in Drosophila (Tamkun et al., 1992). Through interaction with acetylated DNA, BET proteins are capable of regulating transcriptional elongation through recruitment of P-TEFb to DNA (Z. Yang et al., 2005; Zeng & Zhou, 2002). Bromodomains are present in a variety of proteins including histone acetyltransferases such as P/CAF (p300/CBP-associated factor), methyltransferases, helicases, ATP-dependant chromatin remodelling complexes, co-activators, and scaffolding proteins. Bromodomains can promote histone acetylation through linking HATs to specific loci and assembly of

chromatin remodelling complexes (Brownell et al., 1996). Treatment of C2C12 myoblasts with BET inhibitors (BETi) resulted in dose-dependent inhibition of myogenic differentiation (Roberts et al., 2017). While knock-down of BRD3 resulted in enhanced myogenic differentiation, knock-down of BRD4, which preferentially binds to the Myog promoter and is associated with increased presence of H3K27ac resulted in an anti-myogenic phenotype. In addition to reading acetylated lysine residues, BRD4 has also been shown to act as a HAT capable of acetylating histones H3 and H4 (Devaiah et al., 2016).

Histone acetylation can either take place on the core histone proteins (H2A, H2B, H3 and H4), at various regions of the histone tail or at certain surface residues of their C-terminal globular domains (Mizzen & Allis, 1998; Molina-Serrano & Kirmizis, 2013). Acetylation on the histone tail can be read by BET proteins which modulate transcription through recruitment of effector molecules (Zeng & Zhou, 2002). Acetylation is generally associated with an opened, euchromatic DNA through neutralization of negatively charged DNA and destabilization of DNA-histone interactions resulting in a transcriptionally active state. In addition to modifications to the histone tail, acetylation has also been detected on the sides and core of the octamer, effecting histone-histone interactions (Mersfelder & Parthun, 2006). Modulations to the core potentially effect the assembly of the histone octamer while acetylation to the outer regions effect inter-nucleosomal interactions. Acetylation to the histone surface have been suggested to disrupt DNA-histone interactions by decreasing the positive charge of the histone core thereby regulating transcription by directly modulating DNA accessibility, such has been demonstrated for H3K122ac (D. Y. Lee et al., 1993; Tropberger et al., 2013).

Histone deacetylases (HDAC) are catalytic enzymes which control the balance of acetylation by removing acetyl groups deposited by HATs (Wade, 2001). There are four (I-IV) classes of HDACs respectively classified based on homology to homologues found in yeast, Rpd3, Hdal, Sir2 (Ruijter et al., 2003). Contrasting to HAT activity, HDAC's are associated with condensed, inaccessible heterochromatin and transcriptional inactivation. HDACs such as SIRT1, can be recruited to silence developmentally and environmentally regulated genes through formation of facultative heterochromatin (Vaquero et al., 2004). During terminal muscle differentiation, relatively stable constitutive heterochromatin has been suggested to require the presence of HDACs for spatial reorganisation and enhanced histone methylation (Terranova et al., 2005).

1.14 H3K27ac

H3K27ac can be catalyzed through the p300/CBP complex and is marker of active promoters and enhancer regions (Creyghton et al., 2010; Raisner et al., 2018). The presence of H3K27ac has been extensively studied in various regulatory mechanisms and is associated with transcriptional activation. In human skeletal muscle, H3K27ac has been found to be upregulated in aging skeletal tissue (Zhou et al., 2019). The understanding of the mechanism behind H3K27ac activity is largely correlative rather than functional.

Through in vitro RNA binding assays, the BET family protein, BRD4 has been shown to localize at regions enriched with H3K27ac and to directly interact with H3K27-containing peptides in vitro in an acetylation-dependent manner (Rahnamoun et al., 2018). BRD4

bound to acetylated histones is suggested to promote transcriptional elongation through recruitment of the pause-release factor, P-TEFb to promoter-proximal regions (Kanno et al., 2014). It has also been suggested that H3K27ac regulates activation through blocking the repressive trimethylation of H3K27 by PRC2 (Polycomb Repressive Complex 2) (Pasini et al., 2010).

1.15 H3K122ac

In addition to H3K27ac, p300 is also capable of catalyzing the acetylation of H3K122ac, a marker of active functional enhancers and promoters (Tropberger et al., 2013). H3K122ac is located on the nucleosome dyad axis, where histone-DNA binding reaches its maximum strength (Hall et al., 2009). Acetylation on the lateral surface of histone octamers results in nucleosome destabilization and the opening of chromatin, thereby enabling gene transcription (Tropberger et al., 2013).

Although H3K4me1 and H3K27ac are the standard chromatin signatures used for identifying active enhancer regions (Creyghton et al., 2010), Pradeepa et al. identified enhancer regions which lacked H3K27ac and were instead defined by H3 globular domain acetylation on H3K64ac and H3K122ac. A portion of enhancer regions and poised promoters contained H3K122ac but had no detectable levels of H3K27ac. Furthermore, sequential ChIP (chromatin immunoprecipitation) was used to confirm the presence of H3K122ac in addition to H3K4me1 and H3K27me3 at poised enhancers, a potential element of the rapid modulation of genes required during myogenesis.

The presence of H3K122ac at poised promoters and enhancers, as well as its ability to destabilize nucleosomes suggests that H3K122ac may increase DNA accessibility prior to differentiation, allowing for rapid transcriptional upregulation of myogenic genes.

1.16 Nucleosome Destabilization and RNA Polymerase II

For Pol II to effectively traverse across template DNA, additional factors such as transcriptional elongation factors, chromatin remodelling enzymes, chaperone proteins and epigenetic modifications are required for downstream transcription (Henikoff, 2008). While nucleosomes are required for DNA organization and compaction, the structures also pose physical barriers for elongation by RNAPII (RNA Polymerase II). Previous studies have found that RNAPII is unable to efficiently cross genomic regions with nucleosomes without detachment of a H2A/H3B dimer (Bondarenko et al., 2006; Kireeva et al., 2002, 2005). Binding of RNAPII to certain genomic loci is obscured by tight wrapping around histone octamers and can be accessed through the activity of chromatin remodelling factors. Binding of RNAPII can also be obstructed by the rapid and spontaneous re-wrapping of DNA following unwrapping by chromatin remodelling factors (G. Li et al., 2005).

Enzymatic reactions from SWI/SNF complexes can disrupt the interactions between DNA and histones through ATP hydrolysis. BRG1 and BRM are two homologous proteins of the SWI/SNF complex which impart ATPase activity (Kadam & Emerson, 2003). Absence of BRG1 and BRM in mouse NIH 3T3 cells resulted in impairment of chromatin remodelling required for MyoD-mediated myogenic differentiation (de la Serna et al., 2001). Although ectopic expression of myogenin and Mef2D is capable of

restoring differentiation in MyoD deficient B22 cells, in NIH3T3 fibroblasts lacking BRG1, chromatin remodelling mediated by BRG1 is required for Myogenin/Mef2D induction of skeletal muscle differentiation (Ohkawa et al., 2006).

1.17 Pioneer Factors

The activation of precursor muscle stem cells and maintenance of the stem cell niche is collectively orchestrated by numerous transcription factors, enzymes, and epigenetic modifications, requiring precise spatial and temporal organization. Pioneer transcription factors are capable of initial binding to target sites and actively or passively promoting downstream transcriptional activity (Zaret & Carroll, 2011). Pioneer factors work to initiate transcriptional cascades through direct recruitment of transcription factors or chromatin reorganization, while for others their mere presence acts as a barrier to binding of unneeded factors (Magnani et al., 2011).

The pioneer factor FoxA, is characterized by the ability to recognize target sites within compacted regions of DNA and C-terminal domain capable of disrupting the interaction between DNA and certain histones (Cirillo et al., 2002). In early mouse embryonic stem cells (mESCs) lacking FoxA, target regions are bound by the repressor FoxD3 which maintains a demethylated state of DNA (Hanna et al., 2002). During differentiation, FoxA proteins are capable of replacing linker histones (H1) thereby opening DNA and allowing for transcription factors to bind to their target genes (Marsden et al., 1998).

In mature macrophages, stimulation by LPS upregulates enhancer activity and is coupled by p300 association and NFkB binding (Smale, 2010). To investigate

endotoxin-induced transcriptional activation in macrophages, PU.1, a primary regulator of myeloid development and p300 were profiled following LPS stimulation using the 3T3 cell line of mouse embryonic fibroblasts (Ghisletti et al., 2010). Many LPS induced p300 upregulated regions were pre-associated with PU.1, suggesting that both pioneer factor activity of PU.1 prior to LPS stimulation and DNA remodelling primes DNA for immune response.

Myogenic determination factor, MyoD, requires prior Pbx1 binding to the myogenin promoter region to allow for MyoD recruitment during differentiation (Berkes et al., 2004; Maves et al., 2007). It has been suggested that Pbx1 recruits BRG1 to the myogenin promoter and subsequent BRG1-based SWI/SNF chromatin remodelling facilitates MyoD binding (de la Serna et al., 2005).

Six1 interacts with the SWI/SNF complex which is capable of nucleosome displacement during inner ear neurogenesis (W. Wang et al., 1996). Previous work in our lab suggests that Six1 may potentially act as a pioneer factor by establishing a chromatin environment which enables binding of MyoD to the CER of its own gene, thereby potentiating the positive autoregulation of MyoD (Y. Liu et al., 2013).

The presence of pioneer factors allows for organized changes to transcriptional patterns by preparing the nucleosome environment (Magnani et al., 2011). The gene expression program necessary for regeneration is quickly activated in muscle stem cells, suggesting that pioneer factors allow for quick upregulation of genes required for myogenesis. Although different mechanisms for pioneer factor activity have been proposed, several pioneer factors are suggested to function through recruitment of

epigenetic modifications and coincide with the establishment of H3K27ac at enhancer regions (Fuglerud et al., 2018; Lemma et al., 2021; Tamura et al., 2021).

1.18 Hypothesis and Aims

In this research, it was hypothesized that Six1 opens chromatin by recruiting p300 to acetylate H3K122 on the lateral surface of the histone octamer, rendering DNA more accessible, thereby facilitating gene transcription (Figure 5). The primary aim of this work was to determine whether control of DNA accessibility by Six1 has effects on gene expression in muscle precursor cells. To address the hypothesis, this work reports a series of objectives:

Objective 1. To determine the functional relationship between Six1 and p300.

Objective 2. To determine the functional relationship between p300 HAT activity and DNA accessibility.

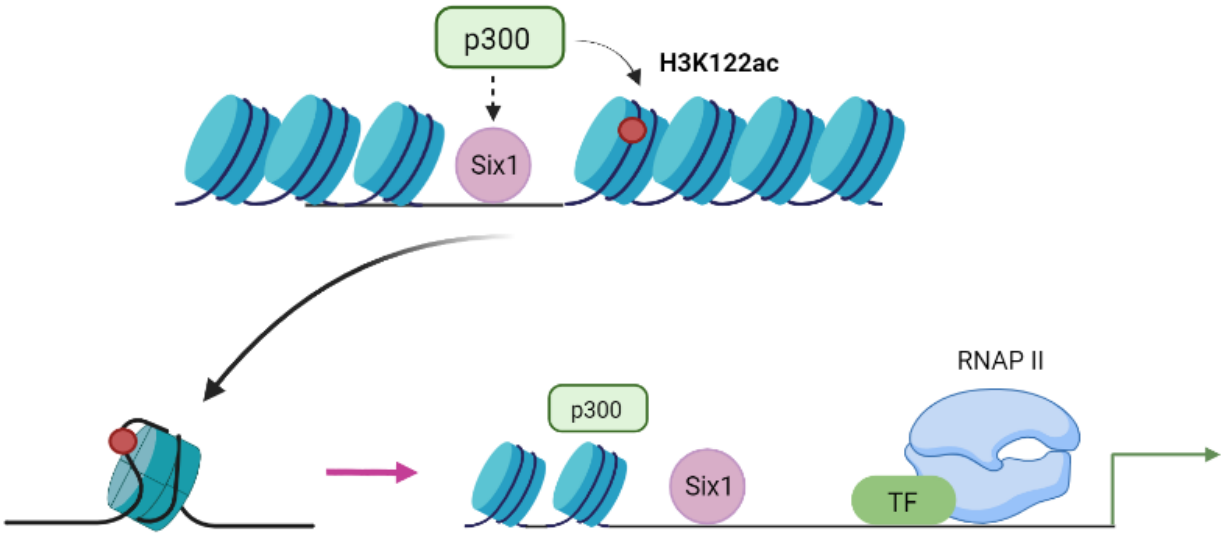

Figure 5 Schematic of the hypothesis illustrating recruitment of p300 through pioneer factor activity of Six1 and H3K122ac mediated nucleosome destabilization and opening of DNA

2. Materials and Methods

2.1 C2C12 Cell Line Maintenance

The C2C12 cells (American Type Culture Collection) were grown in Growth Medium (GM) containing 88% (500 mL) Dulbecco's Modified Eagle's Medium High glucose (Sigma), 10% (5 mL) Fetal Bovine Serum (FBS) (Sigma), 1% (5 mL) L-Glutamine and 1% (5 mL) Penicillin/Streptomycin. Cells were grown and maintained subconfluent in a humidified water-jacketed incubator at 37°C and 5% CO_2.

2.2 siRNA Transfections

A 15 cm cell culture dish was used to seed 200,000 C2C12 cells for each condition. Transfections were performed using Silencer Select siRNAs (small interfering RNA) (Thermo Fisher Scientific) suspended and diluted as described by the manufacturer to a final concentration of 10 µM. Twenty-four hours after seeding, either 38 µL of siRNA siSix1.1 (Silencer™ Select Pre-Designed siRNA cat: 4390771 ID: s73792), siSix1.2 (Silencer™ Select Pre-Designed siRNA cat: 4390771 ID: s201996) or 38 µL of siCtrl (Silencer™ Select Negative Control No. 1 siRNA 40 nmol cat: 4390844) was suspended in 1.8 mL of OptiMEM (Invitrogen). Additionally, 95 µL of Lipofectamine RNAiMax was suspended in 1835 µL of OptiMEM. The Lipofectamine solution was added to the siRNA solution and incubated at room temperature for five minutes. Following the incubation, the solution was added dropwise to adherent cells in 12 mL growth medium. Twenty-four hours after siRNA transfection, medium was aspirated, and 24 mL of fresh growth medium was added.

2.3 Western Blot

Two days after siRNA transfection, cells were scraped and lysed using a urea/SDS lysis buffer (6 M urea, 20 mM Tris pH 6.8, 0.1% SDS). Lysates were briefly sonicated at 10% intensity and subsequently spun down to remove debris. Lysates were separated by 10 % SDS-PAGE gel and transferred to a polyvinylidene fluoride (PVDF) membrane at 100 V. The membrane was blocked for thirty minutes at room temperature with 5% skim milk. The membrane was washed with a wash buffer (TBS with 0.05% TritonX-100 and 0.05% Tween 20) five times for five minutes. The membrane was probed with either anti-Six1 antibody (rabbit, Sigma, cat: HPA001893) or B-Tubulin (mouse, clone E7, DSHB) at a ratio of 1:1000 overnight at 30 V in 4°C. The membrane was washed as previously described prior to incubation with secondary mouse or rabbit specific antibodies conjugated with Horseradish Peroxidase (Promega) for one hour. The membrane was washed in wash buffer as previously described and drained. Exposure was performed using a home-made ECL (enhanced luminol-based chemiluminescent) kit where 10 mL 0.1M Tris pH 8.5 was combined with 50 µL 90 mM Coumaric Acid and 50 µL 250 mM 3-Aminophtalyhydraize Free Azide (Luminol). Prior to exposure, 3 µL of 30% Hydrogen Peroxide was added to the ECL mixture and incubated for 30 seconds with the membrane at room temperature prior to exposure using an SRX-101A Processor.

2.4 p300 inhibition

To inhibit p300, three different doses (0.3 µM, 1.0 µM and 3.0 µM) of 12 mM A-485 (Tocris) in DMSO solvent was added dropwise to cells. DMSO was used as control.

2.5 RNA Extraction

To perform RNA extraction, medium was removed from the cells and the plate was rinsed once with PBS (Phosphate-Buffered Saline) to remove excess growth medium. Extraction was performed using 1 mL of TRIzol reagent (Invitrogen) and samples were transferred into conical tubes before freezing at -80°C. Supernatant was transferred to a new tube and samples were vortexed for 10 seconds. Subsequently, 500 µL of chloroform was added to the lysates and samples were vortexed for an additional 10 seconds and allowed to incubate at room temperature for 3 minutes. Samples were centrifuged at 12,000 g for 15 minutes at 4°C. The RNA from the aqueous phase was precipitated from solution by adding 850 µL of isopropanol, vortexed for 5 seconds and allow to incubate for 10 minutes at room temperature. Following this, samples were centrifuged at 12,000 g at 4°C for 10 minutes. Pellets were washed twice with 75% ethanol and washed once with 100% ethanol. Pellets were centrifuged between washes at 7500 g for 5 minutes at 4°C. The final RNA pellet was resolubilized in 30 µL of DEPC-treated water and incubated for 5 minutes 37°C. Optical density of the samples was measured using a NanoDrop 2000 Spectrophotometer.

2.6 CUT&Tag

Two days after siRNA transfection, cells were scraped and rinsed twice with PBS. The 2.01 version of the CUT&Tag (Cleavage Under Targets and Tagmentation) protocol was used (Kaya-Okur et al., 2019). The H3K122ac (Abcam, cat: ab33309, rabbit), H3K27ac (Abcam, cat: ab4729, rabbit), p300 (Active Motif, cat: 61903, mouse), Six1 (Sigma, cat: HPA001893, rabbit) and IgG (Normal rabbit IgG, Jackson

ImmunoResearch), CUT&Tag-seq was performed as described (Kaya-Okur et al., 2020) with the inclusion of 1 µL of spike in drosophila DNA at 5 fg/µL and qPCR calibration of the amplification procedure added at the post-tagmentation clean-up step. Half of a microliter of primary antibody for each marker was added to each sample with the exception of H3K122ac, where empirical tests showed that 1 µL of primary antibody was optimal. Six replicates of control and Six1 knock-down CUT&Tag experiments were performed with antibodies targeting Six1. Three replicates of control and Six1 knock-down experiments with antibodies targeting H3K122ac, H3K27ac and p300 were also performed. For sequencing, 3.2 µL of 12.5 µM i5 + i7 dual index Nextera for Illumina primers suspended in Tris 10 mM pH 8.0 were used.

2.7 qPCR

qPCR was performed using the real-time PCR system, BioRad CFX 96 using 10 µL reactions in 96-well plates. To prepare the samples two microliters of DNA was diluted in a ratio of 1:50 in 10 mM pH 8 Tris. The DNA solution was added into a solution containing 2 µL detergent free 5X HF Phusion Buffer (Thermo Scientific), 0.2 µL 100 µM SYTO-13 (Invitrogen), 0.2 µL 10 µM dNTP (Promega), 0.5 µL 10µM primer diluted in 10mM Tris pH 8.0, 5 µL dH20 and 0.1 µL Phusion (Prepared in-house by Dr. Adam Rudner).

Prior to submitting libraries for sequencing (Illumina HiSeq), samples were validated using quantitative PCR (qPCR) with primers targeting the MyoD CER, a region internal to the Pax2 gene (heterochromatic in C2C12 cells), the Sf1 gene proximal promoter, and a region of the drosophila genome to detect spike-in DNA.

For each primer, optimal melting temperatures (*T*m) during qPCR amplification were determined by testing a gradient of temperatures between 58°C to 70°C with purified C2C12 genomic DNA diluted in 5-fold decreasing quantities.

Initial validation of samples was performed by comparing melting temperature curves to those determined to be optimal. Samples were quantified by first determining the mean of the quantification cycle (*Cq*) values of biological replicates followed by calculating a transformed *Cq* value (2^{-Cq}). Statistical analysis was performed using a two-sample equal variance, one-sided, t-test ($p>0.05$).

2.8 HepG2 Transfection

HepG2 were obtained from the ATCC and cultured as recommended. They were transfected in 24 well plates using Lipofectamine 3000 using 1 microgram of DNA mixture, consisting of 100 ng of firefly luciferase reporter plasmid (pGL3-Basic with four E-box elements, 3 MEF3 elements and a TATA box, (Y. Liu et al., 2010) ,10 ng of normalizing plasmid (Renilla luciferase pRL-Null), and 450 ng each of p3xFlag-Six1-myc (Y. Liu et al., 2010) and pCI/CMV-p300 (kindly provided by Dr. Qiao Li, U. of Ottawa), or the respective empty plasmids. Medium was changed 24 hours after lipofection and cells were harvested in 100 μL passive lysis buffer (Promega Inc.) after another day. Five μL of lysate were used to assay firefly and Renilla luciferase with the Dual luciferase assay kit (Promega). Firefly activity was divided by Renilla activity, and normalized numbers were further divided by the condition without Six1 or p300 overexpression.

2.9 Co-immunoprecipitation

C2C12 myoblasts were harvested in growth phase and nuclear proteins were extracted following a modification of the Dignam method where Dounce homogenization is replaced passing through a 27 gauge syringe needle and extract dialysis is replaced by dilution with buffer of a lower salt concentration (Dignam et al., 1983). Antibodies used were a custom-made rabbit anti-Six1(Y. Liu et al., 2013) or normal rabbit IgG (Jackson Immunoresearch). The extract was precleared for two hours with protein A/G agarose beads, antibodies were applied overnight at 4^{o}C with rotation, immune complexes were captured with protein A/G agarose beads, beads were washed four times in RIPA buffer and immune complexes were eluted by boiling in sample buffer. Eluates were resolved on 4-20% gradient SDS-PAGE gels and proteins were detected by western blot. Rabbit anti-p300 (sc-585X, Santa Cruz Biotechnology) was used.

2.8 ATAC-seq

ATAC-seq libraries were prepared using the OMNI ATAC-seq protocol as described (Corces et al., 2017). Three replicates of samples were prepared in control and Six1 knock-down conditions using an equimolar pool of siSix1.1 and siSix1.2 small-interfering RNA. Additionally, ATAC-seq was performed using the p300-inhibitor A-485 (Tocris) and DMSO as control for 3, 6, 24 hour treatment durations and 0.3 µM, 1.0 µM, 3.0 µM dosages.

2.9 Bioinformatics Analyses

Quality of FASTQ files was analyzed using fastQC 0.11.9. Files were trimmed of low quality regions and contaminating sequencing adapters using fastp 0.20.1 (S. Chen et al., 2018). STAR v2.7.3a was used to align reads to the mm9 genome with a maximum intron size of 1 base pair using a mm9 genome index created without a GTF file (Dobin et al., 2013). SAMTools v1.11 was used for indexing of BAM files (H. Li et al., 2009). Picard v2.23.3 was to for mark duplicate reads, and duplicates were removed for downstream analysis (Picard Tools, Broad Institute). deepTools bamCoverage, with arguments set to exclude duplicate reads and bin sizes set to 10, was used to calculate sequencing coverage across the genome and generate bigwig files (Ramírez et al., 2016). For CUT&Tag sequencing data, libraries were limited to fragments between 10 and 2000 base pairs. MACS2 v2.2.7.1 was used for peak calling in BAMPE format using the --nomodel option and excluding duplicate fragments (Y. Zhang et al., 2008). MSPC v4.0.2 (Multiple Sample Peak Calling) was used to generate consensus peak files for CUT&Tag markers (Jalili et al., 2015). The intersect tool from the v.2.29.2 bedtools package was used for removal of blacklisted genomic loci, including mitochondrial DNA (Quinlan & Hall, 2010). featureCounts was used to summarized sequenced fragments (defined by read pairs) over peaks (Liao et al., 2014). For CUT&Tag samples, fragments ranging in 10 – 2000 bp in length were counted whereas for ATAC data, the 5' end of each read was used to query Tn5 cleavage sites in open regions of DNA. CUT&Tag peak consensus files for each marker were filtered to have a less than 5% False Discovery Rate (FDR), calculated based on overlap with the IgG

peak consensus file. A-485 treatment ATAC-seq peaks were filtered to have over 20 counts in at least 14 samples determined by the number of control samples.

Downstream differential analysis was carried out using the R package, Bioconductor (Huber et al., 2015). edgeR was used to perform differential analysis (Robinson et al., 2010a) based on sample conditions. Read counts were normalized using Trimmed means of M Values (TMM) converted to counts per million reads. Batch effects were accounted for using the RUVseq package with the RUVr algorithm with the number of co-variables (k) optimized to reduce unwanted variation based on Principal Components Analysis (PCA) (Risso et al., 2014). K-means clustering (k=3) was used to group peaks according to log-fold change values of median-centered counts. anti-Six1 CUT&TAG samples were normalized by the number of thousands of drosophila spike-in reads present in each sequencing library. The Bioconductor package, liftOver was used to convert peaks from the mm9 to mm10 genome. ChIPpeakAnno v.4.0.2 was used to annotate peaks from each cluster using the ENSEMBL mm10 assembly (Zhu et al., 2010). Peaks were annotated to genes using the shortest distance within a maximum of 60 kb around the transcription start site (TSS) and limited to those with greater than 30 counts in at least 5 samples. Panther was used to perform Gene Ontology (GO) term enrichment analysis using the Overrepresentation Test against the whole mouse genome (Mi et al., 2013). Raw P-values were calculated using the Fisher's Exact Test and the FDR was corrected with the Benjamini-Hochberg algorithm ($p < 0.05$) (Benjamini & Hochberg, 1995).

2.10 Data Visualization and Statistical Analysis

Graphs were generated using R packages, pheatmap and ggplot. regioneR was used to perform statistical association analysis using a permutation procedure (Gel et al., 2015). PlotCorrelation was used to calculate pairwise correlation between samples to determine reliability of data (Ramírez et al., 2016).

3 Results

3.1 Description of the study system employed

Six1 cooperates with various cofactors to regulate skeletal muscle development and regeneration (X. Li, Ohgi, et al., 2003; Maire et al., 2020). Assays using C2C12 myoblasts have established the involvement of the HAT p300 in myogenesis by acting as a transcriptional coactivator of the MRF's, MyoD and Myogenin, and a previous report has shown an interaction between Eya3 and the HAT, CBP (X. Li, Ohgi, et al., 2003; Puri, Avantaggiati, et al., 1997). Thousands of Six1 binding sites were found to coincide with p300-bound gene enhancers (Khilji et al., 2018) (Figure 6). In order to determine if there is a functional association between Six1 and p300 in C2C12 myoblasts, a co-IP assay was performed. The results of this unpublished experiment, performed by a former colleague reveal an interaction between Six1 and p300 (Figure 7A). The correlation between Six1 and p300 is consistent with a mechanism involving Six1 recruitment of p300 in myoblast regulation.

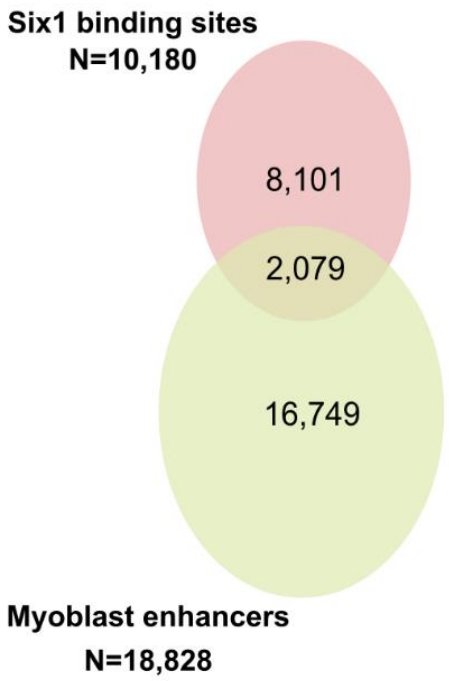

Figure 6 In proliferating myoblasts, several Six1 binding sites (Girgis et al., 2021) qualify as p300-bound gene enhancers (defined as promoter-distal loci with high levels of H3K4me1 (Lilja et al., 2017), H3K27ac (Lilja et al., 2017) and p300 (Khilji et al., 2018).

An interaction between Six1 and co-activator p300 is likely considering that an interaction between CBP and a Six1-binding protein (Eya3) has previously been reported (X. Li, Ohgi, et al., 2003), and that Six1 and p300 are often located at the same genomic loci (Khilji et al., 2018; Y. Liu et al., 2010). Co-immunoprecipitation in C2C12 myoblasts was used to determine if Six1 and p300 are part of the same complex. Cells were harvested in growth phase and nuclear protein extracts were immunoprecipitated with antibodies against Six1 or negative control normal rabbit IgG. The results show that Six1 and p300 form a stable multiprotein complex (Figure 7A)

To examine whether the Six1-p300 association is functional, the transcriptional activities of Six1 and p300 were assayed. For this, a heterologous cell line expressing minimal levels of Six1 was needed. The HepG2 hepatocarcinoma cell line was selected for this

purpose, as the Cancer Cell Line Encyclopedia indicates that it expresses relatively low levels of the Six1 mRNA (Barretina et al., 2012). This was confirmed by western blots using an anti-Six1 antibody, which revealed that HepG2 cells indeed express low levels of this protein compared to the mouse myoblast cell line C2C12 or human HEK293T cells (Figure 7B).

Transcriptional reporter assays were performed using an artificial reporter plasmid containing binding sites for Six1, co-transfected with expression plasmids for Six1, p300 or both. The results indicate that p300 has a Six1-dependent effect on transcription from the reporter (Figure 7C), suggesting that p300 acts as a *bona fide* co-activator for Six1.

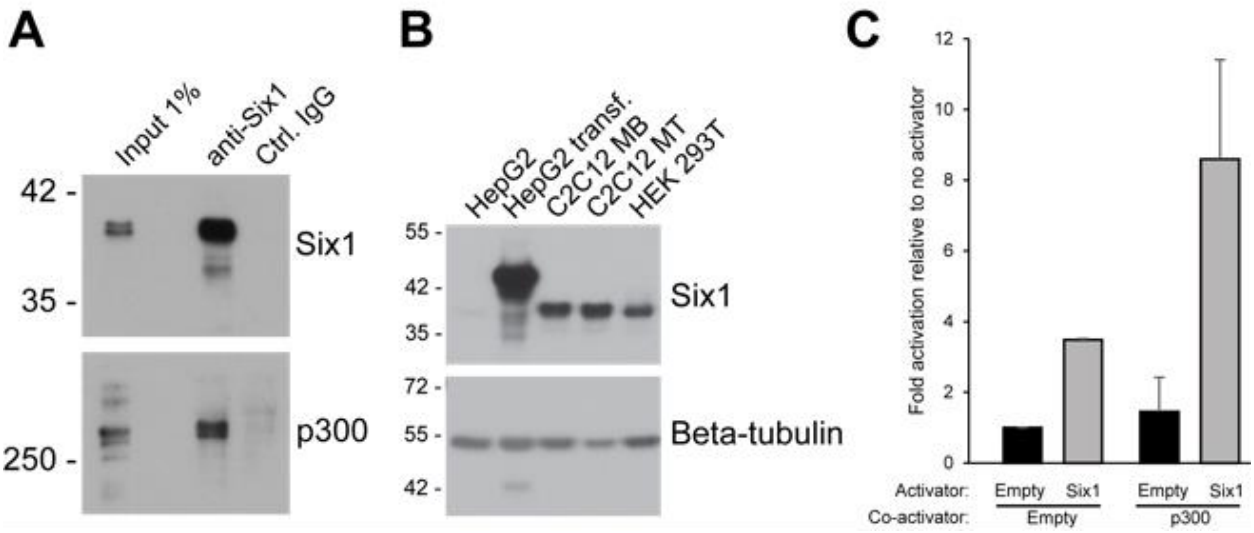

Figure 7 (A) Co-immunoprecipitation of p300 with anti-Six1 in nuclear extracts of proliferating C2C12 myoblasts. Normal rabbit IgG was used as negative control. An aliquot representing 1% of the starting material was loaded alongside. (B) Western blot showing low expression of Six1 various cell lines. The lysate from lane two is from HepG2 cells transfected with a 3xFlag-Six1 expression plasmid. The C2C12 lysates are from cells in the growth phase (myoblasts, "MB") or differentiated for four days (myotubes, "MT"). (C) Luciferase assay performed in HepG2 cells in the presence of combinations of Six1 and p300 or the respective empty expression plasmids. Results are shown as fold reporter gene activity over the condition with both empty plasmids and are the average of two biological replicates. Experiments performed by Yubing Liu (panel A) and Caleb Labonté (panels B and C).

To establish the functional mechanism of Six1 by which Six1 regulates gene expression in skeletal myoblasts, dynamic changes in regulating skeletal muscle development and regeneration, dynamic changes to DNA accessibility and epigenetic landscape were examined in C2C12 myoblasts following Six1 knock-down. Six1 binding sites were profiled using CUT&Tag. Epigenetic regulation by Six1 was investigated by assessing variations in H3K27ac, H3K122ac and p300 CUT&Tag signals following Six1 knock-down. DNA accessibility dynamics following either Six1 siRNA knockdown or p300 chemical inhibition were also profiled using ATAC-seq. Finally, gene expression levels were evaluated at regions where both accessibility and epigenetic landscape were suggested to be regulated by Six1 recruitment of p300.

3.2 Identification of Six1 binding sites using CUT&Tag

To assess the role of Six1 in establishing the epigenetic landscape of myoblasts, Six1 binding sites were initially identified. ChIP-seq and ChIP-on-chip Six1 binding sites in C2C12 myoblasts were previously reported by our lab (Girgis et al., 2021; Y. Liu et al., 2010). CUT&Tag was used as an alternative method to profile Six1 binding sites in C2C12 myoblasts with a high signal-to-noise ratio and affording the possibility to work with low cell numbers typically used for siRNA transfections.

A confirmatory western blot was performed to assess the efficiency of Six1 knockdown using two different siRNAs (Figure 8). PlotCorrelation was used to ensure reliability of anti-Six1 CUT&Tag data against anti-Six1ChIP-seq peaks (Figure 9) (Ramírez et al., 2016). Six1 ChIP-seq peaks were obtained in primary myoblasts as opposed to C2C12 cells, which may explain the cloud of spots of strong ChIP-seq signal that correlate

differently with CUT&Tag signal. Additionally, the Six1 antibody used in the ChIP-seq experiment was performed using a homemade, polyclonal antibody as opposed to a commercially available antibody.

Three biological replicates of CUT&Tag samples were prepared under Six1 knock-down conditions using two siRNA's targeting Six1. Six1 binding sites were filtered to have <0.05% FDR, determined by overlap with nonspecific IgG CUT&Tag binding sites. A total of 9596 significant Six1 binding sites were identified. The CUT&Tag signal at representative Six1 binding sites is shown, displaying a reduction in Six1 signal at these loci following Six1 knock-down (Figure 10-Figure 12).

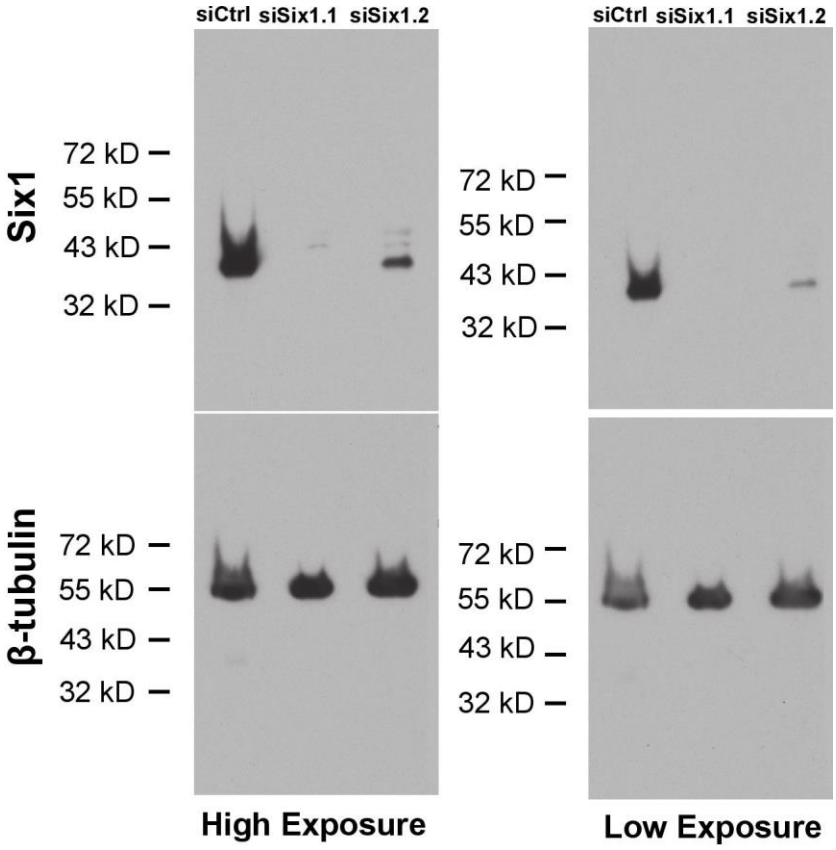

Figure 8 Western blot of C2C12 control and Six1 KD conditions with primary antibodies against Six1 and second against beta-tubulin.

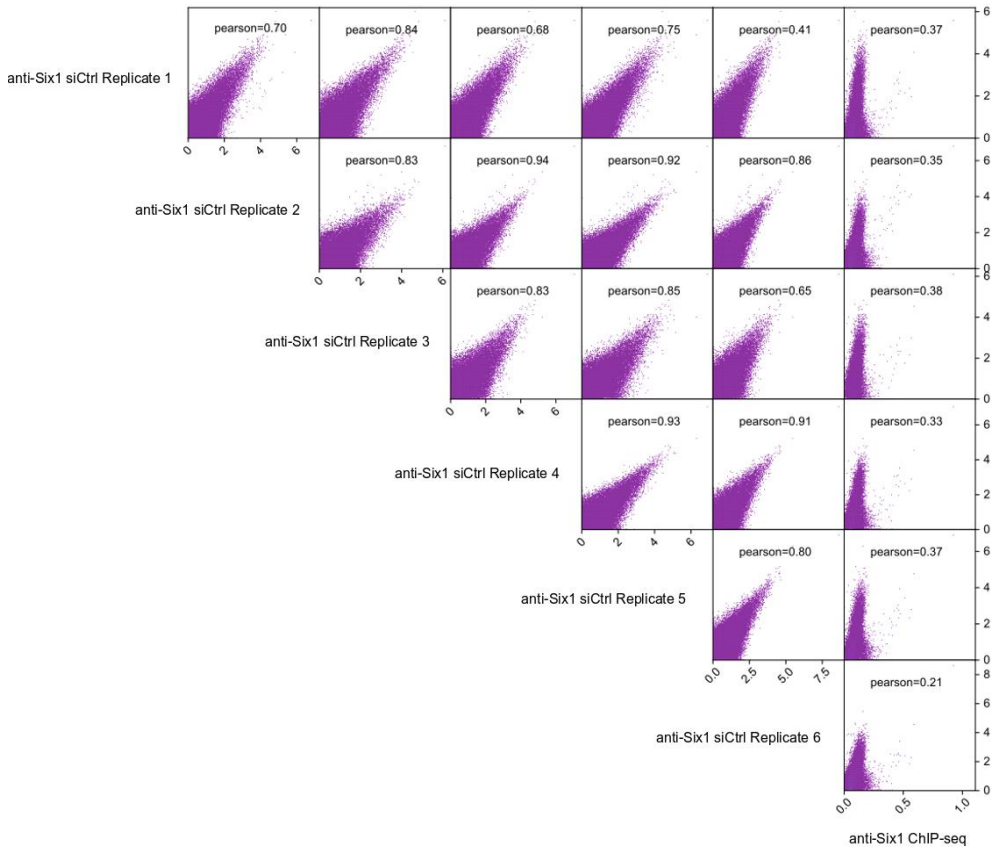

Figure 9 Computation of sample correlations between six replicates of Six1 control treatment CUT&Tag C2C12 cell samples and Six1 ChIP-seq data obtained from primary myoblasts over the entire genome using the plotCorrelation tool. CUT&Tag and ChIP-seq data was scaled and normalized by 10 counts per million (CPM) on the mm9 genome. Each dot on the figure is representative of the number of fragments between two samples in a single genome region. Correlation coefficients were calculated using the Pearson method.

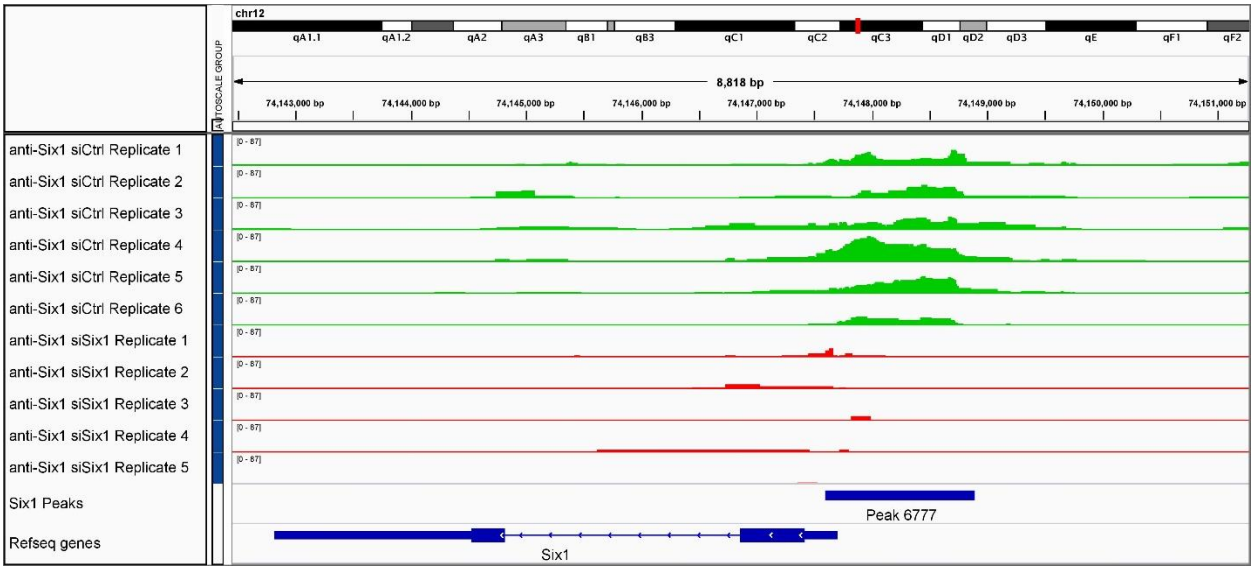

Figure 10 IGV screenshot at Six1 with bigwig files representing read density distribution in identically scaled tracks for all Six1 control and knock-down samples and a track representing Six1 binding sites.

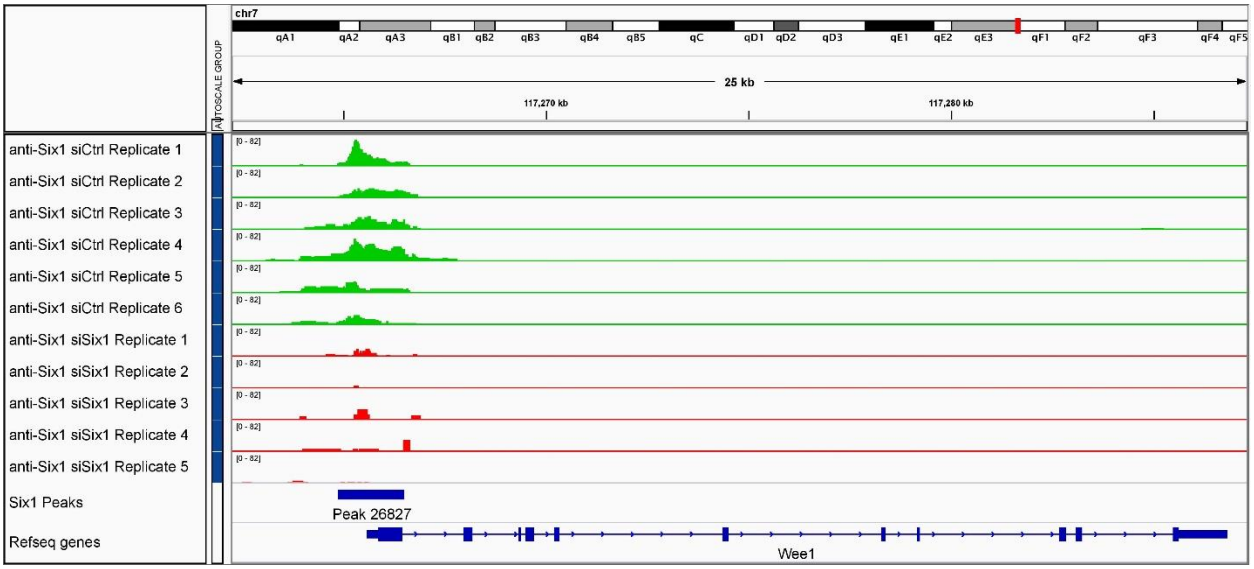

Figure 11 IGV screenshot at Wee1 with bigwig files representing read density distribution in identically scaled tracks for all Six1 control and knock-down samples and a track representing Six1 binding sites.

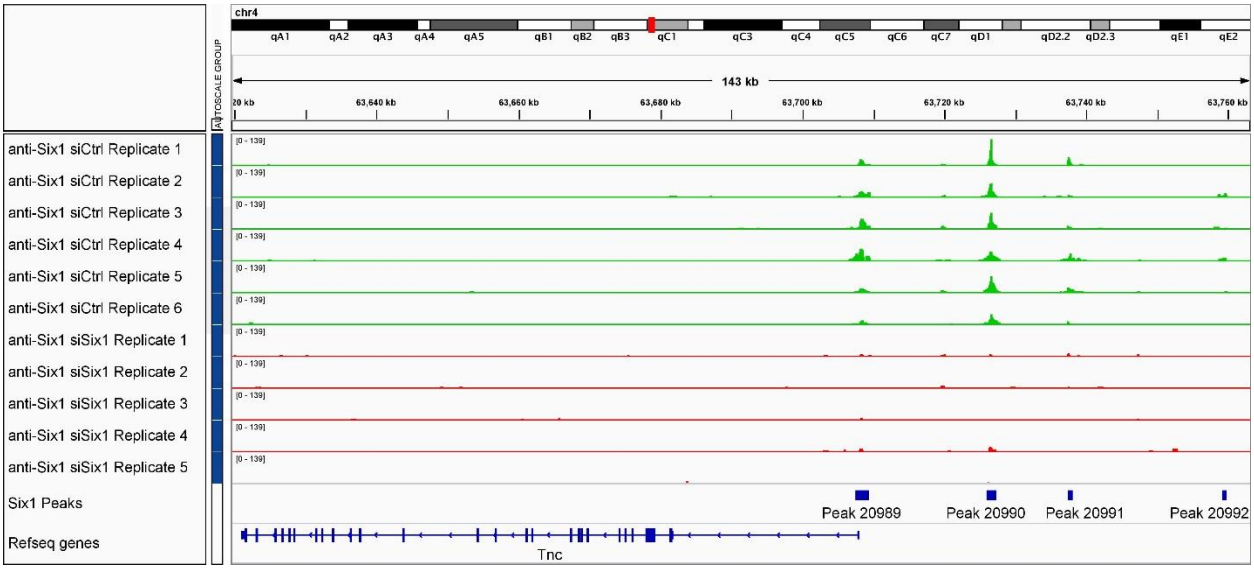

Figure 12 IGV screenshot at Tnc with bigwig files representing read density distribution in identically scaled tracks for all Six1 control and knock-down samples and a track representing Six1 binding sites.

To quantitate the CUT&Tag signal, a strategy related to RNA-seq was employed where binding site “peaks” were considered as genes and CUT&Tag sequence tag abundance was treated as RNA-seq tags. CUT&Tag signal at Six1 binding sites were subsequently normalized using TMM normalization. Unwanted variation was removed using residuals with the Bioconductor package RUVSeq (Figure 13) (Risso et al., 2014)

To quantify the effect of Six1 knock-down on CUT&Tag signal at Six1 binding sites, differential analysis was performed using edgeR (Robinson et al., 2010). These results illustrate the expected behavior for most peaks with the Six1 CUT&Tag signal decreasing markedly following Six1 knock-down (Figure 14-Figure 15).

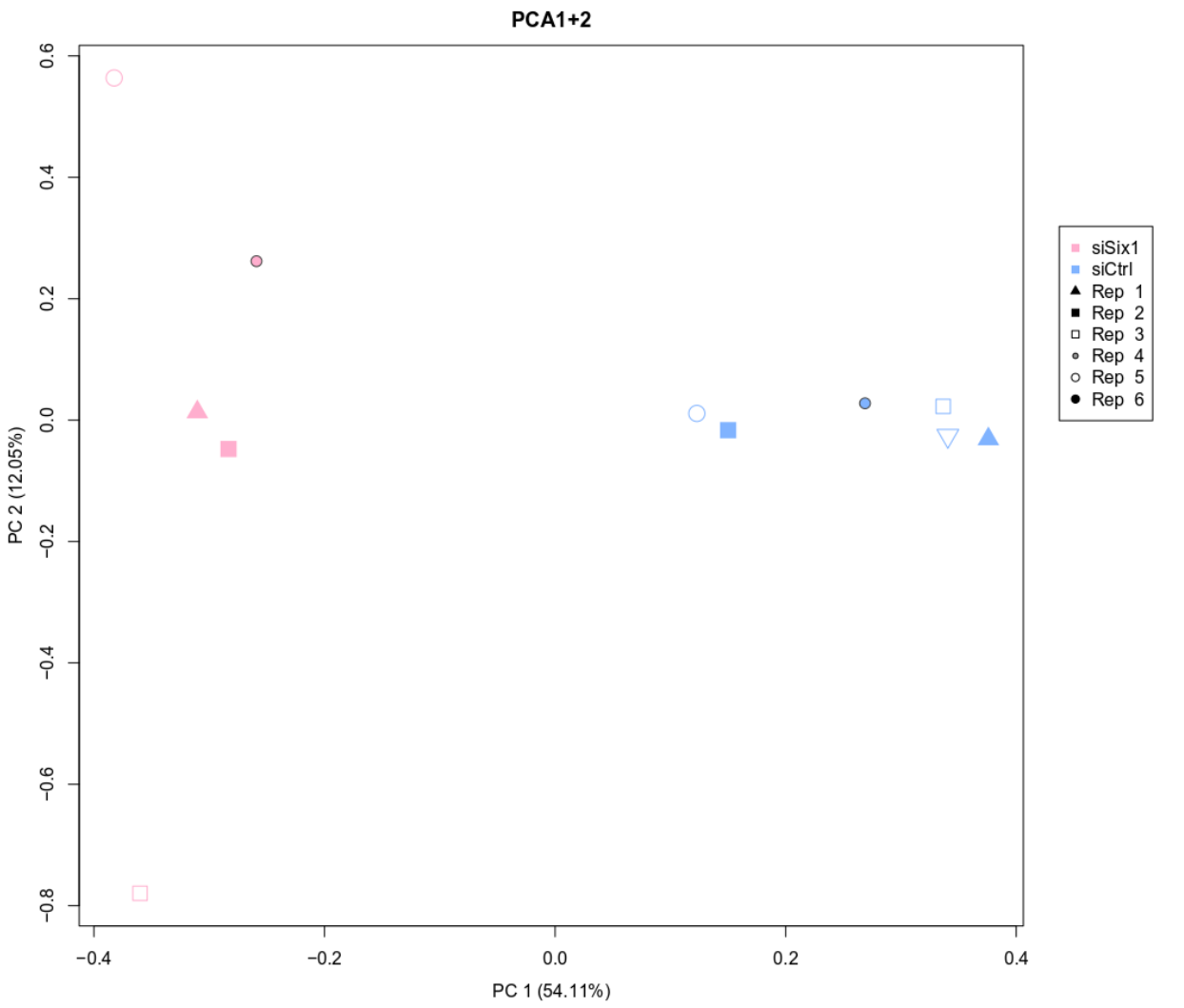

Figure 13 PCA of anti-Six1 CUT&Tag samples showing the variation in signal between control and Six1 knock-down treatment conditions following TMM normalization and removal of unwanted variation using RUVseq. Symbols correspond to the six replicates for each condition excluding one low quality knock-down sample omitted from analysis. The first two principal axes explained 66.16 % of the variance

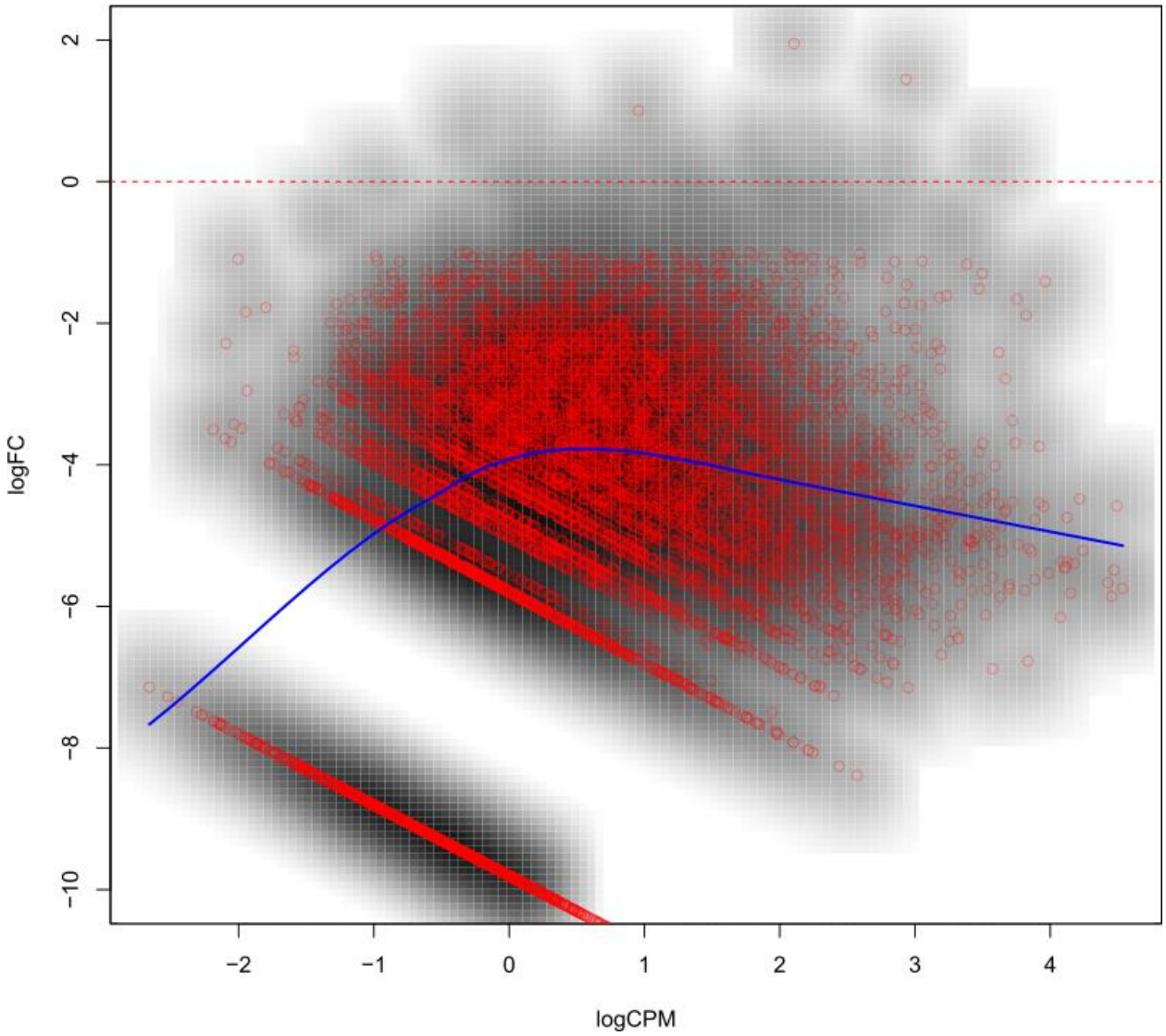

Figure 14 MA illustrating log-scaled difference between the average Six1 knock-down and control signal at Six1 CUT&Tag peaks. Read counts were divided by the number of thousands of Drosophila spike-in reads, library-wise.

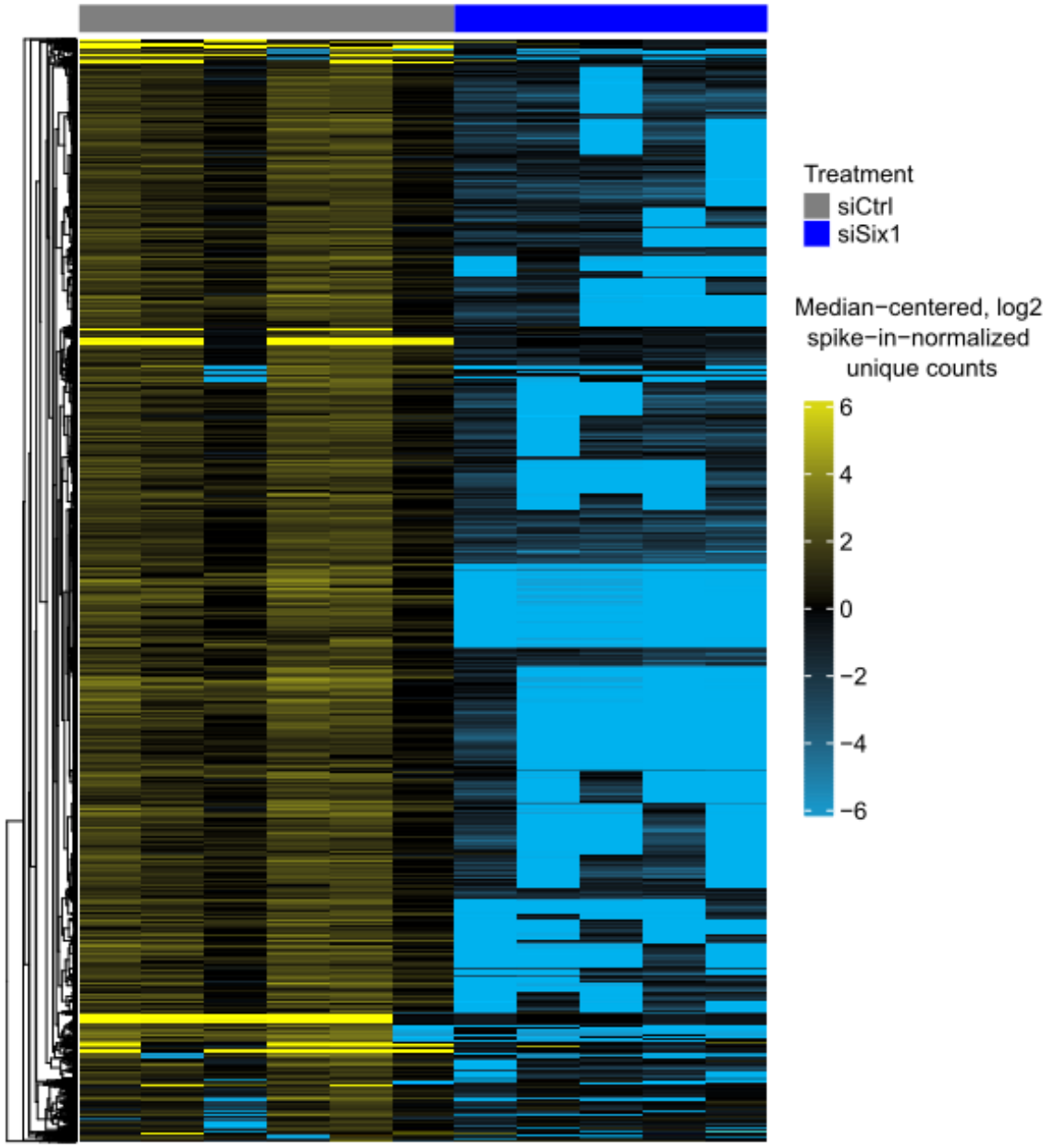

Figure 15 Heatmap illustrating Six1 signal at Six1 binding sites between siCtrl and siSix1 treatment samples. Samples were normalized by the number of thousands of drosophila spike-in reads present in each sample sequencing library. The Six1 signal colour scale indicates log-scaled CUT&Tag signal after median-centering. Samples were plotted using hierarchical clustering.

3.3 Identification of genomic loci which decrease or increase in H3K122ac, H3K27ac and p300 signal following Six1 knock-down

To study the effect of Six1 on the epigenetic landscape of myoblasts, CUT&Tag was performed using antibodies against H3K122ac, H3K27ac and p300 following Six1 knock-down. One control (Replicate 1) and one Six1 knock-down (Replicate 3) anti-p300 sample were identified as outliers based on PCA and excluded from further analysis (Figure 16).

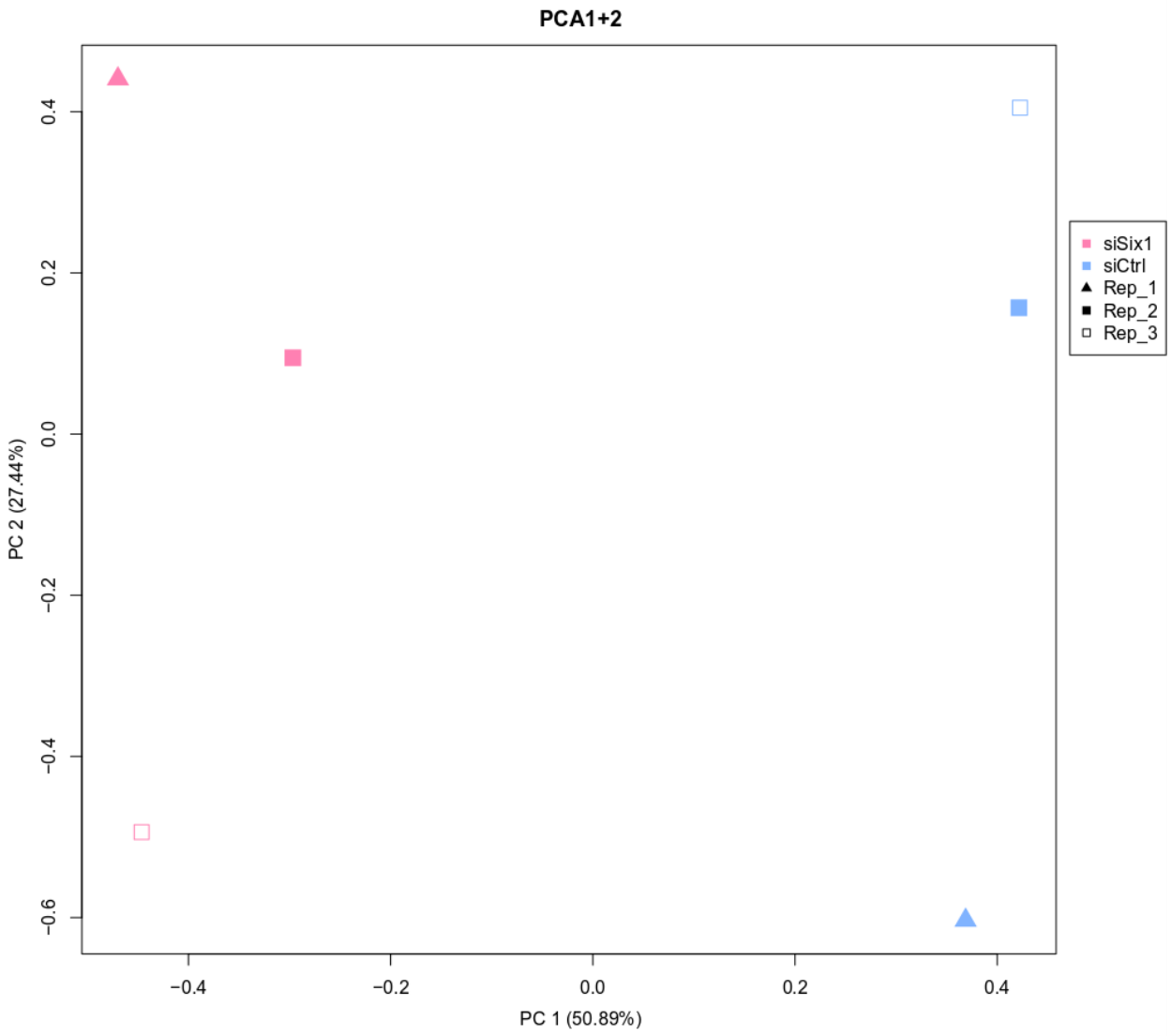

Figure 16 PCA of anti-p300 CUT&Tag samples showing the variation in signal between control and Six1 knock-down treatment conditions. Symbols correspond to the three replicates for each condition. One control and one knock-down sample was omitted from downstream analysis due to poor clustering. The first two principal axes explained 78.33 % of the variance.

CUT&Tag-seq signal was normalized using TMM normalization and unwanted variation was removed by residuals with RUVSeq. Differential binding of p300, H3K122ac and H3K27ac at previously identified Six1 binding sites following Six1 knock-down was evaluated using edgeR. K-means clustering (k=3) of Six1 binding sites according to differential p300 signal following Six1 knock-down was used to identify loci where p300

is potentially recruited by Six1 (Figure 17-Figure 18). Both Cluster 1 (n=982) and Cluster 2 (n=2436) contain Six1 binding sites which decrease in p300 signal following Six1 knockdown whereas Cluster 3 (n=6178) contains peaks with no significant change to p300 signal. These results suggest that Six1 is responsible for the recruitment of p300 to binding sites within the first two clusters while p300 binding in regions within Cluster 3 are unaffected by the presence of Six1.

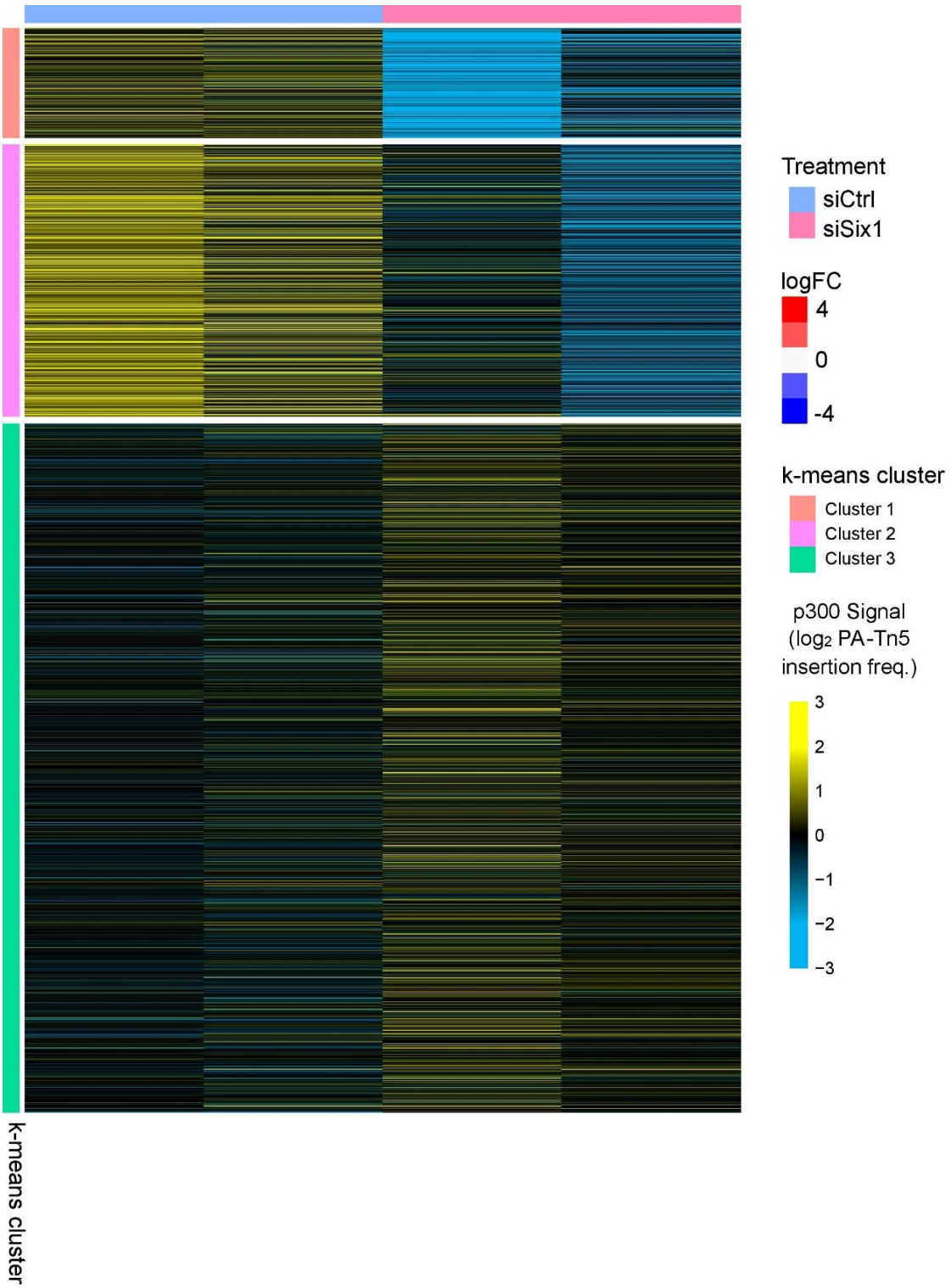

Figure 17 Heatmap illustrating p300 signal at Six1 binding sites between siCtrl and siSix1 treatment samples normalized with TMM RUVr k=2. K-means clustering was applied to the data with k set to 3. C.1 n= 982, C.2 n=2436, C.3 n=6178. The p300 signal colour scale indicates log-scaled CUT&Tag signal after median-centering.

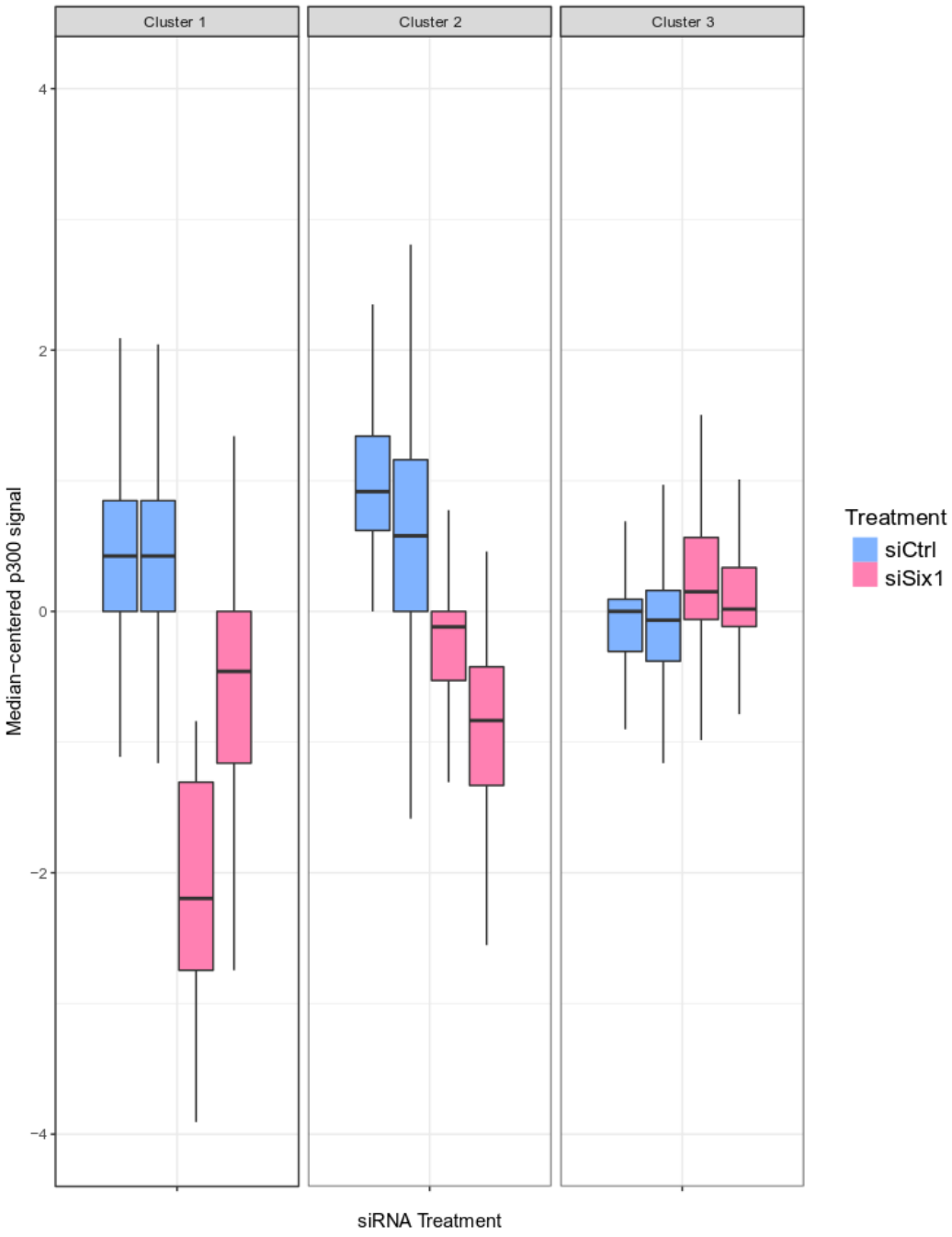

Figure 18 Boxplot illustrating p300 signal in Six1 knockdown and control conditions grouped according to the p300 clustering solution.

When anti-Six1 CUT&Tag signal established Six1 binding sites were grouped according to the p300 clustering solution (Figure 19-Figure 20), the effect of Six1 knock-down appears most prominent in Cluster 1 and Cluster 2, coinciding with loci which decrease in p300 signal following Six1 knock-down.

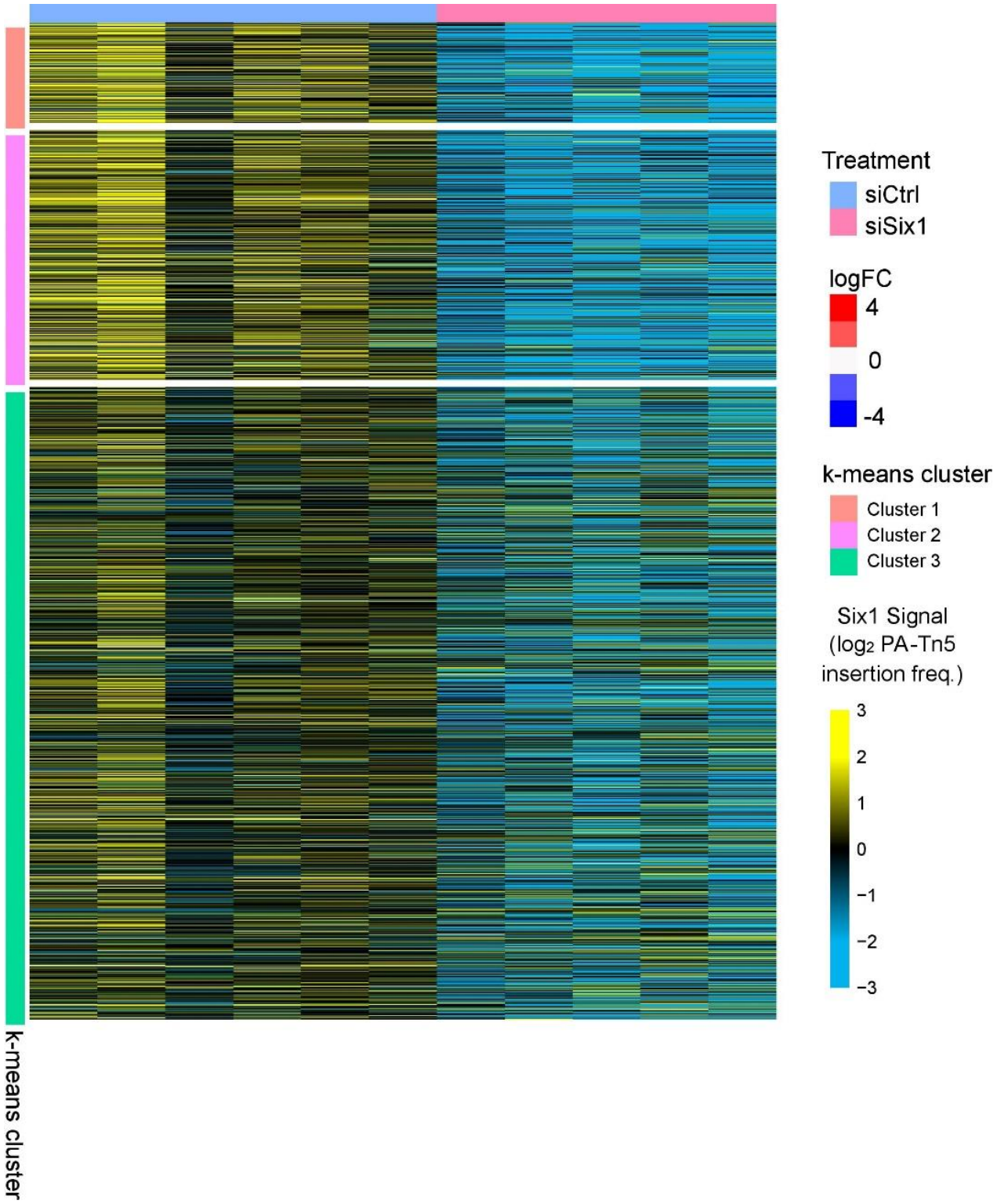

Figure 19 Heatmap illustrating anti-Six1 CUT&Tag signal between siCtrl and siSix1 treatment samples normalized with TMM RUVr k=1. The p300 clustering solution was used to cluster Six1 peaks. C.1 n= 982, C.2 n=2436, C.3 n=6178. The Six1 signal colour scale indicates log-scaled CUT&Tag signal after median-centering.

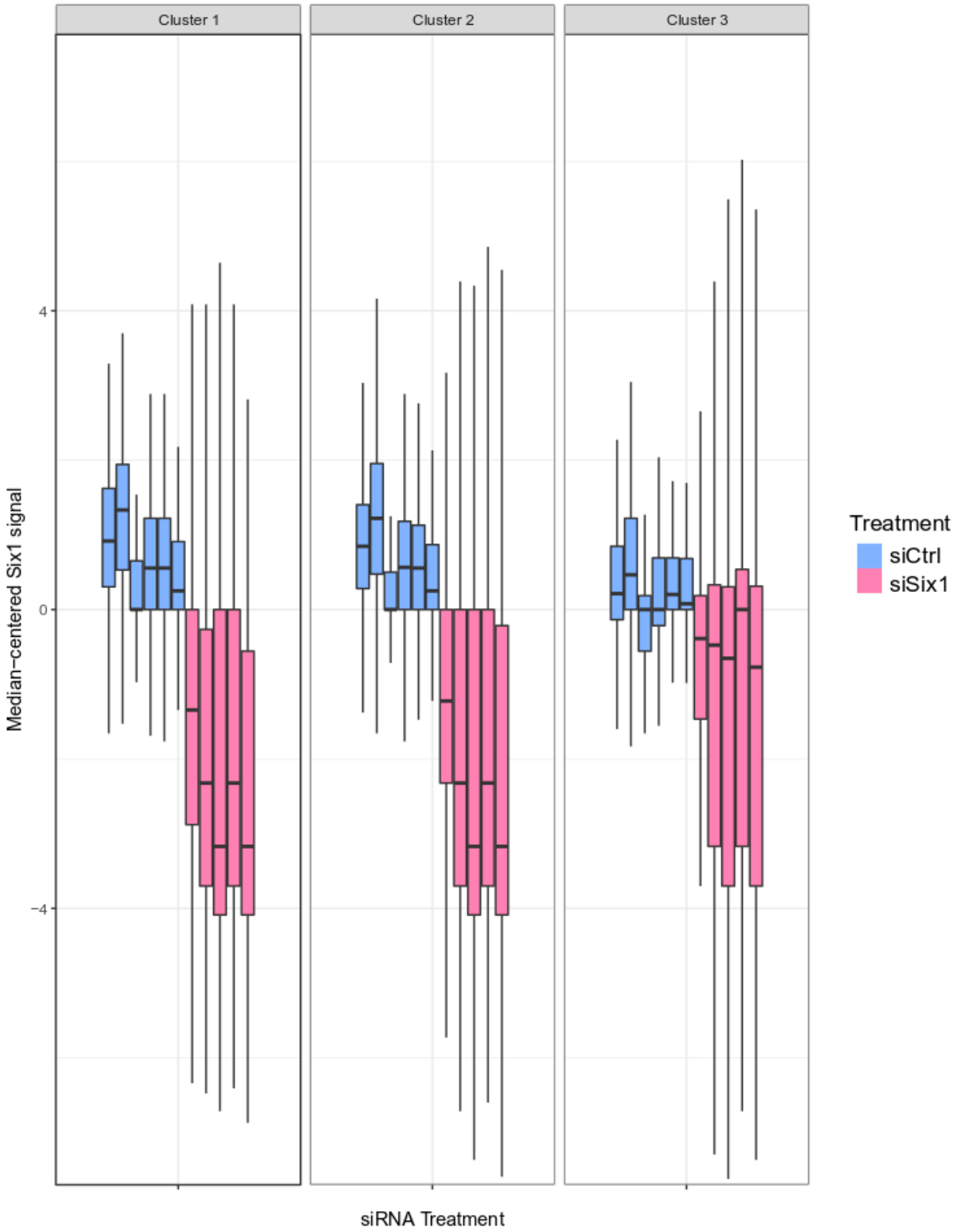

Figure 20 Boxplot illustrating Six1 signal in Six1 knockdown and control conditions grouped according to the p300 clustering solution.

Since p300 is capable of acetylating both H3K27 and H3K122 (Tie et al., 2009; Tropberger et al., 2013), the p300 k-means clustering solution was also used to cluster the CUT&Tag signal of the two acetylation marks at Six1 binding sites (Figure 21-Figure 22). It is expected that following Six1 knock-down and the corresponding reduced presence of p300, HDACs which are globally more abundant will quickly deacetylate lysine's resulting in lower signal of acetylation marks. The effect of Six1 knock-down on the acetylation signals are more subtle, potentially a result of antagonistic histone methyltransferase activity (Pasini et al., 2010). If a methyltransferase methylates H3K27 this should also translate to lower H3K27ac signal. Another possibility is that other HATs recruited in a Six1-independent manner compensate for the reduction in p300. Acetylation marks may also persist despite a reduced presence of p300 due to absence of HDAC activity. The reduction in histone acetylation signal at Six1 binding sites which also decrease in p300 signal following Six1 knock-down supports the involvement of Six1 recruitment of p300 in regulating the epigenetic landscape of myoblasts.

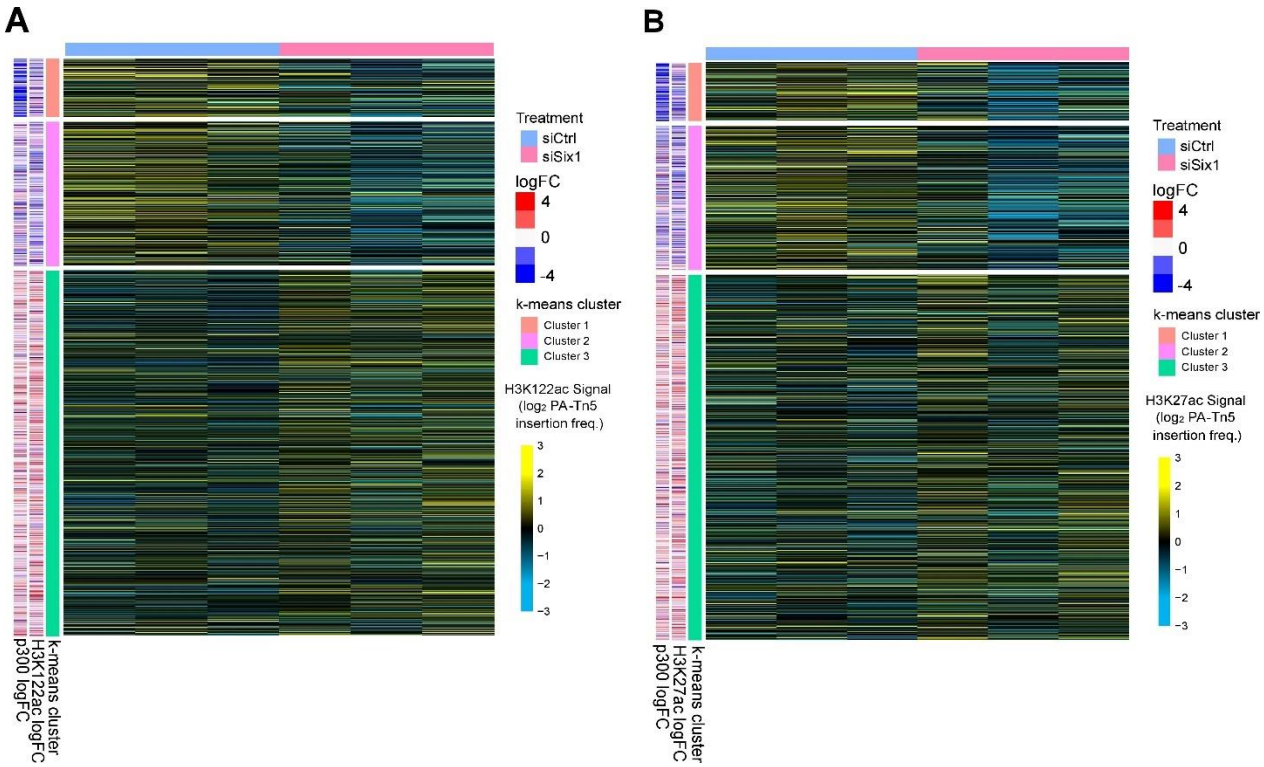

Figure 21 Panel A: Heatmap illustrating H3K122ac signal at Six1 binding sites between siCtrl and siSix1 treatment samples normalized with TMM RUVr k=2. The p300 clustering solution was used to cluster H3K122ac peaks. C.1 n= 982, C.2 n=2436, C.3 n=6178. The H3K122ac signal colour scale indicates log-scaled CUT&Tag signal after median-centering. Panel B: Heatmap illustrating H3K27ac signal at Six1 binding sites between siCtrl and siSix1 treatment samples normalized with TMM RUVr k=1. The p300 clustering solution was used to cluster H3K27ac peaks. C.1 n= 982, C.2 n=2436, C.3 n=6178. The H3K27ac signal colour scale indicates log-scaled CUT&Tag signal after median-centering.

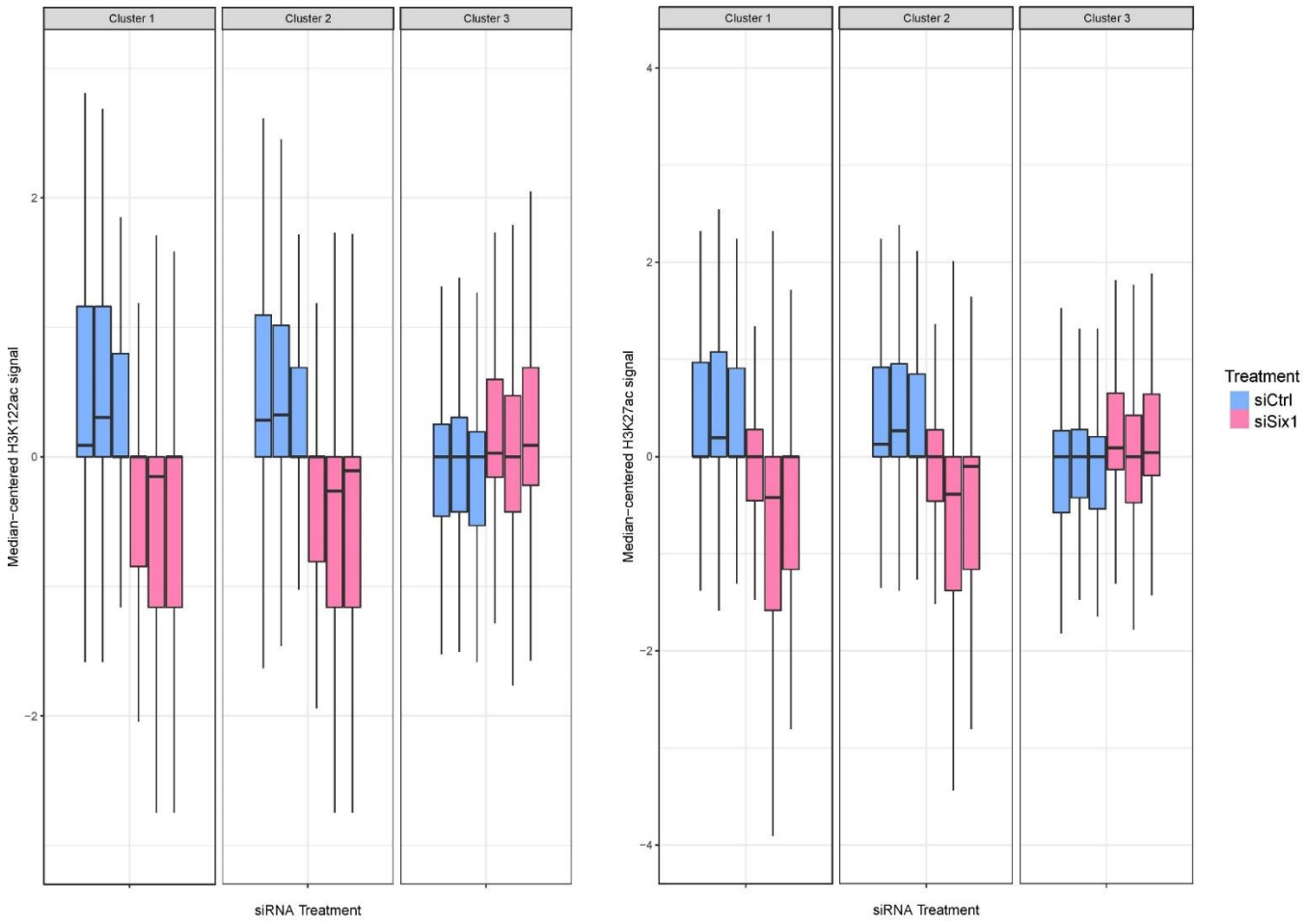

Figure 22 Panel A: Boxplot illustrating H3K122ac signal in Six1 knockdown and control conditions grouped according to the p300 clustering solution. Panel B: Boxplot illustrating H3K27ac signal in Six1 knockdown and control conditions grouped according to the p300 clustering solution.

3.4 Identification of dynamically accessible genomic loci following Six1 knock-down

Transcriptionally active, euchromatin is generally enriched with lysine acetylation marks which disrupt DNA-histone interactions and increase the accessibility of DNA at particular genomic loci (Hebbes et al., 1988; Klemm et al., 2019). To determine the effect of Six1 on DNA accessibility dynamics, ATAC-seq was previously performed using two separate siRNA's targeting Six1 (siSix1.1, siSix1.2).

To evaluate differences in accessibility in conjunction with regions where Six1 knock-down at Six1 binding sites resulted in a decrease of p300, H3K122ac and H3K27ac signal, ATAC-seq signal was also identified at Six1 binding sites. ATAC-seq signal was normalized using TMM normalization and unwanted variation was removed using residuals with RUVSeq. ATAC-seq signal at Six1 binding sites were subsequently clustered using the p300 k-means clustering solution (Figure 23-Figure 24).

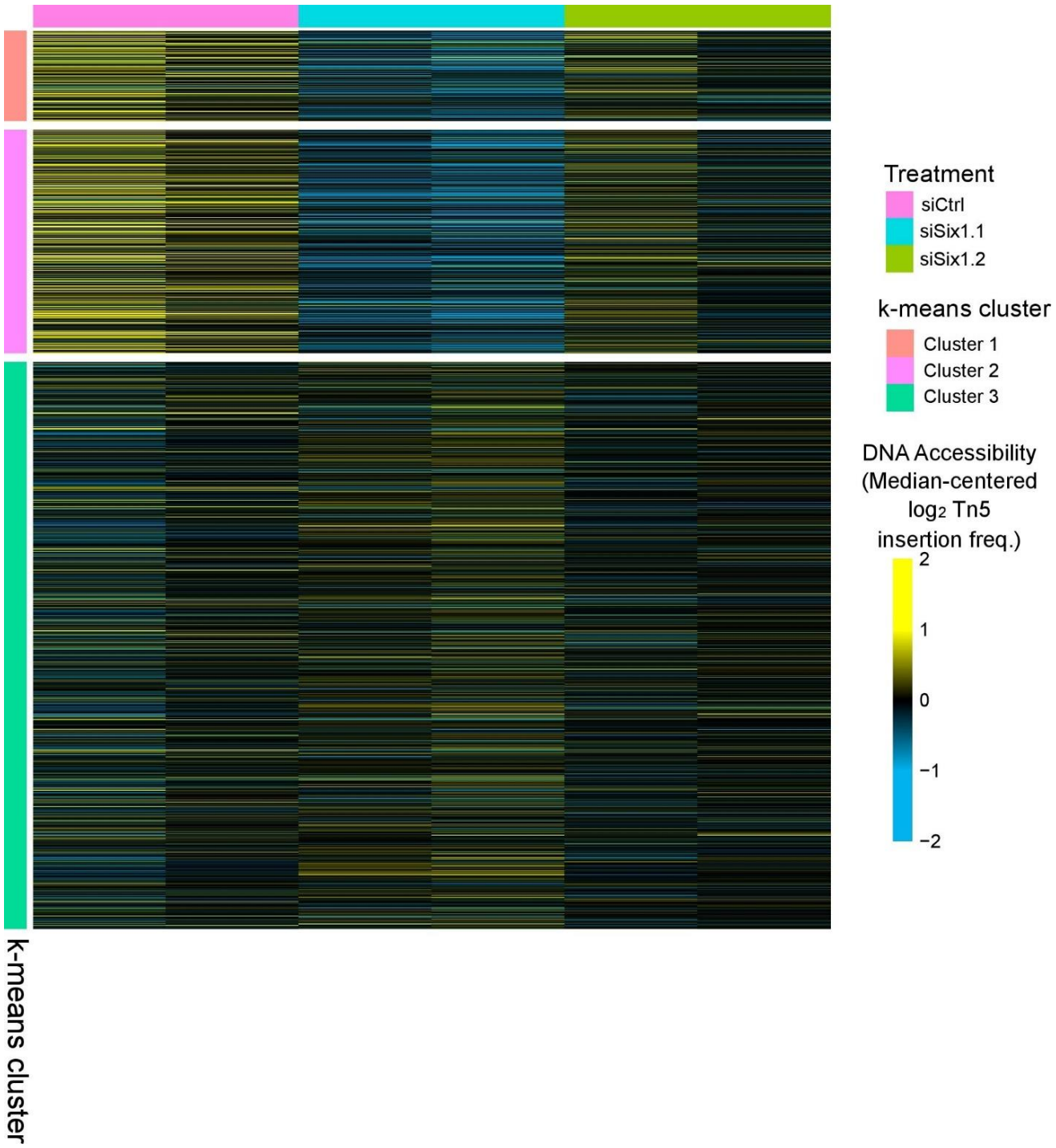

Figure 23 Heatmap illustrating ATAC-seq DNA accessibility dynamics at Six1 binding sites between siCtrl and siSix1.1/siSix1.2 treatment samples normalized with TMM RUVr k=2. The p300 clustering solution was used to cluster ATAC-seq peaks. C.1 n= 982, C.2 n=2436, C.3 n=6178. DNA accessibility colour scale indicates DNA accessibility after median-centering.

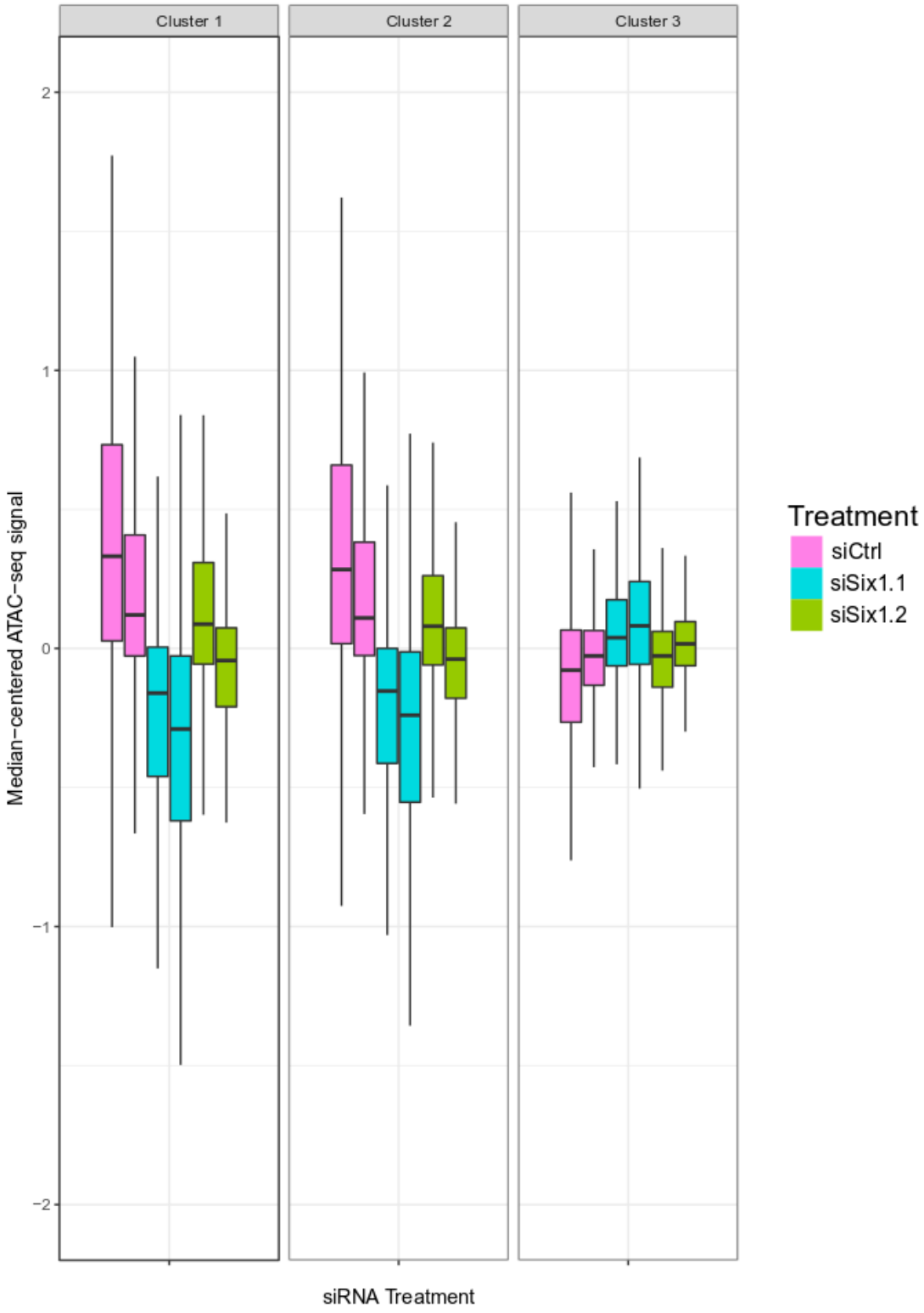

Figure 24 Boxplot illustrating the log fold-change of the mean ATAC-seq signal between siCtrl and siSix1 treatment conditions.

Cluster's 1 and 2 illustrate a decrease in accessibility while Cluster 3 illustrates a modest global increase in accessibility with Six1 knock-down. The effects of Six1 knock-down on accessibility are more pronounced with siSix1.1 treatment as opposed to siSix1.2. Treatment by siSix1.1 alone may not be sufficient in knocking down Six1 to generate an impact on DNA accessibility. The Six1 binding sites which decrease in p300, H3K122ac and H3K27ac signal coincide with regions which decrease in accessibility following Six1 knock-down. Previous reports using shRNA knock-down of p300-related protein CBP, demonstrated minimal effect on H3K27ac enrichment and DNA accessibility (Martire et al., 2020). Prior research has indicated that p300 but not CBP inhibition results in reduced expression of muscle determination genes and that recruitment of p300 alone is sufficient in inducing enhancer acetylation and promoter proximal transcription of MyoD (Hilton et al., 2015). Here we show that p300 inhibition coincides with decreased DNA accessibility, providing support for the increased impact of p300 over CBP in transcriptional regulation. The result of these analysis supports the hypothesis that Six1 regulates accessibility in myoblasts by recruiting the HAT p300, to acetylate certain Six1 binding sites which is correlated with greater DNA accessibility.

3.5 Identification of dynamically accessible genomic loci following p300 inhibition

Numerous transcription factors, chromatin remodelers and histone modifying enzymes are known to be involved in regulation of DNA accessibility. Having established the capability of Six1 in altering DNA accessibility in myoblasts, we next wanted to determine whether accessibility dynamics regulated by Six1 are also dependent on p300 recruitment.

ATAC-seq was initially performed for a 24-hour treatment duration of three different doses (0.3 μM, 1.0 μM and 3.0 μM) of the p300 inhibitor, A-485. In a recent publication by Narita et al., it was found that the recruitment of BRD4 through p300/CBP catalyzed acetylation, facilitates the release of promoter-proximal paused RNAPII and the rapid activation of enhancer mediated transcription. In this work, three biological replicates of ATAC-seq were performed by treating mESCs with a thirty and sixty-minute duration of 10 μM A-485. ATAC-seq was subsequently repeated using shorter treatment durations of 3 and 6 hours of 1.0 μM A-485 treatment to rule out the possibility of secondary effects.

ATAC-seq signal was identified at significant Six1 peaks and signal values were normalized using TMM normalization. Unwanted variation was removed using residuals with RUVSeq. One 6-hour duration, 1.0 μM replicate sample was determined to be an outlier and excluded from analysis based on PCA. To evaluate changes in accessibility following p300 inhibition alongside regions where Six1 knock-down at Six1 binding sites resulted in a decrease in accessibility, as well as p300, H3K122ac and H3K27ac signal, ATAC-seq signal was identified at Six1 binding sites and clustered according to the p300 k-means clustering solution (Figure 25-Figure 26).

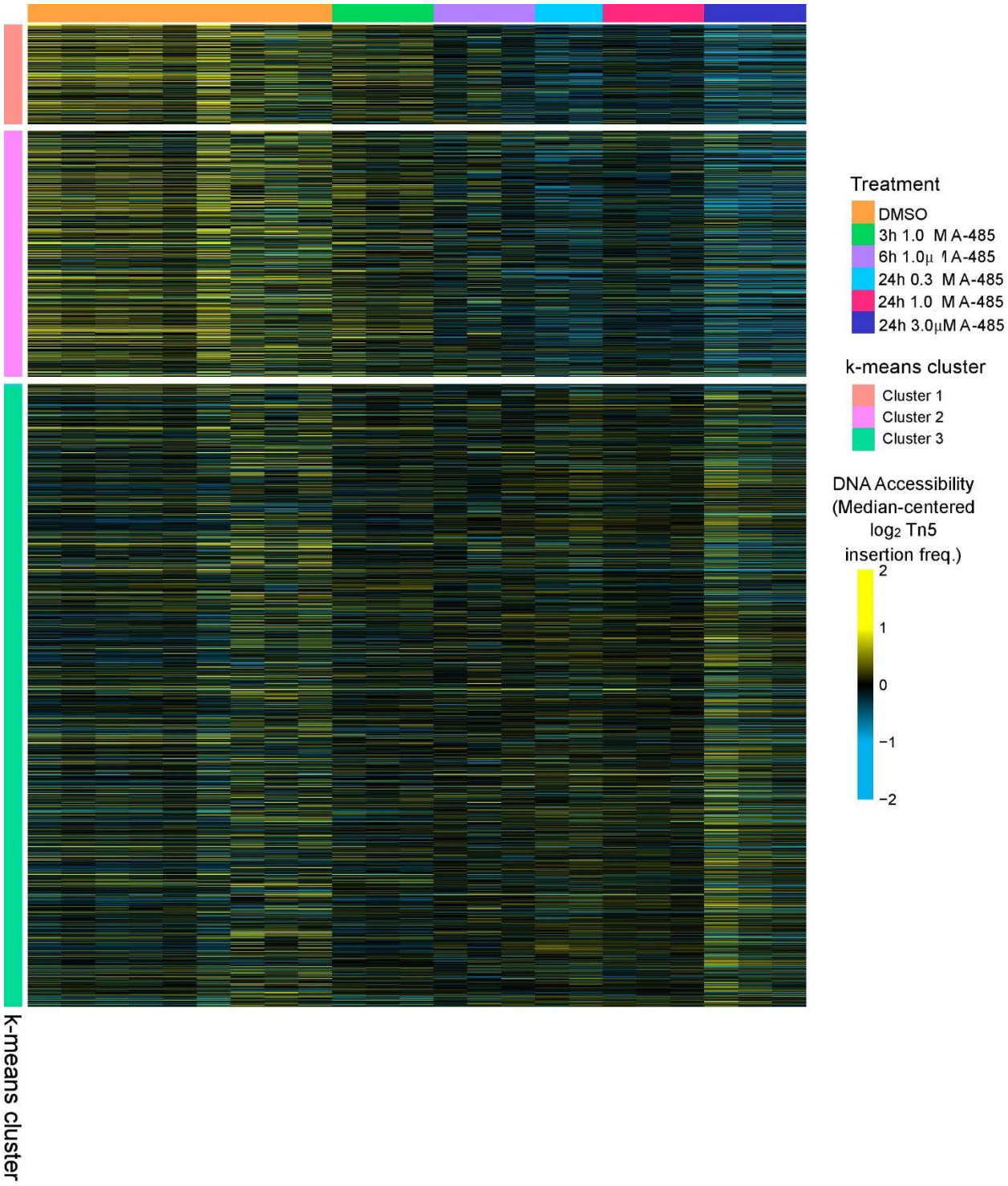

Figure 25 Heatmap illustrating ATAC-seq DNA accessibility dynamics at Six1 binding sites between DMSO and A-485 treatment samples using various treatment durations (3-hours, 6-hours, 24-hours) and A-485 doses (0.3 μM, 1.0 μM, 3.0 μM). ATAC-seq signal was normalized with TMM RUVr k=1. The p300 clustering solution was used to cluster ATAC-seq peaks. C.1 n= 982, C.2 n=2436, C.3 n=6178. DNA accessibility colour scale indicates DNA accessibility after median-centering.

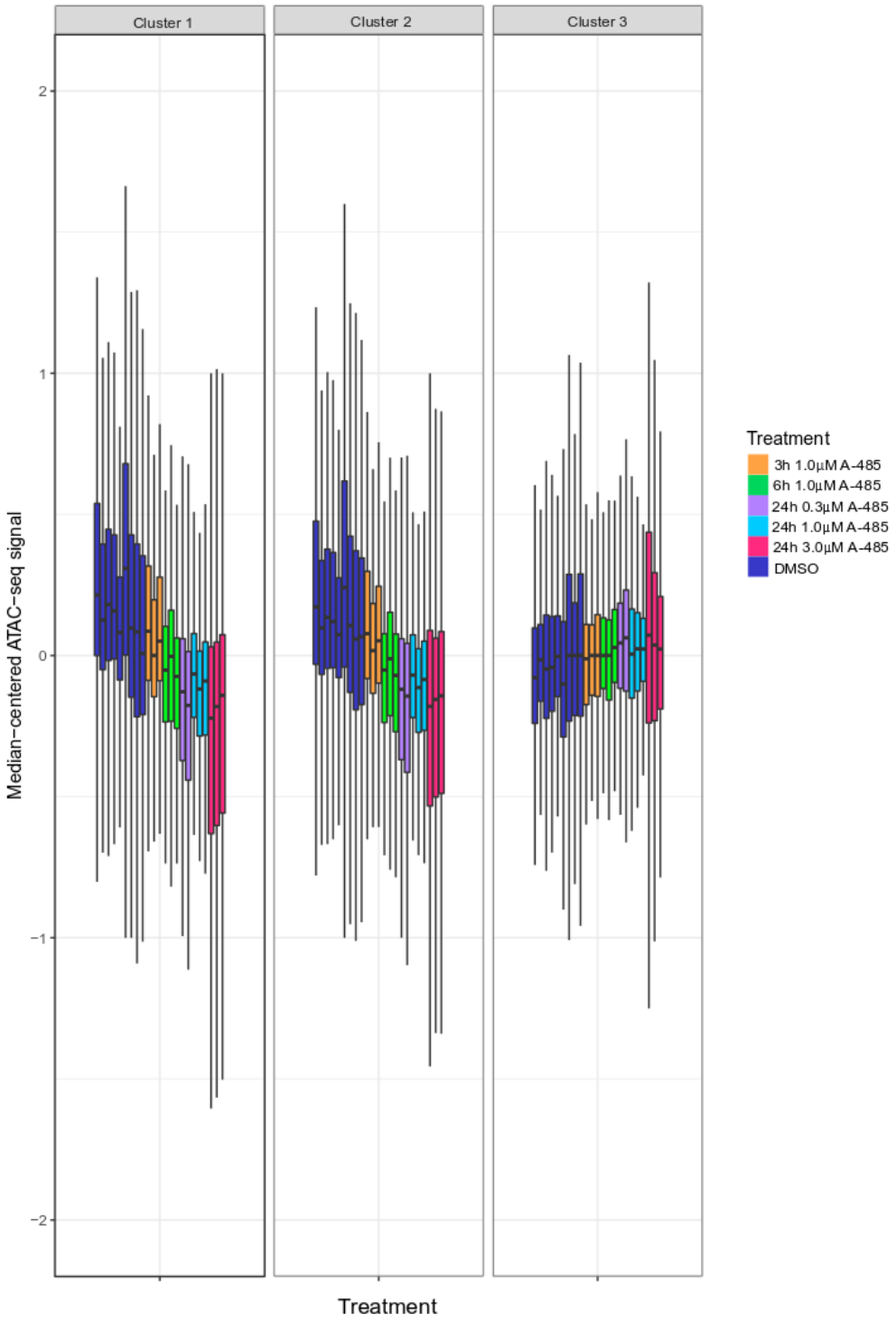

Figure 26 Boxplot illustrating the log fold-change of the mean ATAC-seq signal between DMSO and A-485 treatment conditions.

Analogous to ATAC-seq samples treated with Six1 targeting siRNA, Six1 binding sites in Cluster's 1 and 2 were also found to decrease in accessibility following p300 inhibition. While the most striking effect of p300 inhibition on accessibility is demonstrated by a 24-hour treatment duration of 3.0 μM A-485, effects on accessibility are apparent with just 24-hours of 0.3 μM A-485 treatment or after 3-hours of 1.0 μM A-485 treatment. Analysis of acetylation levels in the NIH 3T3 fibroblast cell line demonstrated that histone deacetylase activity is largely responsible for high turnover of acetylation (McShane et al., 2016). The rapid reduction in acetylation following Six1 knock-down may be resulting from reduced presence of p300 HAT activity alongside activity by lysine deacetylases.

3.6 Effect of Six1 knock-down on gene expression where p300 inhibition or Six1 knock-down impacts accessibility and epigenetic landscape

To identify regions where Six1 knock-down affects gene expression, previous and newly generated RNA-seq data from cells treated with Six1 targeting siRNA was analyzed. C2C12 cells were treated with two types of small interfering RNA targeting Six1, siSix1.1, siSix1.2 or a combination of the two.

Gene expression was evaluated at Six1 binding sites and loci were annotated to genes using the shortest distance with a maximum of 60 kb around the TSS. A total of 4234 loci were annotated to genes. Genes were limited to those with greater than 30 counts in at least 5 samples. Genes were clustered according to the p300 clustering solution to evaluate changes in their mRNA abundance at loci where Six1 recruitment of p300 had been found to regulate DNA accessibility and epigenetic landscape in myoblasts (Figure 27-Figure 28).

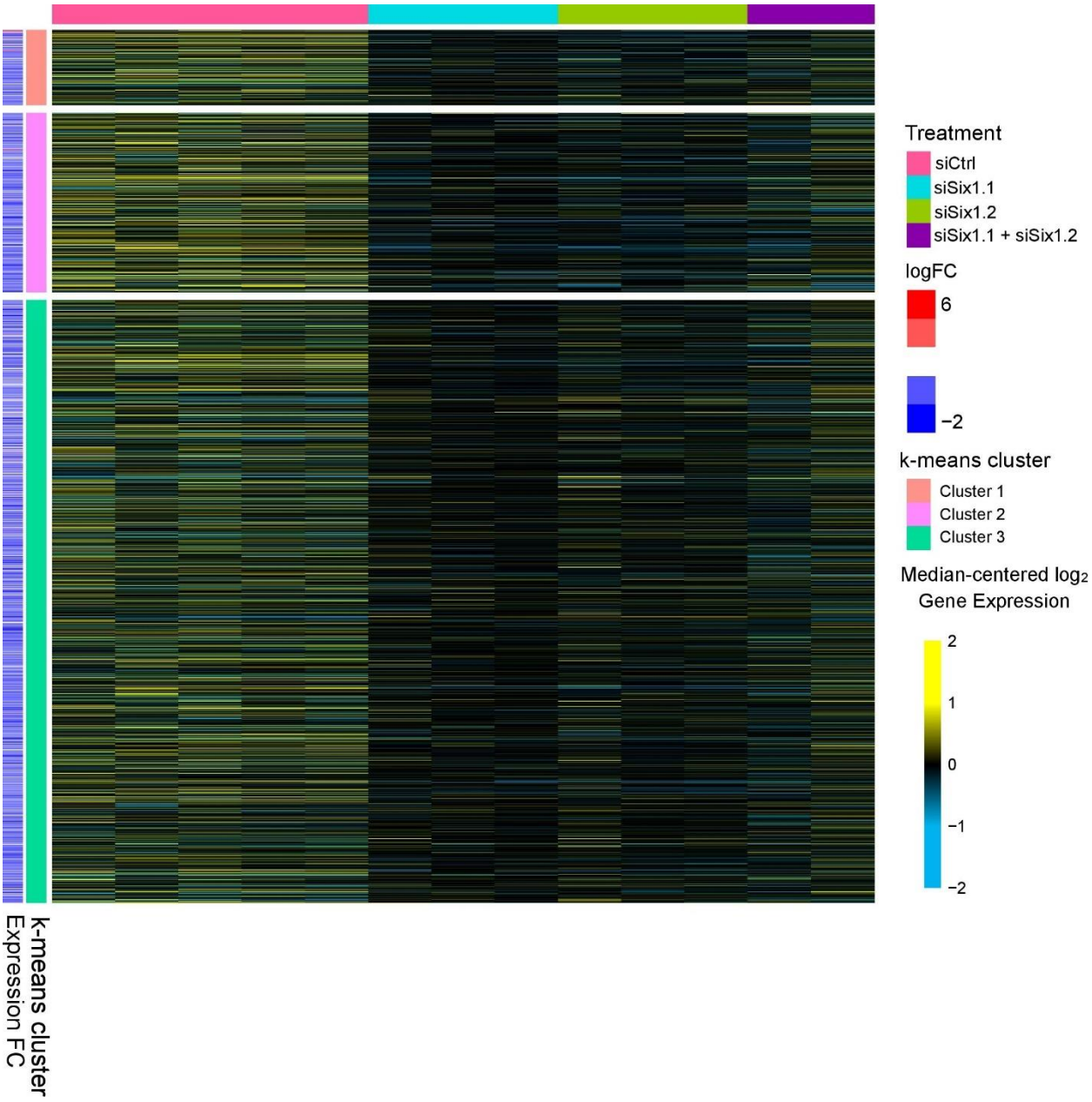

Figure 27 Heatmap illustrating RNA-seq expression data at Six1 binding sites between siCtrl and siSix1 treatment samples normalized with TMM RUVr k=2. Peaks were annotated to genes using the shortest distance with a maximum of 60kb around the TSS. Peaks were limited to those with greater than 30 counts in at least 5 samples. The p300 clustering solution was used to cluster RNA-seq peaks. C.1 n= 376, C.2 n=895, C.3 n=2963. The gene expression colour scale indicates expression after median-centering.

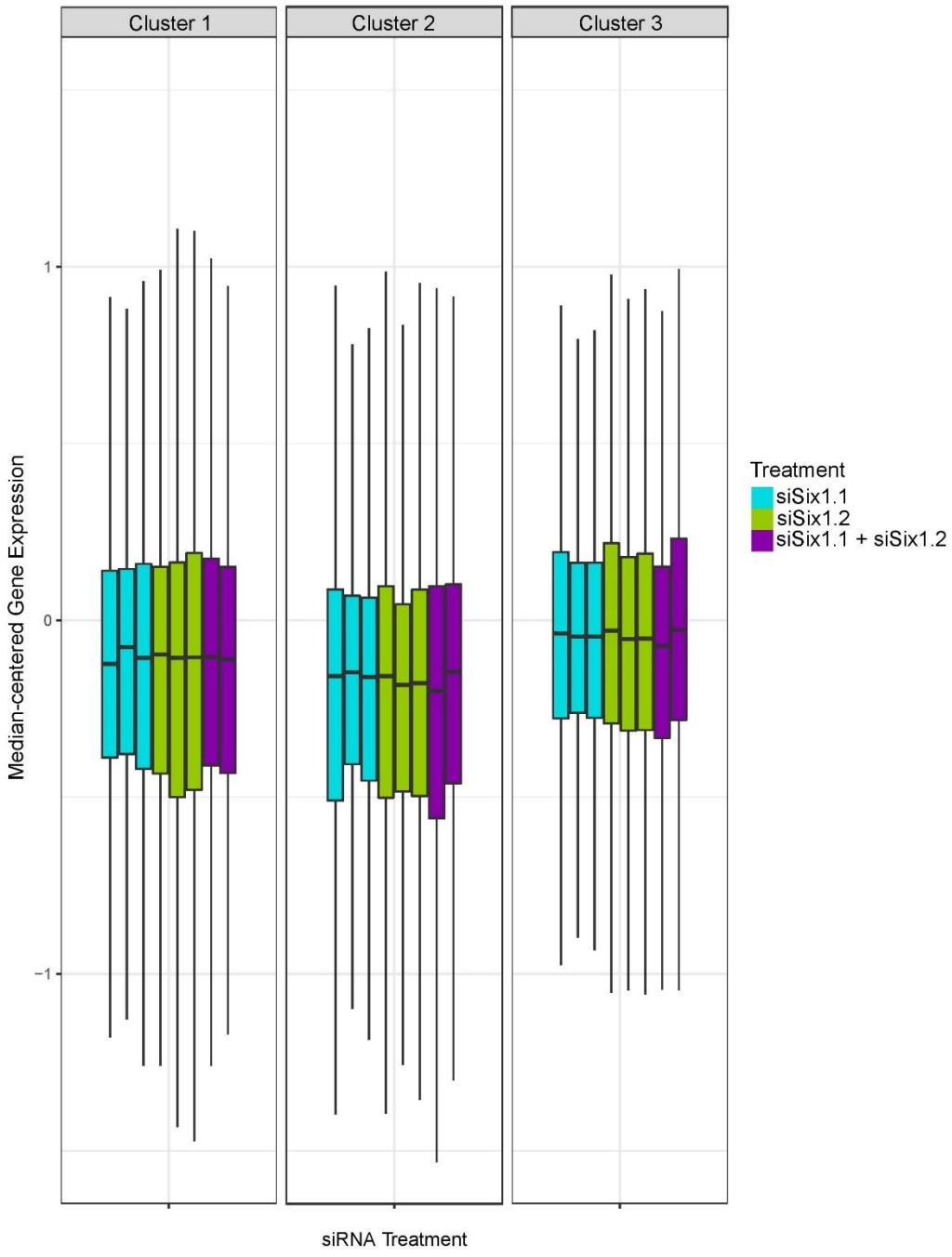

Figure 28 Boxplot illustrating the log fold-change of RNA-seq signal between siCtrl and siSix1 treatment conditions.

Cluster's 1 and 2 show a modest decrease in expression whereas Cluster 3 illustrates a slight increase (Figure 28). Numerous muscle-related genes are present in Cluster 1 (i.e. Eya1, Eya4, Myo9b, Ski, Actr2) and Cluster 2 (i.e. Actn3, Myof, Myom1, Myo1d,

Myo18a, Lama2, Sox5, Tnnt2, Myo1b). Overall, the gene expression data reveals a decrease in gene expression at loci where Six1 knock-down or p300 inhibition results in a decrease in accessibility as well as p300, H3K122ac and H3K27ac signal. The result of this analysis also supports a potential mode of action for Six1 in myoblast regulation wherein recruitment of p300 acetylates H3K122ac, which then destabilizes nucleosomes, rendering DNA more accessible thereby increasing gene expression. A previous report by Narita et al. suggests that p300 catalyzed acetylation promotes transcriptional initiation by allowing for pre-initiation complex assembly and recruitment of RNA Polymerase II. Our results provide support for a mechanism whereby Six1 recruitment of p300 is involved in transcriptional regulation.

3.7 GO Term Analysis of genes controlled by Six1 regulation of DNA accessibility and epigenetic landscape

To gain a functional understanding of the role of Six1 in myoblast regulation, GOterm analysis was performed on genes with TSS within each of the three p300 k-means clusters. GOterm analysis was conducted using Panther with the Overrepresentation Test using the whole mouse genome (Figure 29-Figure 30) (Mi et al., 2021). P-values

were calculated using the Binomial Test with FDR correction. REViGO was used to remove redundancy in the GO-term analysis (Supek et al., 2011).

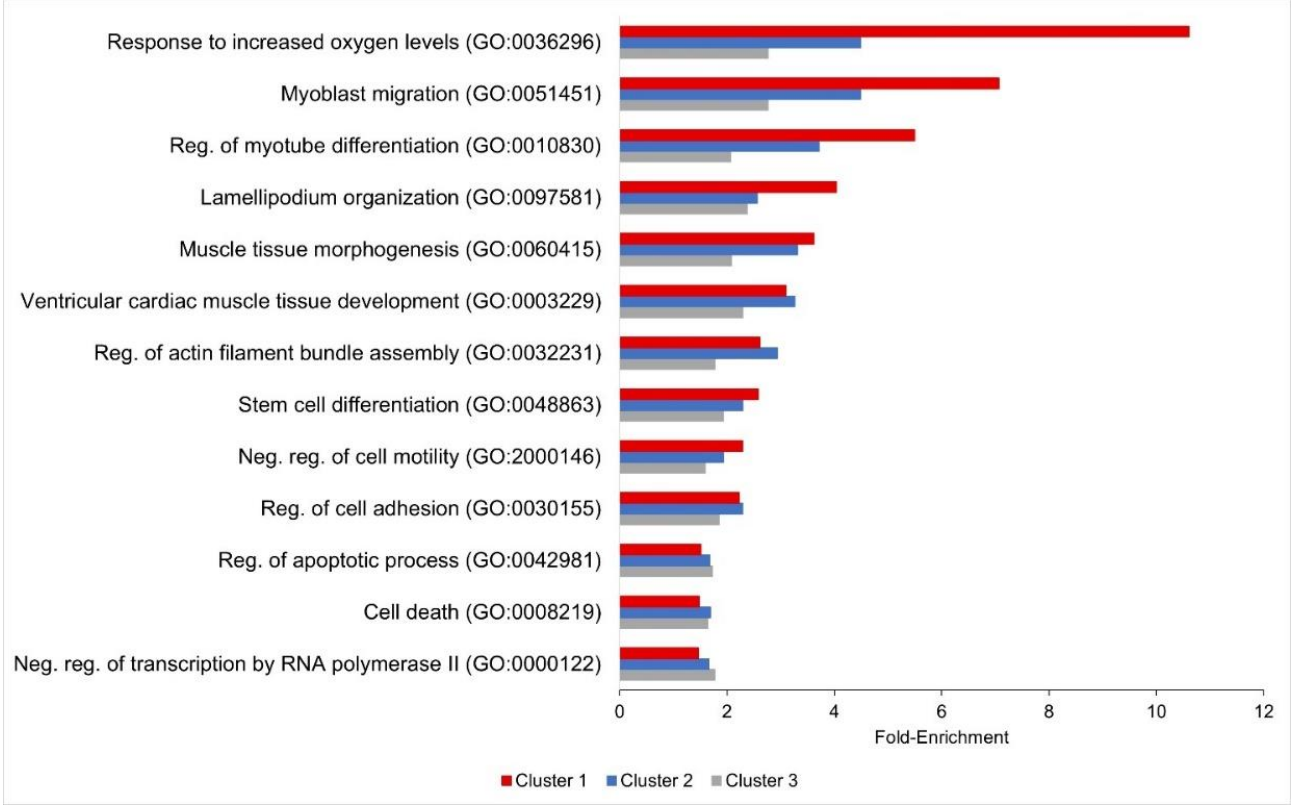

Figure 29 Gene ontology enrichment analysis performed using PantherDB GO Resources using genes annotated to Six1 peaks for each cluster from the p300 CUT&Tag k-means clustering (k=3) solution. All GO-terms pass the Benjamini-Hochberg False Discovery Rate (FDR) cut-off of <0.05. Gene ontology enrichment analysis performed using PantherDB GO Resources using genes annotated to Six1 peaks for each cluster from the p300 CUT&Tag k-means clustering (k=3) solution.

GO Terms	Cluster 1 p-value	Cluster 2 p-value	Cluster 3 p-value	Cluster 1 Genes Enriched / Total	Cluster 2 Genes Enriched / Total	Cluster 3 Genes Enriched / Total	Cluster 1 Genes / Cluster Length	Cluster 2 Genes / Cluster Length	Cluster 3 Genes / Cluster Length
Response to increased oxygen levels (GO:0036296)	0.00303	0.0304	0.0366	3/14	3/14	5/14	5/4731	3/1593	3/688
Myoblast migration (GO:0051451)	0.0331	0.0304	0.0366	2/14	3/14	5/14	5/4731	3/1593	2/688
Reg. of myotube differentiation (GO:0010830)	0.00241	0.00169	0.0158	5/45	8/45	12/45	12/4731	8/1593	5/688
Lamellipodium organization (GO:0097581)	0.0182	0.032	0.00223	4/49	6/49	15/49	15/4731	6/1593	4/688
Muscle tissue morphogenesis (GO:0060415)	0.00696	0.000216	0.00136	6/82	13/82	22/82	22/4731	13/1593	6/688
Ventricular cardiac muscle tissue development (GO:0003229)	0.0421	0.00124	0.000903	4/64	10/64	19/64	19/4731	10/1593	4/688
Reg. of actin filament bundle assembly (GO:0032231)	0.0297	0.00017	0.00468	6/114	16/114	26/114	26/4731	16/1593	6/688
Stem cell differentiation (GO:0048863)	0.00947	0.000892	0.0000591	9/173	19/173	43/173	43/4731	19/1593	9/688
Neg. reg. of cell motility (GO:2000146)	0.00401	0.000943	0.000383	14/303	28/303	62/303	62/4731	28/1593	14/688
Reg. of cell adhesion (GO:0030155)	0.0000121	4.08E-12	6.3E-15	35/778	85/778	185/778	185/4731	85/1593	35/688
Reg. of apoptotic process (GO:0042981)	0.00392	2.79E-08	3.21E-22	46/1511	121/1511	337/1511	337/4731	121/1593	46/688
Cell death (GO:0008219)	0.0304	0.000015	3.92E-11	27/906	73/906	192/906	192/4731	73/1593	27/688
Neg. reg. of transcription by RNA polymerase II (GO:0000122)	0.03	0.0000194	1.85E-15	28/946	75/946	216/946	216/4731	75/1593	28/688

Figure 30 Table including p-values and the count of total enriched genes annotated to Six1 peaks for each cluster from the p300 CUT&Tag k-means clustering (k=3) solution.

GO terms associated with Cluster 1 and Cluster 2 where Six1 knock-down or p300 inhibition results in a decrease in accessibility as well as p300, H3K122ac and H3K27ac

signal were found to be associated with genes related to muscle development. Six1 may selectively recruit p300 to enhance the transcription of a set of genes required for myogenesis. Interestingly, GO Terms which were more enriched in Cluster 3 as opposed to the first two clusters were enriched in genes related to apoptosis (Lsp1, Notch1, Dapk2, Fas, Tnfrsf1b) and cell death. A possible explanation for the increased levels of genes associated with apoptosis is that a stress response was elicited following Six1 knock-down by siRNA treatment.

4 Discussion

4.1 Effect of Six1 knock-down on H3K122ac, H3K27ac and p300

My initial goal was to determine the binding sites of Six1, p300 and regions marked by H3K27ac and H3K122ac in C2C12 myoblasts. If Six1 recruits p300 to DNA, it would be expected that Six1 and p300 co-occur at certain regions along with p300 catalyzed acetylation marks. In proliferating myoblasts, ChIP-seq targeting both Six1 and p300 identified several Six1 binding sites which qualify as p300-bound gene enhancer. A strong correlation between Six1 ChIP-seq and Six1 CUT&Tag binding sites was identified. Further, a partial correlation was observed between the presence of Six1 and p300.

Six1 knock-down was associated with a striking reduction in p300 signal at Six1 binding sites in clusters 1 and 2 whereas recruitment to regions within Cluster 3 was unaffected. Notably, only a small number of p300 molecules are present within individual cells, as such, numerous transcription factors compete for p300 recruitment and binding (Gillespie et al., 2020). As the majority of discovered pioneer factors have been found to interact with p300, other transcription factors may continue to recruit p300 to these loci (Choi et al., 2016; Dai & Markham, 2001; Grossman, 2001; Tsuda et al., 2003).

As p300 is capable of catalyzing both H3K122ac and H3K27ac, the signal of these acetylation was also profiled. In Cluster 1 and Cluster 2, regions where p300 recruitment was determined to be dependent on Six1, H3K122ac and H3K27ac signal was reduced after Six1 knockdown indicating that Six1 recruitment of p300 regulates the acetylation of H3K122 and H3K27 at certain regions. Although H3K27ac has recurrently been found to correlate with active enhancer regions, no causal or functional

associations have yet been identified (T. Zhang et al., 2020). In fact, previous studies have suggested that H3K27ac alone is dispensable for enhancer activity as mutations to lysine 27 on the H3.3 histone in mESCs had inconsequential effects on the transcriptome, chromatin accessibility or lysine acetylation at other regions (Pengelly et al., 2013; T. Zhang et al., 2020). Additionally, in both flies and mice, active enhancer regions were found to not solely be characterized by H3K27ac but also by the presence of additional chromatin marks including H3K122ac, H3K64ac and H3K79me3 and the loading of histone variants such as H3.3 and H2aZ (Bonn et al., 2012; Pradeepa, 2016). Although H3K27ac appears not to be required for transcription, it may be a piece of the mechanism involved in transcriptional activation through either nucleosome destabilization or recruitment of additional factors. The overlap of regions found to decrease in p300 signal, H3K27ac and H3K122ac signal following Six1 knock-down suggests that transcriptional activation may involve p300 acetylation of chromatin features beyond H3K27.

Inhibiting p300-mediated acetylation through Six1 knock-down may concomitantly allow for binding of methyltransferases and increase the presence of inactive chromatin marks (H3K27me3). Treatment of U2OS human osteosarcoma cells using a small molecule inhibitor of CBP was found to reduce H3K27ac while increasing levels of H3K27me3 (Vincek et al., 2018). To better understand epigenetic regulation of myogenesis, future work should determine whether levels of inactive chromatin marks are elevated in regions where acetylation of H3K122 decreases following Six1 knock-down. Analysis of the presence methylation marks should also consider that the Six family member, Six4 has been found to recruit the histone demethylase UTX to erase

the repressive mark H3K27me3 (Chakroun et al., 2015; Seenundun et al., 2010). Future work should examine the involvement of Six4 in establishing the epigenetic landscape in myoblasts as it is also expressed in muscle stem cells. Of note, the analysis here was limited to growing C2C12 cells which have not undergone differentiation wherein Six4 recruitment of UTX may vary. In the scenario where the presence of H3K27me3 is dependent on Six1, it is also not clear whether Six1 may increase the presence of H3K27me3 by freeing H3K27 for deposition of the mark and/or by reducing the presence of the UTX eraser function.

Recruitment of p300 has been shown to be facilitated by the UTX-MLL4 complex (Wang et al., 2017). Future work should also explore whether Six1 recruitment of p300 is dependent on UTX.

In comparison to the striking reduction observed in p300 signal, more subtle effects of Six1 knock-down were observed for the acetylation of H3K122 and H3K27. The interplay of activity between histone acetyltransferases and histone deacetylases maintains an equilibrium between acetylation and deacetylation essential to the epigenetic regulation of gene expression (Eckschlager et al., 2017). For instance, hyperacetylated histones may be established not only through increased levels of acetylation but also reduced HDAC activity. Muscle wasting during sepsis was found to be associated with increased levels of p300 and hyperacetylation alongside a reduction in HDAC activity (Alamdari et al., 2010). Impairment of p300 recruitment as a result of Six1 knock-down would be expected to shift the balance towards an accumulation of hypoacetylated histones. Although Six1 and p300 coincide at certain regions, the net level of histone acetylation may also implicate p300 recruitment by a different

transcription factor or activity by other HATs such as CBP, BRD4 or P/CAF acting independently of Six1 binding.

This and previous work support the idea that recruitment of p300 at gene regulatory regions may occur synergistically by Six1 and MyoD. Synergy can occur when several transcription factors cooperate to recruit a coactivator. Here it was shown that Six1 recruits p300 to 3,418 Six1 binding sites. Previous reports have indicated that p300 also directly interacts with and is recruited by MyoD (Puri, Avantaggiati, et al., 1997). Through correlation analysis, MyoD recruitment of p300 was found to be associated with acetylation of active enhancer regions and the Six1 binding motif was found to be enriched at p300 bound regions (Khilji et al., 2018). It is possible that Six1 and MyoD work synergistically to recruit p300. Another possibility is a mechanism involving stepwise recruitment and stabilization of p300 at target sites. Six1 may initially recruit MyoD, and subsequently both factors could work to retain p300 there (Y. Liu et al., 2013). In principle, this mechanism may represent the mechanism for the pioneer activity of Six1 for MyoD.

4.2 Effect of Six1 knock-down on DNA accessibility

Histone acetylation is capable of disrupting interactions between DNA and histones by neutralizing histone charges resulting in a more accessible state of DNA. Dynamic changes to DNA conformation affect the ability of transcriptional machinery to bind and initiate transcription. To characterize the involvement of Six1 on the accessibility landscape of DNA, we investigated whether DNA accessibility was dependent on Six1 expression at certain loci. Here it was found that regions that decrease in accessibility

following Six1 knock-down coincide with those which also exhibited a decrease in p300, H3K122ac and H3K27ac signal. These results are consistent with Six1 playing a role of a pioneer factor through recruitment of p300 to acetylate H3K122 and H3K27 which establish an accessible and active state of DNA.

Pax7 was similarly profiled by changes to DNA accessibility and presence of epigenetic markers H3K27ac and H3K4me1 in C2C12 myoblasts following ectopic expression or removal (Lilja et al., 2017). Pax7 was found to be associated with euchromatic regions, and its removal also resulted in localized reductions in both active histone marks and accessibility at Pax7 dependant enhancer regions. By demonstrating that Pax7 is capable of reorganizing DNA to a more accessible state and that its removal is accompanied with a loss of active histone markers the authors suggested that Pax7 may be a pioneer factor. Although strong evidence associated Pax7 presence with DNA accessibility and important chromatin marks, the molecular mechanism by which Pax7 acts in this context remains largely unknown. Interestingly, Pax7 bound regions also bound by MyoD were found to be the most strikingly reduced in both accessibility and histone marks following Pax7 removal. Additionally, while certain Pax7 bound regions lose accessibility following Pax7 removal, a group of regions continue to maintain accessibility. As previously mentioned, MyoD is also capable of recruiting p300 (Khilji et al., 2018). It is possible that Pax7 may also be involved in a stepwise recruitment mechanism of p300 alongside Six1 and/or MyoD to promote a more accessible state of DNA.

A limitation to this work was that only the effects of Six1 and p300 were profiled for effects on DNA accessibility. In reality, numerous regulatory factors are likely at play in

establishing the accessibility and epigenetic landscape of DNA. As Six1 is a known regulator of MyoD, the two transcription factors may act in cooperation to establish the accessible state of DNA. Future research should simultaneously explore the effect of additional MRFs involved in muscle stem cell activity on DNA accessibility, such as Myf5 and myogenin.

4.3 Effect of p300 inhibition on DNA accessibility

To characterize the role of p300 histone acetyltransferase activity on the DNA accessibility landscape, we examined changes to DNA accessibility following p300 catalytic inhibition. Narita et al. demonstrated that p300 activity contributes to transcriptional activation through assembly of the pre-initiation complex and recruitment of RNA polymerase II. Treatment of mESCs with the p300 inhibitor A-485 was expectedly associated with a decrease in H3K27ac levels, but also with a strong transcriptional inhibition and decrease in DNA accessibility. While Narita et al. observed a decrease in accessibility following p300 inhibition, changes were subtle in comparison to the reduction in transcription suggesting that the decrease in accessibility may not fully explain the strong reduction in transcription. Here, a decrease in accessibility was found when myoblasts were treated with A-485 at regions coinciding with those that decrease in p300, H3K27ac and H3K1ac following Six1 knock-down. Remarkably, effects on accessibility were observed here after just three hours of A-485 treatment. The results of this work fall in line with those observed by Narita et al. where a time-course analysis of A-485 treatment revealed that CBP/p300 regulated sites demonstrated a rapid (less than 30 minutes) turnover of acetylation markers.

Our results suggest the possibility that p300-mediated changes to DNA accessibility may impact transcription (see below) at certain regions (Figure 31-Figure 33) but not others. Notably, at certain regions (Figure 34) the opposite phenomenon is seen and accessibility, p300 recruitment and acetylation of the histone lysine's increase with Six1 knock-down or p300 inhibition. Six1 knock-down could potentially affect the activity of another factor which increases the accessibility or recruits an alternative HAT.

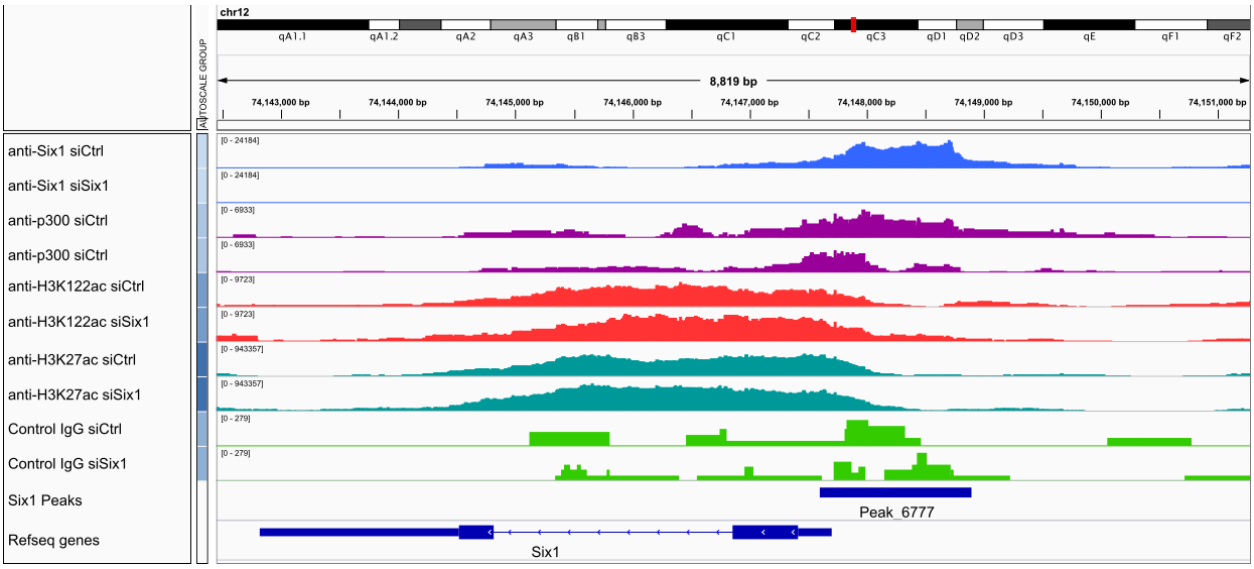

Figure 31 IGV screenshot at Six1 with bigwig files representing read density distribution in identically scaled tracks for merged Six1 control and knock-down samples and a track representing Six1 binding sites.

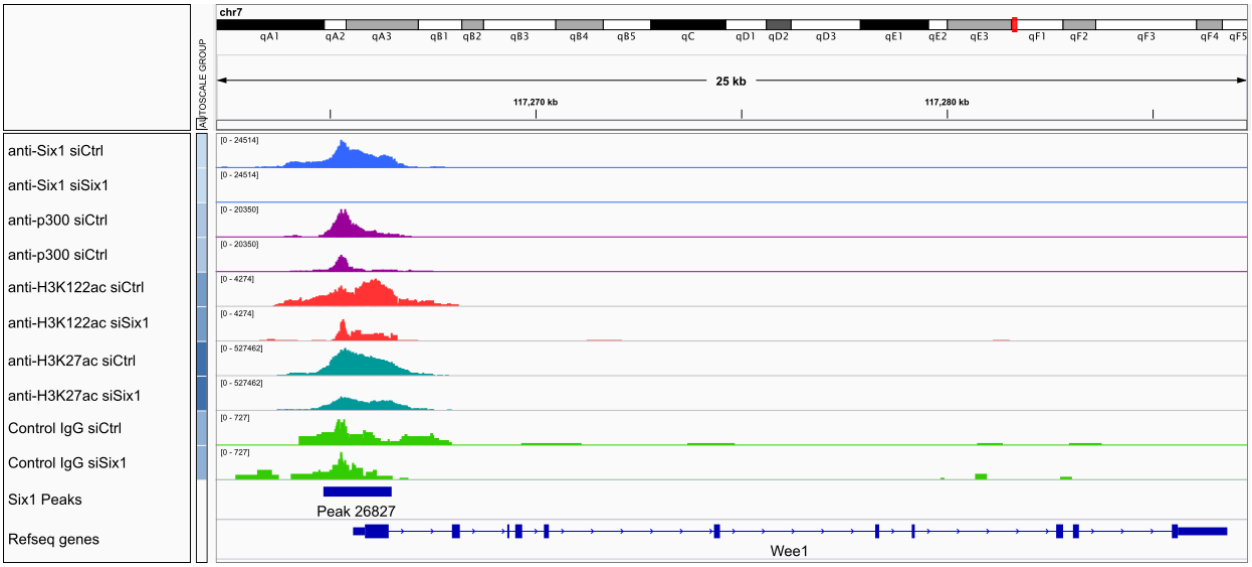

Figure 32 IGV screenshot at Wee1 with bigwig files representing read density distribution in identically scaled tracks for merged Six1 control and knock-down samples and a track representing Six1 binding sites.

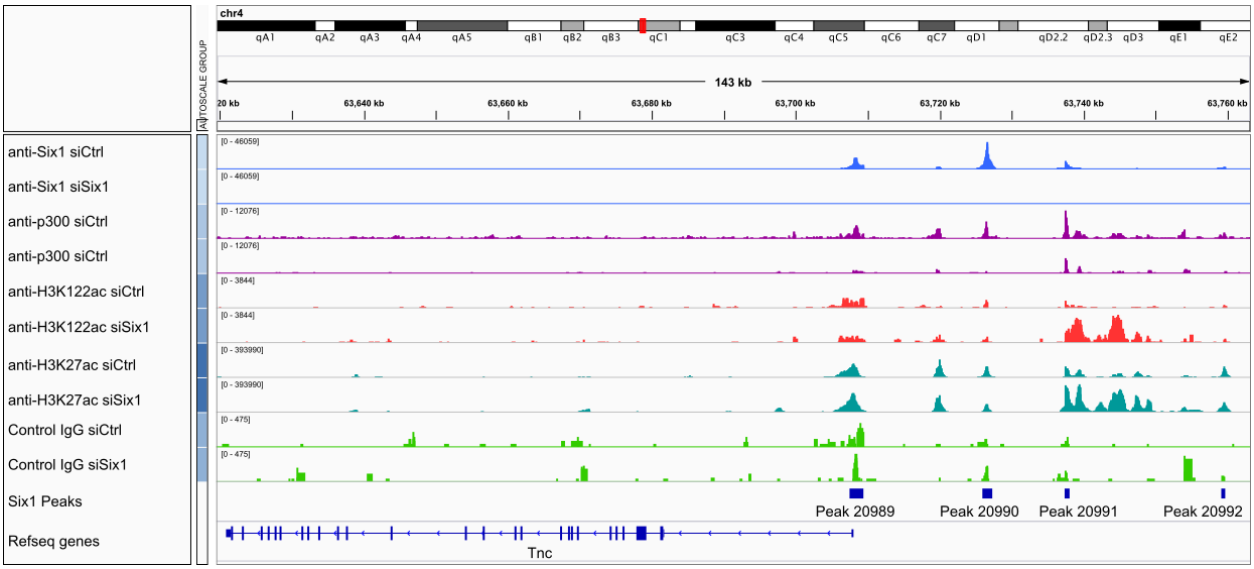

Figure 33 IGV screenshot at Tnc with bigwig files representing read density distribution in identically scaled tracks for merged Six1 control and knock-down samples and a track representing Six1 binding sites.

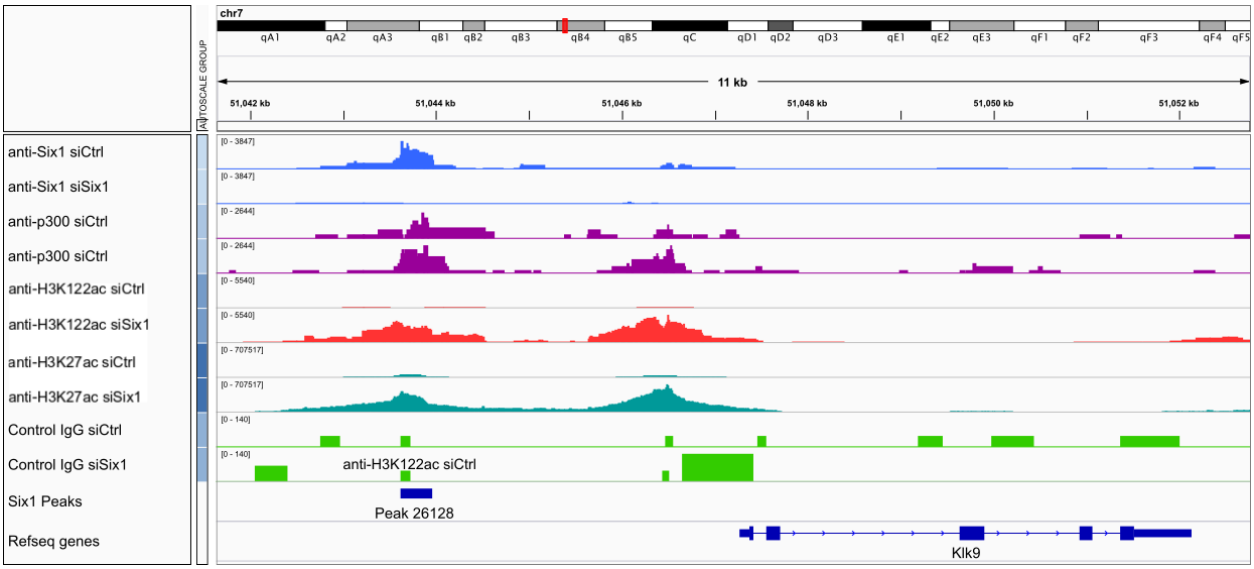

Figure 34 IGV screenshot at Klk9 with bigwig files representing read density distribution in identically scaled tracks for merged Six1 control and knock-down samples and a track representing Six1 binding sites.

Additionally, knock-down of Six1 may allow for binding of a competitive repressive factor, potentially inhibiting p300-mediated acetylation or allowing for binding of a HDAC. Increased activity by HATs not studied here, and not inhibited by A-485, may also affect the accessibility and epigenetic landscape such that reverse effects are seen at certain genomic loci following Six1 knock-down. Alternatively, Six1 and/or p300 may be involved in the recruitment of an unidentified HDAC, such that when Six1 is knocked down or p300 inhibited, deacetylase activity is impaired, allowing for increased HAT activity. Future work should examine how regions that increase in acetylation following Six1 knock-down behave with the inclusion of inhibitors against various HDACs.

The functional mechanisms by which pioneer factors bind to compact regions of DNA and mediate transcriptional activation is not yet fully understood. Additionally, not all pioneer factors appear to function the same way (X. Zhang et al., 2014). As evidenced through this work and previous research demonstrating the role of p300 in histone

eviction, p300 has a probable role in establishing the DNA accessibility landscape (Narita et al., 2021; Tropberger et al., 2013). p300 has previously been found to bind several known pioneer factors. In addition to its capacity to acetylate H3K27 on lysine tails, p300 is also capable of acetylating the surface of the histone octamer, non-histone proteins and components of the preinitiation complex (Gu & Roeder, 1997; Narita et al., 2021; Pradeepa et al., 2016). Notably, acetylation of H3K122 on the lateral surface of the histone octamer was found to be associated with regions where p300 signal, accessibility and transcription was decreased following Six1 knockdown (Tropberger et al., 2013). p300 mediated acetylation of H3K122 and resulting destabilization of nucleosomes may also in part contribute to the accessibility landscape of DNA. Furthermore, through introduction of point mutations to the DNA binding domain of c-Myb, it was suggested that c-Myb may act as a co-factor to p300 by positioning histone tails in closed regions of DNA for efficient acetylation by p300 (Fuglerud et al., 2018). Given that p300 can acetylate many regions and has reported involvement in numerous signalling pathways a complete mode of action for p300 in pioneer factor activity has not yet been determined. Furthermore, although here we focus on p300 activity due to its specific importance towards myogenesis, A-485 can inhibit the histone acetyltransferase activity of both p300 and CBP. As C2C12 cells are also capable of expressing CBP, future work should also examine the accessibility of sites bound by CBP.

Here we provide additional evidence for the implication of p300 in pioneer factor activity during myogenesis. MyoD, which acts both in parallel with and downstream of Six1, is capable of recruiting p300/CBP to DNA (Puri, Sartorelli, et al., 1997). Six1 and MyoD

may both work to shape the accessibility landscape of DNA during myogenesis through a p300 recruitment mechanism.

p300 activity is also capable of recruiting BRD4, a HAT which is associated with increased DNA accessibility (J.-E. Lee et al., 2017). Similarly to p300, BRD4 is capable of acetylating H3K122, resulting in nucleosomal destabilization (Devaiah et al., 2016). Furthermore, BRD4 regulates transcriptional elongation through both recruitment of P-TEFb and by phosphorylating Serine-2 of the RNA Polymerase II carboxy-terminal domain (Devaiah et al., 2012). Knock-down of BRD4 in C2C12 myoblasts was found to inhibit myogenesis (J.-E. Lee et al., 2017). The authors demonstrated BRD4 is a epigenomic reader of acetylation marks deposited by p300/CBP which is recruited to and colocalizes with lineage determining transcription factors (LDTFs) to allow for modulation of cell identity during myogenic differentiation. A mechanism involving p300 recruitment of BRD4 and subsequent BRD4-mediated nucleosome destabilization may enable transcription of LDTRs during differentiation. It is possible, and even likely, that the activity of additional factors not studied here collaborate to establish the epigenetic and accessibility landscape of DNA during myogenesis through a mechanism which implicates p300 recruitment. To further understand changes to the epigenetic and accessibility landscape during myogenesis future work should profile additional factors which implicate p300, including c-Myb, BRD4, and MyoD.

4.4 Effect of Six1 knock-down on gene expression in regions which decrease in accessibility with Six1 knock-down or H3K122ac and H3K27ac signal with p300 inhibition

Overexpression of Six1 is correlated with poor clinical outcomes in a variety of diseases including ovarian, esophageal, lung, and pancreatic cancer (Behbakht et al., 2007; He et al., 2017; Z. Li et al., 2013; Q. Liu et al., 2016). Additionally, Six1 knock-out in mice leads to cell death and reduced proliferation, resulting in organ failure (Laclef, Hamard, et al., 2003). To assess how expression is affected through Six1 regulation of epigenetic and accessibility landscape, RNA-seq was performed following Six1 knock-down.

Genes within or near the regions comprised in cluster 1 and cluster 2 were shown to have a trend towards lower expression following Six1 knock-down. Narita et al. reported that impairment of p300 activity disrupts RNA Polymerase II mediated transcriptional elongation. Given that BRD4 is recruited to acetylated nucleosomes, it was postulated that p300 promotes transcriptional elongation not by allowing for the binding of transcription factors but through promotion of BRD4 mediated RNA Polymerase II pause release (Narita et al., 2021). Our finding that gene expression following Six1 knock-down decreases at regions which coincide with those that decrease in p300, and acetylation signal are consistent to those reported by Narita et al. Future work should directly assess how transcriptional elongation is impacted by p300 inhibition in myoblasts.

Collectively, genes within Cluster 3 showed the least changes in mRNA abundance following Six1 knock-down. Genes within Cluster 3 represent Six1 binding sites where expression is independent of the presence of Six1. Notably, H3K122ac and p300 signal

was shown to increase following Six1 knock-down. Regions within Cluster 3 may continue to be acetylated through recruitment of p300 by a transcription factor other than Six1 resulting in little or no consequence on gene transcription.

GO terms analysis was used to associate terms with Cluster 1 and Cluster 2 where Six1 knock-down or p300 inhibition resulted in a decrease in accessibility as well as where p300, H3K122ac and H3K27ac signal were found to be associated with genes related to muscle development. Six1 may selectively recruit p300 to regions within Cluster 1 and Cluster 2 to promote transcription at enhancer regions implicated in myogenesis. Opposingly, genes within Cluster 3 were most enriched for those associated to GO terms related to apoptosis and cell death. Apoptosis is an essential component of skeletal muscle proliferation as it allows for damaged cells to be removed from progressing towards differentiation (King & Cidlowski, 1998). Double knockdown of CBP/p300 in human primary myoblasts was also associated with a group of upregulated genes involved in apoptosis indicating that CBP and p300 may have a role in cell protection and survival (Fauquier et al., 2018). Furthermore, Six1 deficient mouse embryos were not found to have increased levels of apoptosis (Laclef, Hamard, et al., 2003). Inhibition of p300 has been found in other cases to supress apoptosis. It is possible that p300 may be recruited by transcription factors other than Six1 to certain p300 bound regions within Cluster 3.

4.5 Conclusion

Here, ATAC-seq, RNA-seq and CUT&Tag-seq data was cross-referenced to reveal a mechanism whereby Six1 exhibits pioneer factor activity in proliferating myoblasts of the C2C12 cell line during myogenesis. Analyzing changes in accessibility following Six1 knockdown or p300 inhibition revealed that Six1 is a regulator of DNA accessibility through recruitment of p300. Knock-down of Six1 reduces the presence of p300 established acetylation at regions that are associated with nucleosome destabilization and transcriptional activation. Our findings demonstrate that knock-down of Six1 and inhibition of p300 correlate with decreased accessibility; however, we cannot rule out the possibility that additional factors also regulated by Six1 have a role in altering the epigenetic and accessibility landscape. Although p300 but not CBP was determined to be necessary for myogenesis (J. Chen et al., 2015), the contribution of CBP towards the epigenetic and accessibility landscape in myoblasts was not examined here. Although p300 is indispensable for skeletal myogenesis, the presence of histone deacetylases far outweighs the number of acetyltransferases (Gillespie et al., 2020; Puri, Sartorelli, et al., 1997). The overall abundance of HDACs suggests that these enzymes are ubiquitous and result in high rates of histone deacetylation. Previous research suggests that MyoD associates with HDAC1 in undifferentiated but not differentiating cells to supress transcription of muscle-specific genes (Mal et al., 2001). Whether HDACs are explicitly recruited by transcription factors involved in myogenesis and the extent to which HDAC activity impacts myogenesis is not yet known. For a comprehensive assessment of the epigenetic regulation of myoblasts, changes to p300 binding and function should be examined in conjunction with HDAC binding and activity. To further the understanding of

regulatory mechanisms involved during myogenesis, the contribution of additional factors towards the accessibility and epigenetic landscape in myoblasts should be profiled. Myoblasts were examined only in a proliferative state, to better characterize the regulation of muscle stem cells, changes to accessibility and the epigenetic landscape during quiescence, differentiation and activation should be studied. While use of the mouse muscle derived C2C12 cell line offered the advantages of reduced animal use and simplified siRNA transfection and drug treatment, there are known limitations with the use of cell lines as a model for skeletal muscle. One factor that makes C2C12 cells grown in culture dissimilar to real isolated myoblasts is that they are absent of an in vivo microenvironment that contributes towards differentiation to the myogenic lineage. Additionally, C2C12 myoblasts are a model of already activated MuSC, so they cannot offer direct evidence of what happens during the activation of quiescent MuSCs. Further, C2C12 cells are immortal and have undergone an unknown but possibly large number of genetic changes. For instance, C2C12 cells are aneuploid and have lost parts of the Cdkn2a locus.

To explore the therapeutic potential of muscle stem cells for treatment of muscular degenerative diseases, analyzing the accessibility and epigenetic landscape in human cells would be advantageous. Although there is an overlap between human and rodent genomes, similar analysis using primate skeletal muscle may expose key differences in epigenetic regulatory mechanisms. While human skeletal muscle cells contain high levels of proteins associated with type I fibers, C2C12 cells are highly expressed in proteins associated with type I glycolytic fibers (Schiaffino & Reggiani, 2011). The surrounding microenvironment of stem cells are known to be crucial to the regulation

and maintenance of a quiescent state and towards the differentiation of stem cells to specific tissues (Dinulovic et al., 2017). It is likely that there are changes in the DNA accessibility and epigenetic landscape as muscle stem cells transition from quiescence to early activation. Future work profiling changes to accessibility and epigenetic landscape of skeletal muscle using real isolated muscle stem cells could provide insight into functional mechanisms that occur during muscle stem cell activation.

References

Abe, S., Takeda, H., Nishio, S., & Usami, S. (2018). Sensorineural hearing loss and mild cardiac phenotype caused by an EYA4 mutation. *Human Genome Variation*, *5*(1), 1–4. https://doi.org/10.1038/s41439-018-0023-9

Ahmed, M., Xu, J., & Xu, P.-X. (2012). EYA1 and SIX1 drive the neuronal developmental program in cooperation with the SWI/SNF chromatin-remodeling complex and SOX2 in the mammalian inner ear. *Development (Cambridge, England)*, *139*(11), 1965–1977. https://doi.org/10.1242/dev.071670

Alamdari, N., Smith, I. J., Aversa, Z., & Hasselgren, P.-O. (2010). Sepsis and glucocorticoids upregulate p300 and downregulate HDAC6 expression and activity in skeletal muscle. *American Journal of Physiology-Regulatory, Integrative and Comparative Physiology*, *299*(2), R509–R520. https://doi.org/10.1152/ajpregu.00858.2009

Anand, A., Nambirajan, A., Kumar, V., Agarwal, S., Sharma, S., Mohta, S., Gopi, S., Kaushal, K., Gunjan, D., Singh, N., Madhusudhan, K. S., Chauhan, S. S., Sharma, M. C., Bansal, V. K., & Saraya, A. (2021). Alterations in Autophagy and Mammalian Target of Rapamycin (mTOR) Pathways Mediate Sarcopenia in Patients with Cirrhosis. *Journal of Clinical and Experimental Hepatology*. https://doi.org/10.1016/j.jceh.2021.05.004

Appolloni, I., Calzolari, F., Corte, G., Perris, R., & Malatesta, P. (2008). Six3 Controls the Neural Progenitor Status in the Murine CNS. *Cerebral Cortex*, *18*(3), 553–562. https://doi.org/10.1093/cercor/bhm092

Armand, A.-S., Bourajjaj, M., Martínez-Martínez, S., Azzouzi, H. el, Martins, P. A. da C., Hatzis, P., Seidler, T., Redondo, J. M., & Windt, L. J. D. (2008). Cooperative Synergy between NFAT and MyoD Regulates Myogenin Expression and Myogenesis ∗. *Journal of Biological Chemistry*, *283*(43), 29004–29010. https://doi.org/10.1074/jbc.M801297200

Balasubramanyam, K., Altaf, M., Varier, R. A., Swaminathan, V., Ravindran, A., Sadhale, P. P., & Kundu, T. K. (2004). Polyisoprenylated Benzophenone, Garcinol, a Natural Histone Acetyltransferase Inhibitor, Represses Chromatin Transcription and Alters Global Gene Expression *. *Journal of Biological Chemistry*, *279*(32), 33716–33726. https://doi.org/10.1074/jbc.M402839200

Bannister, A. J., & Kouzarides, T. (1996). The CBP co-activator is a histone acetyltransferase. *Nature*, *384*(6610), 641–643. https://doi.org/10.1038/384641a0

Barretina, J., Caponigro, G., Stransky, N., Venkatesan, K., Margolin, A. A., Kim, S., Wilson, C. J., Lehár, J., Kryukov, G. V., Sonkin, D., Reddy, A., Liu, M., Murray, L., Berger, M. F., Monahan, J. E., Morais, P., Meltzer, J., Korejwa, A., Jané-Valbuena, J., … Garraway, L. A. (2012). The Cancer Cell Line Encyclopedia enables predictive modelling of anticancer drug sensitivity. *Nature*, *483*(7391), 603–607. https://doi.org/10.1038/nature11003

Beggs, A. H., Hoffman, E. P., Snyder, J. R., Arahata, K., Specht, L., Shapiro, F., Angelini, C., Sugita, H., & Kunkel, L. M. (1991). Exploring the molecular basis for variability among patients with Becker muscular dystrophy: Dystrophin gene and protein studies. *American Journal of Human Genetics*, *49*(1), 54–67.

Behbakht, K., Qamar, L., Aldridge, C. S., Coletta, R. D., Davidson, S. A., Thorburn, A., & Ford, H. L. (2007). Six1 Overexpression in Ovarian Carcinoma Causes Resistance to TRAIL-Mediated Apoptosis and Is Associated with Poor Survival. *Cancer Research*, *67*(7), 3036–3042. https://doi.org/10.1158/0008-5472.CAN-06-3755

Behrens, J., von Kries, J. P., Kühl, M., Bruhn, L., Wedlich, D., Grosschedl, R., & Birchmeier, W. (1996). Functional interaction of beta-catenin with the transcription factor LEF-1. *Nature*, *382*(6592), 638–642. https://doi.org/10.1038/382638a0

Bello, L., Morgenroth, L. P., Gordish-Dressman, H., Hoffman, E. P., McDonald, C. M., & Cirak, S. (2016). DMD genotypes and loss of ambulation in the CINRG Duchenne Natural History Study. *Neurology*, *87*(4), 401–409. https://doi.org/10.1212/WNL.0000000000002891

Benjamini, Y., & Hochberg, Y. (1995). Controlling the False Discovery Rate: A Practical and Powerful Approach to Multiple Testing. *Journal of the Royal Statistical Society. Series B (Methodological)*, *57*(1), 289–300.

Berkes, C. A., Bergstrom, D. A., Penn, B. H., Seaver, K. J., Knoepfler, P. S., & Tapscott, S. J. (2004). Pbx Marks Genes for Activation by MyoD Indicating a Role for a Homeodomain Protein in Establishing Myogenic Potential. *Molecular Cell*, *14*(4), 465–477. https://doi.org/10.1016/S1097-2765(04)00260-6

Bernier, G., Panitz, F., Zhou, X., Hollemann, T., Gruss, P., & Pieler, T. (2000). Expanded retina territory by midbrain transformation upon overexpression of Six6

(Optx2) in Xenopus embryos. *Mechanisms of Development*, *93*(1), 59–69. https://doi.org/10.1016/S0925-4773(00)00271-9

Bissel, M. J., & Barcellos-Hoff, M. H. (1987). The Influence of Extracellular Matrix on Gene Expression: Is Structure the Message? *Journal of Cell Science*, *1987*(Supplement_8), 327–343. https://doi.org/10.1242/jcs.1987.Supplement_8.18

Bladen, C. L., Salgado, D., Monges, S., Foncuberta, M. E., Kekou, K., Kosma, K., Dawkins, H., Lamont, L., Roy, A. J., Chamova, T., Guergueltcheva, V., Chan, S., Korngut, L., Campbell, C., Dai, Y., Wang, J., Barišić, N., Brabec, P., Lahdetie, J., … Lochmüller, H. (2015). The TREAT-NMD DMD Global Database: Analysis of More than 7,000 Duchenne Muscular Dystrophy Mutations. *Human Mutation*, *36*(4), 395–402. https://doi.org/10.1002/humu.22758

Bladt, F., Riethmacher, D., Isenmann, S., Aguzzi, A., & Birchmeier, C. (1995). Essential role for the c-met receptor in the migration of myogenic precursor cells into the limb bud. *Nature*, *376*(6543), 768–771. https://doi.org/10.1038/376768a0

Blais, A. (2015). Myogenesis in the Genomics Era. *Journal of Molecular Biology*, *427*(11), 2023–2038. https://doi.org/10.1016/j.jmb.2015.02.009

Bondarenko, V. A., Steele, L. M., Újvári, A., Gaykalova, D. A., Kulaeva, O. I., Polikanov, Y. S., Luse, D. S., & Studitsky, V. M. (2006). Nucleosomes Can Form a Polar Barrier to Transcript Elongation by RNA Polymerase II. *Molecular Cell*, *24*(3), 469–479. https://doi.org/10.1016/j.molcel.2006.09.009

Bonn, S., Zinzen, R. P., Girardot, C., Gustafson, E. H., Perez-Gonzalez, A., Delhomme, N., Ghavi-Helm, Y., Wilczyński, B., Riddell, A., & Furlong, E. E. M. (2012).

Tissue-specific analysis of chromatin state identifies temporal signatures of enhancer activity during embryonic development. *Nature Genetics*, *44*(2), 148–156. https://doi.org/10.1038/ng.1064

Boonen, K. J. M., & Post, M. J. (2008). The Muscle Stem Cell Niche: Regulation of Satellite Cells During Regeneration. *Tissue Engineering Part B: Reviews*, *14*(4), 419–431. https://doi.org/10.1089/ten.teb.2008.0045

Borrow, J., Stanton, V. P., Andresen, J. M., Becher, R., Behm, F. G., Chaganti, R. S. K., Civin, C. I., Disteche, C., Dubé, I., Frischauf, A. M., Horsman, D., Mitelman, F., Volinia, S., Watmore, A. E., & Housman, D. E. (1996). The translocation t(8;16)(p11;p13) of acute myeloid leukaemia fuses a putative acetyltransferase to the CREB–binding protein. *Nature Genetics*, *14*(1), 33–41. https://doi.org/10.1038/ng0996-33

Bostick, B., Shin, J.-H., Yue, Y., & Duan, D. (2011). AAV-microdystrophin Therapy Improves Cardiac Performance in Aged Female mdx Mice. *Molecular Therapy*, *19*(10), 1826–1832. https://doi.org/10.1038/mt.2011.154

Boudreau, N. J., & Jones, P. L. (1999). Extracellular matrix and integrin signalling: The shape of things to come. *Biochemical Journal*, *339*(3), 481–488. https://doi.org/10.1042/bj3390481

Bovolenta, P., Mallamaci, A., Puelles, L., & Boncinelli, E. (1998). Expression pattern of cSix3, a member of the Six/sine oculis family of transcription factors. *Mechanisms of Development*, *70*(1–2), 201–203. https://doi.org/10.1016/s0925-4773(97)00183-4

Bowers, E. M., Yan, G., Mukherjee, C., Orry, A., Wang, L., Holbert, M. A., Crump, N. T., Hazzalin, C. A., Liszczak, G., Yuan, H., Larocca, C., Saldanha, S. A., Abagyan, R., Sun, Y., Meyers, D. J., Marmorstein, R., Mahadevan, L. C., Alani, R. M., & Cole, P. A. (2010). Virtual Ligand Screening of the p300/CBP Histone Acetyltransferase: Identification of a Selective Small Molecule Inhibitor. *Chemistry & Biology*, *17*(5), 471–482. https://doi.org/10.1016/j.chembiol.2010.03.006

Braun, T., Rudnicki, M. A., Arnold, H. H., & Jaenisch, R. (1992). Targeted inactivation of the muscle regulatory gene Myf-5 results in abnormal rib development and perinatal death. *Cell*, *71*(3), 369–382. https://doi.org/10.1016/0092-8674(92)90507-9

Brownell, J. E., Zhou, J., Ranalli, T., Kobayashi, R., Edmondson, D. G., Roth, S. Y., & Allis, C. D. (1996). Tetrahymena Histone Acetyltransferase A: A Homolog to Yeast Gcn5p Linking Histone Acetylation to Gene Activation. *Cell*, *84*(6), 843–851. https://doi.org/10.1016/S0092-8674(00)81063-6

Bultman, S., Gebuhr, T., Yee, D., La Mantia, C., Nicholson, J., Gilliam, A., Randazzo, F., Metzger, D., Chambon, P., Crabtree, G., & Magnuson, T. (2000). A Brg1 Null Mutation in the Mouse Reveals Functional Differences among Mammalian SWI/SNF Complexes. *Molecular Cell*, *6*(6), 1287–1295. https://doi.org/10.1016/S1097-2765(00)00127-1

Bushby, K. M. D., Thambyayah, M., & Gardner-Medwin, D. (1991). Prevalence and incidence of Becker muscular dystrophy. *The Lancet*, *337*(8748), 1022–1024. https://doi.org/10.1016/0140-6736(91)92671-N

Carrozza, M. J., Utley, R. T., Workman, J. L., & Côté, J. (2003). The diverse functions of histone acetyltransferase complexes. *Trends in Genetics*, *19*(6), 321–329. https://doi.org/10.1016/S0168-9525(03)00115-X

Chakroun, I., Yang, D., Girgis, J., Gunasekharan, A., Phenix, H., Kærn, M., & Blais, A. (2015). Genome-wide association between Six4, MyoD, and the histone demethylase Utx during myogenesis. *The FASEB Journal*, *29*(11), 4738–4755. https://doi.org/10.1096/fj.15-277053

Chen, J., Wang, Y., Hamed, M., Lacroix, N., & Li, Q. (2015). Molecular Basis for the Regulation of Transcriptional Coactivator p300 in Myogenic Differentiation. *Scientific Reports*, *5*(1), 13727. https://doi.org/10.1038/srep13727

Chen, K., Wu, K., Gormley, M., Ertel, A., Wang, J., Zhang, W., Zhou, J., Disante, G., Li, Z., Rui, H., Quong, A. A., McMahon, S. B., Deng, H., Lisanti, M. P., Wang, C., & Pestell, R. G. (2013). Acetylation of the cell-fate factor dachshund determines p53 binding and signaling modules in breast cancer. *Oncotarget*, *4*(6), 923–935. https://doi.org/10.18632/oncotarget.1094

Chen, S., Zhou, Y., Chen, Y., & Gu, J. (2018). fastp: An ultra-fast all-in-one FASTQ preprocessor. *Bioinformatics*, *34*(17), i884–i890. https://doi.org/10.1093/bioinformatics/bty560

Cheng, X., Huang, H., Luo, X., Shi, B., & Li, J. (2018). Wnt7a induces satellite cell expansion, myofiber hyperplasia and hypertrophy in rat craniofacial muscle. *Scientific Reports*, *8*(1), 10613. https://doi.org/10.1038/s41598-018-28917-6

Cheyette, B. N. R., Green, P. J., Martin, K., Garren, H., Hartenstein, V., & Zipursky, S. L. (1994). The drosophila sine oculis locus encodes a homeodomain-containing

protein required for the development of the entire visual system. *Neuron*, *12*(5), 977–996. https://doi.org/10.1016/0896-6273(94)90308-5

Choi, S. H., Gearhart, M. D., Cui, Z., Bosnakovski, D., Kim, M., Schennum, N., & Kyba, M. (2016). DUX4 recruits p300/CBP through its C-terminus and induces global H3K27 acetylation changes. *Nucleic Acids Research*, *44*(11), 5161–5173. https://doi.org/10.1093/nar/gkw141

Christ, B., & Ordahl, C. (1995). Early stages of chick somite development. *Anatomy and Embryology*, *191*(5), 381–396. https://doi.org/10.1007/BF00304424

Chrivia, J. C., Kwok, R. P. S., Lamb, N., Hagiwara, M., Montminy, M. R., & Goodman, R. H. (1993). Phosphorylated CREB binds specifically to the nuclear protein CBP. *Nature*, *365*(6449), 855–859. https://doi.org/10.1038/365855a0

Cirillo, L. A., Lin, F. R., Cuesta, I., Friedman, D., Jarnik, M., & Zaret, K. S. (2002). Opening of Compacted Chromatin by Early Developmental Transcription Factors HNF3 (FoxA) and GATA-4. *Molecular Cell*, *9*(2), 279–289. https://doi.org/10.1016/S1097-2765(02)00459-8

Colella, P., Ronzitti, G., & Mingozzi, F. (2018). Emerging Issues in AAV-Mediated In Vivo Gene Therapy. *Molecular Therapy - Methods & Clinical Development*, *8*, 87–104. https://doi.org/10.1016/j.omtm.2017.11.007

Connuck, D. M., Sleeper, L. A., Colan, S. D., Cox, G. F., Towbin, J. A., Lowe, A. M., Wilkinson, J. D., Orav, E. J., Cuniberti, L., Salbert, B. A., & Lipshultz, S. E. (2008). Characteristics and outcomes of cardiomyopathy in children with Duchenne or Becker muscular dystrophy: A comparative study from the Pediatric

Cardiomyopathy Registry. *American Heart Journal*, *155*(6), 998–1005. https://doi.org/10.1016/j.ahj.2008.01.018

Corces, M. R., Trevino, A. E., Hamilton, E. G., Greenside, P. G., Sinnott-Armstrong, N. A., Vesuna, S., Satpathy, A. T., Rubin, A. J., Montine, K. S., Wu, B., Kathiria, A., Cho, S. W., Mumbach, M. R., Carter, A. C., Kasowski, M., Orloff, L. A., Risca, V. I., Kundaje, A., Khavari, P. A., … Chang, H. Y. (2017). An improved ATAC-seq protocol reduces background and enables interrogation of frozen tissues. *Nature Methods*, *14*(10), 959–962. https://doi.org/10.1038/nmeth.4396

Cossu, G., & Sampaolesi, M. (2007). New therapies for Duchenne muscular dystrophy: Challenges, prospects and clinical trials. *Trends in Molecular Medicine*, *13*(12), 520–526. https://doi.org/10.1016/j.molmed.2007.10.003

Creyghton, M. P., Cheng, A. W., Welstead, G. G., Kooistra, T., Carey, B. W., Steine, E. J., Hanna, J., Lodato, M. A., Frampton, G. M., Sharp, P. A., Boyer, L. A., Young, R. A., & Jaenisch, R. (2010). Histone H3K27ac separates active from poised enhancers and predicts developmental state. *Proceedings of the National Academy of Sciences*, *107*(50), 21931–21936. https://doi.org/10.1073/pnas.1016071107

Dai, Y.-S., & Markham, B. E. (2001). P300 Functions as a Coactivator of Transcription Factor GATA-4 *. *Journal of Biological Chemistry*, *276*(40), 37178–37185. https://doi.org/10.1074/jbc.M103731200

Davis, R. J., Shen, W., Heanue, T. A., & Mardon, G. (1999). Mouse Dach, a homologue of Drosophila dachshund, is expressed in the developing retina, brain and limbs.

Development Genes and Evolution, *209*(9), 526–536. https://doi.org/10.1007/s004270050285

Davis, R. L., Weintraub, H., & Lassar, A. B. (1987). Expression of a single transfected cDNA converts fibroblasts to myoblasts. *Cell*, *51*(6), 987–1000. https://doi.org/10.1016/0092-8674(87)90585-x

de la Serna, I. L., Carlson, K. A., & Imbalzano, A. N. (2001). Mammalian SWI/SNF complexes promote MyoD-mediated muscle differentiation. *Nature Genetics*, *27*(2), 187–190. https://doi.org/10.1038/84826

de la Serna, I. L., Ohkawa, Y., Berkes, C. A., Bergstrom, D. A., Dacwag, C. S., Tapscott, S. J., & Imbalzano, A. N. (2005). MyoD Targets Chromatin Remodeling Complexes to the Myogenin Locus Prior to Forming a Stable DNA-Bound Complex. *Molecular and Cellular Biology*, *25*(10), 3997–4009. https://doi.org/10.1128/MCB.25.10.3997-4009.2005

Devaiah, B. N., Case-Borden, C., Gegonne, A., Hsu, C. H., Chen, Q., Meerzaman, D., Dey, A., Ozato, K., & Singer, D. S. (2016). BRD4 is a Histone Acetyltransferase that Evicts Nucleosomes from Chromatin. *Nature Structural & Molecular Biology*, *23*(6), 540–548. https://doi.org/10.1038/nsmb.3228

Devaiah, B. N., Lewis, B. A., Cherman, N., Hewitt, M. C., Albrecht, B. K., Robey, P. G., Ozato, K., Sims, R. J., & Singer, D. S. (2012). BRD4 is an atypical kinase that phosphorylates Serine2 of the RNA Polymerase II carboxy-terminal domain. *Proceedings of the National Academy of Sciences*, *109*(18), 6927–6932. https://doi.org/10.1073/pnas.1120422109

Dignam, J. D., Lebovitz, R. M., & Roeder, R. G. (1983). Accurate transcription initiation by RNA polymerase II in a soluble extract from isolated mammalian nuclei. *Nucleic Acids Research*, *11*(5), 1475–1489.

Dilworth, F. J., & Blais, A. (2011). Epigenetic regulation of satellite cell activation during muscle regeneration. *Stem Cell Research & Therapy*, *2*(2), 18. https://doi.org/10.1186/scrt59

Dilworth, F. J., Seaver, K. J., Fishburn, A. L., Htet, S. L., & Tapscott, S. J. (2004). In vitro transcription system delineates the distinct roles of the coactivators pCAF and p300 during MyoD/E47-dependent transactivation. *Proceedings of the National Academy of Sciences*, *101*(32), 11593–11598. https://doi.org/10.1073/pnas.0404192101

Dinulovic, I., Furrer, R., & Handschin, C. (2017). Plasticity of the Muscle Stem Cell Microenvironment. *Advances in Experimental Medicine and Biology*, *1041*, 141–169. https://doi.org/10.1007/978-3-319-69194-7_8

Dirks, A., & Leeuwenburgh, C. (2002). Apoptosis in skeletal muscle with aging. *American Journal of Physiology-Regulatory, Integrative and Comparative Physiology*, *282*(2), R519–R527. https://doi.org/10.1152/ajpregu.00458.2001

Dobin, A., Davis, C. A., Schlesinger, F., Drenkow, J., Zaleski, C., Jha, S., Batut, P., Chaisson, M., & Gingeras, T. R. (2013). STAR: Ultrafast universal RNA-seq aligner. *Bioinformatics*, *29*(1), 15–21. https://doi.org/10.1093/bioinformatics/bts635

Dumont, N. A., Wang, Y. X., von Maltzahn, J., Pasut, A., Bentzinger, C. F., Brun, C. E., & Rudnicki, M. A. (2015). Dystrophin expression in muscle stem cells regulates

their polarity and asymmetric division. *Nature Medicine*, *21*(12), 1455–1463. https://doi.org/10.1038/nm.3990

Dupont-Versteegden, E. E. (2005). Apoptosis in muscle atrophy: Relevance to sarcopenia. *Experimental Gerontology*, *40*(6), 473–481. https://doi.org/10.1016/j.exger.2005.04.003

Duprez, D., Fournier-Thibault, C., & Douarin, N. (1998). Sonic Hedgehog induces proliferation of committed skeletal muscle cells in the chick limb. *Development (Cambridge, England)*, *125*, 495–505.

Duxon, Usson, & Harris. (1989). *The origin of secondary myotubes in mammalian skeletal muscles: Ultrastructural studies | Development | The Company of Biologists*. https://journals.biologists.com/dev/article/107/4/743/36496/The-origin-of-secondary-myotubes-in-mammalian

Eckner, R., Ewen, M. E., Newsome, D., Gerdes, M., DeCaprio, J. A., Lawrence, J. B., & Livingston, D. M. (1994). Molecular cloning and functional analysis of the adenovirus E1A-associated 300-kD protein (p300) reveals a protein with properties of a transcriptional adaptor. *Genes & Development*, *8*(8), 869–884. https://doi.org/10.1101/gad.8.8.869

Eckschlager, T., Plch, J., Stiborova, M., & Hrabeta, J. (2017). Histone Deacetylase Inhibitors as Anticancer Drugs. *International Journal of Molecular Sciences*, *18*(7), 1414. https://doi.org/10.3390/ijms18071414

Emery, A. E. (2002). The muscular dystrophies. *The Lancet*, *359*(9307), 687–695. https://doi.org/10.1016/S0140-6736(02)07815-7

Fauquier, L., Azzag, K., Parra, M. A. M., Quillien, A., Boulet, M., Diouf, S., Carnac, G., Waltzer, L., Gronemeyer, H., & Vandel, L. (2018). CBP and P300 regulate distinct gene networks required for human primary myoblast differentiation and muscle integrity. *Scientific Reports*, *8*(1), 12629. https://doi.org/10.1038/s41598-018-31102-4

Feige, P., Brun, C. E., Ritso, M., & Rudnicki, M. A. (2018). Orienting Muscle Stem Cells for Regeneration in Homeostasis, Aging, and Disease. *Cell Stem Cell*, *23*(5), 653–664. https://doi.org/10.1016/j.stem.2018.10.006

Fougerousse, F., Durand, M., Lopez, S., Suel, L., Demignon, J., Thornton, C., Ozaki, H., Kawakami, K., Barbet, P., Beckmann, J. S., & Maire, P. (2002). Six and Eya expression during human somitogenesis and MyoD gene family activation. *Journal of Muscle Research and Cell Motility*, *23*(3), 255–264. https://doi.org/10.1023/a:1020990825644

Fuglerud, B. M., Ledsaak, M., Rogne, M., Eskeland, R., & Gabrielsen, O. S. (2018). The pioneer factor activity of c-Myb involves recruitment of p300 and induction of histone acetylation followed by acetylation-induced chromatin dissociation. *Epigenetics & Chromatin*, *11*(1), 35. https://doi.org/10.1186/s13072-018-0208-y

Garcez, R. C., Le Douarin, N. M., & Creuzet, S. E. (2014). Combinatorial activity of Six1-2-4 genes in cephalic neural crest cells controls craniofacial and brain development. *Cellular and Molecular Life Sciences*, *71*(11), 2149–2164. https://doi.org/10.1007/s00018-013-1477-z

Gel, B., Díez-Villanueva, A., Serra, E., Buschbeck, M., Peinado, M. A., & Malinverni, R. (2015). regioneR: An R/Bioconductor package for the association analysis of

genomic regions based on permutation tests. *Bioinformatics*, btv562. https://doi.org/10.1093/bioinformatics/btv562

Ghisletti, S., Barozzi, I., Mietton, F., Polletti, S., De Santa, F., Venturini, E., Gregory, L., Lonie, L., Chew, A., Wei, C.-L., Ragoussis, J., & Natoli, G. (2010). Identification and Characterization of Enhancers Controlling the Inflammatory Gene Expression Program in Macrophages. *Immunity*, *32*(3), 317–328. https://doi.org/10.1016/j.immuni.2010.02.008

Gillespie, M. A., Palii, C. G., Sanchez-Taltavull, D., Shannon, P., Longabaugh, W. J. R., Downes, D. J., Sivaraman, K., Espinoza, H. M., Hughes, J. R., Price, N. D., Perkins, T. J., Ranish, J. A., & Brand, M. (2020). Absolute Quantification of Transcription Factors Reveals Principles of Gene Regulation in Erythropoiesis. *Molecular Cell*, *78*(5), 960-974.e11. https://doi.org/10.1016/j.molcel.2020.03.031

Giordani, L., & Puri, P. L. (2013). Epigenetic control of skeletal muscle regeneration. *The FEBS Journal*, *280*(17), 4014–4025. https://doi.org/10.1111/febs.12383

Girgis, J., Yang, D., Chakroun, I., Liu, Y., & Blais, A. (2021). Six1 promotes skeletal muscle thyroid hormone response through regulation of the MCT10 transporter. *Skeletal Muscle*, *11*(1), 26. https://doi.org/10.1186/s13395-021-00281-6

Grifone, R., Laclef, C., Spitz, F., Lopez, S., Demignon, J., Guidotti, J.-E., Kawakami, K., Xu, P.-X., Kelly, R., Petrof, B. J., Daegelen, D., Concordet, J.-P., & Maire, P. (2004). Six1 and Eya1 Expression Can Reprogram Adult Muscle from the Slow-Twitch Phenotype into the Fast-Twitch Phenotype. *Molecular and Cellular Biology*, *24*(14), 6253–6267. https://doi.org/10.1128/MCB.24.14.6253-6267.2004

Gross, M. K., Moran-Rivard, L., Velasquez, T., Nakatsu, M. N., Jagla, K., & Goulding, M. (2000). Lbx1 is required for muscle precursor migration along a lateral pathway into the limb. *Development*, *127*(2), 413–424. https://doi.org/10.1242/dev.127.2.413

Grossman, S. R. (2001). P300/CBP/p53 interaction and regulation of the p53 response. *European Journal of Biochemistry*, *268*(10), 2773–2778. https://doi.org/10.1046/j.1432-1327.2001.02226.x

Gu, W., & Roeder, R. G. (1997). Activation of p53 sequence-specific DNA binding by acetylation of the p53 C-terminal domain. *Cell*, *90*(4), 595–606. https://doi.org/10.1016/s0092-8674(00)80521-8

Haddix, S. G., Lee, Y. il, Kornegay, J. N., & Thompson, W. J. (2018). Cycles of myofiber degeneration and regeneration lead to remodeling of the neuromuscular junction in two mammalian models of Duchenne muscular dystrophy. *PLOS ONE*, *13*(10), e0205926. https://doi.org/10.1371/journal.pone.0205926

Halevy, O., Novitch, B. G., Spicer, D. B., Skapek, S. X., Rhee, J., Hannon, G. J., Beach, D., & Lassar, A. B. (1995). Correlation of Terminal Cell Cycle Arrest of Skeletal Muscle with Induction of p21 by MyoD. *Science*, *267*(5200), 1018–1021.

Hall, J. K., Banks, G. B., Chamberlain, J. S., & Olwin, B. B. (2010). Prevention of muscle aging by myofiber-associated satellite cell transplantation. *Science Translational Medicine*, *2*(57), 57ra83. https://doi.org/10.1126/scitranslmed.3001081

Hammitzsch, A., Tallant, C., Fedorov, O., O'Mahony, A., Brennan, P. E., Hay, D. A., Martinez, F. O., Al-Mossawi, M. H., de Wit, J., Vecellio, M., Wells, C.,

Wordsworth, P., Müller, S., Knapp, S., & Bowness, P. (2015). CBP30, a selective CBP/p300 bromodomain inhibitor, suppresses human Th17 responses. *Proceedings of the National Academy of Sciences*, *112*(34), 10768–10773. https://doi.org/10.1073/pnas.1501956112

Hammond, K. L., Hanson, I. M., Brown, A. G., Lettice, L. A., & Hill, R. E. (1998). Mammalian and Drosophila dachshund genes are related to the Ski proto-oncogene and are expressed in eye and limb. *Mechanisms of Development*, *74*(1), 121–131. https://doi.org/10.1016/S0925-4773(98)00071-9

Handy, D. E., Castro, R., & Loscalzo, J. (2011). Epigenetic Modifications: Basic Mechanisms and Role in Cardiovascular Disease. *Circulation*, *123*(19), 2145–2156. https://doi.org/10.1161/CIRCULATIONAHA.110.956839

Hanna, L. A., Foreman, R. K., Tarasenko, I. A., Kessler, D. S., & Labosky, P. A. (2002). Requirement for Foxd3 in maintaining pluripotent cells of the early mouse embryo. *Genes & Development*, *16*(20), 2650–2661. https://doi.org/10.1101/gad.1020502

Hasty, P., Bradley, A., Morris, J. H., Edmondson, D. G., Venuti, J. M., Olson, E. N., & Klein, W. H. (1993). Muscle deficiency and neonatal death in mice with a targeted mutation in the myogenin gene. *Nature*, *364*(6437), 501–506. https://doi.org/10.1038/364501a0

Haynes, S. R., Dollard, C., Winston, F., Beck, S., Trowsdale, J., & Dawid, I. B. (1992). The bromodomain: A conserved sequence found in human, Drosophila and yeast proteins. *Nucleic Acids Research*, *20*(10), 2603.

He, Z., Li, G., Tang, L., & Li, Y. (2017). SIX1 overexpression predicts poor prognosis and induces radioresistance through AKT signaling in esophageal squamous cell carcinoma. *OncoTargets and Therapy*, *10*, 1071–1079. https://doi.org/10.2147/OTT.S125330

Heanue, T. A., Reshef, R., Davis, R. J., Mardon, G., Oliver, G., Tomarev, S., Lassar, A. B., & Tabin, C. J. (1999). Synergistic regulation of vertebrate muscle development by Dach2, Eya2, and Six1, homologs of genes required for Drosophila eye formation. *Genes & Development*, *13*(24), 3231–3243.

Hebbes, T. R., Thorne, A. W., & Crane-Robinson, C. (1988). A direct link between core histone acetylation and transcriptionally active chromatin. *The EMBO Journal*, *7*(5), 1395–1402. https://doi.org/10.1002/j.1460-2075.1988.tb02956.x

Henikoff, S. (2008). Nucleosome destabilization in the epigenetic regulation of gene expression. *Nature Reviews Genetics*, *9*(1), 15–26. https://doi.org/10.1038/nrg2206

Henry, R. A., Kuo, Y.-M., & Andrews, A. J. (2013). Differences in Specificity and Selectivity Between CBP and p300 Acetylation of Histone H3 and H3/H4. *Biochemistry*, *52*(34), 5746–5759. https://doi.org/10.1021/bi400684q

Hilton, I. B., D'Ippolito, A. M., Vockley, C. M., Thakore, P. I., Crawford, G. E., Reddy, T. E., & Gersbach, C. A. (2015). Epigenome editing by a CRISPR-Cas9-based acetyltransferase activates genes from promoters and enhancers. *Nature Biotechnology*, *33*(5), 510–517. https://doi.org/10.1038/nbt.3199

Hsieh, C. L. (1994). Dependence of transcriptional repression on CpG methylation density. *Molecular and Cellular Biology*. https://doi.org/10.1128/mcb.14.8.5487-5494.1994

Huber, W., Carey, V. J., Gentleman, R., Anders, S., Carlson, M., Carvalho, B. S., Bravo, H. C., Davis, S., Gatto, L., Girke, T., Gottardo, R., Hahne, F., Hansen, K. D., Irizarry, R. A., Lawrence, M., Love, M. I., MacDonald, J., Obenchain, V., Oleś, A. K., … Morgan, M. (2015). Orchestrating high-throughput genomic analysis with Bioconductor. *Nature Methods*, *12*(2), 115–121. https://doi.org/10.1038/nmeth.3252

Huo, S., Liu, X., Zhang, S., Lyu, Z., Zhang, J., Wang, Y., Nie, B., & Yue, B. (2021). P300/CBP inhibitor A-485 inhibits the differentiation of osteoclasts and protects against osteoporotic bone loss. *International Immunopharmacology*, *94*, 107458. https://doi.org/10.1016/j.intimp.2021.107458

Ikeya, M., & Takada, S. (1998). Wnt signaling from the dorsal neural tube is required for the formation of the medial dermomyotome. *Development (Cambridge, England)*, *125*(24), 4969–4976.

Imhof, A., Yang, X.-J., Ogryzko, V. V., Nakatani, Y., Wolffe, A. P., & Ge, H. (1997). Acetylation of general transcription factors by histone acetyltransferases. *Current Biology*, *7*(9), 689–692. https://doi.org/10.1016/S0960-9822(06)00296-X

Jalili, V., Matteucci, M., Masseroli, M., & Morelli, M. J. (2015). Using combined evidence from replicates to evaluate ChIP-seq peaks. *Bioinformatics*, *31*(17), 2761–2769. https://doi.org/10.1093/bioinformatics/btv293

Jayandharan, Zhong, & Sack. (2010). *Optimized Adeno-Associated Virus (AAV)–Protein Phosphatase-5 Helper Viruses for Efficient Liver Transduction by Single-Stranded AAV Vectors: Therapeutic Expression of Factor IX at Reduced Vector Doses*. https://www.liebertpub.com/doi/epub/10.1089/hum.2009.100

Jones, P. A., & Taylor, S. M. (1980). Cellular differentiation, cytidine analogs and DNA methylation. *Cell*, *20*(1), 85–93. https://doi.org/10.1016/0092-8674(80)90237-8

Kadam, S., & Emerson, B. M. (2003). Transcriptional Specificity of Human SWI/SNF BRG1 and BRM Chromatin Remodeling Complexes. *Molecular Cell*, *11*(2), 377–389. https://doi.org/10.1016/S1097-2765(03)00034-0

Kanno, T., Kanno, Y., LeRoy, G., Campos, E., Sun, H.-W., Brooks, S. R., Vahedi, G., Heightman, T. D., Garcia, B. A., Reinberg, D., Siebenlist, U., O'Shea, J. J., & Ozato, K. (2014). BRD4 assists elongation of both coding and enhancer RNAs guided by histone acetylation. *Nature Structural & Molecular Biology*, *21*(12), 1047–1057. https://doi.org/10.1038/nsmb.2912

Kassar-Duchossoy, L., Gayraud-Morel, B., Gomès, D., Rocancourt, D., Buckingham, M., Shinin, V., & Tajbakhsh, S. (2004). Mrf4 determines skeletal muscle identity in Myf5:Myod double-mutant mice. *Nature*, *431*(7007), 466–471. https://doi.org/10.1038/nature02876

Kawakami, K. (1996). Structure, function and expression of a murine homeobox protein AREC3, a homologue of Drosophila sine oculis gene product, and implication in development. *Nucleic Acids Research*, *24*(2), 303–310. https://doi.org/10.1093/nar/24.2.303

Kaya-Okur, H. S., Janssens, D. H., Henikoff, J. G., Ahmad, K., & Henikoff, S. (2020). Efficient low-cost chromatin profiling with CUT&Tag. *Nature Protocols*, *15*(10), 3264–3283. https://doi.org/10.1038/s41596-020-0373-x

Kaya-Okur, H. S., Wu, S. J., Codomo, C. A., Pledger, E. S., Bryson, T. D., Henikoff, J. G., Ahmad, K., & Henikoff, S. (2019). CUT&Tag for efficient epigenomic profiling of small samples and single cells. *Nature Communications*, *10*(1), 1930. https://doi.org/10.1038/s41467-019-09982-5

Khilji, S., Hamed, M., Chen, J., & Li, Q. (2018). Loci-specific histone acetylation profiles associated with transcriptional coactivator p300 during early myoblast differentiation. *Epigenetics*, *13*(6), 642–654. https://doi.org/10.1080/15592294.2018.1489659

King, K. L., & Cidlowski, J. A. (1998). Cell cycle regulation and apoptosis. *Annual Review of Physiology*, *60*, 601–617. https://doi.org/10.1146/annurev.physiol.60.1.601

Kirby, R. J., Hamilton, G. M., Finnegan, D. J., Johnson, K. J., & Jarman, A. P. (2001). Drosophila homolog of the myotonic dystrophy-associated gene, SIX5, is required for muscle and gonad development. *Current Biology*, *11*(13), 1044–1049. https://doi.org/10.1016/S0960-9822(01)00319-0

Kireeva, M. L., Hancock, B., Cremona, G. H., Walter, W., Studitsky, V. M., & Kashlev, M. (2005). Nature of the Nucleosomal Barrier to RNA Polymerase II. *Molecular Cell*, *18*(1), 97–108. https://doi.org/10.1016/j.molcel.2005.02.027

Kireeva, M. L., Walter, W., Tchernajenko, V., Bondarenko, V., Kashlev, M., & Studitsky, V. M. (2002). Nucleosome Remodeling Induced by RNA Polymerase II: Loss of

the H2A/H2B Dimer during Transcription. *Molecular Cell*, *9*(3), 541–552. https://doi.org/10.1016/S1097-2765(02)00472-0

Klemm, S. L., Shipony, Z., & Greenleaf, W. J. (2019). Chromatin accessibility and the regulatory epigenome. *Nature Reviews Genetics*, *20*(4), 207–220. https://doi.org/10.1038/s41576-018-0089-8

Klesert, T. R., Cho, D. H., Clark, J. I., Maylie, J., Adelman, J., Snider, L., Yuen, E. C., Soriano, P., & Tapscott, S. J. (2000). Mice deficient in Six5 develop cataracts: Implications for myotonic dystrophy. *Nature Genetics*, *25*(1), 105–109. https://doi.org/10.1038/75490

Koenig, M., Hoffman, E. P., Bertelson, C. J., Monaco, A. P., Feener, C., & Kunkel, L. M. (1987). Complete cloning of the duchenne muscular dystrophy (DMD) cDNA and preliminary genomic organization of the DMD gene in normal and affected individuals. *Cell*, *50*(3), 509–517. https://doi.org/10.1016/0092-8674(87)90504-6

Kung, A. L., Rebel, V. I., Bronson, R. T., Ch'ng, L.-E., Sieff, C. A., Livingston, D. M., & Yao, T.-P. (2000). Gene dose-dependent control of hematopoiesis and hematologic tumor suppression by CBP. *Genes & Development*, *14*(3), 272–277.

Kunkel, L. M. (1986). Analysis of deletions in DNA from patients with Becker and Duchenne muscular dystrophy. *Nature*, *322*(6074), 73–77. https://doi.org/10.1038/322073a0

Laclef, C., Hamard, G., Demignon, J., Souil, E., Houbron, C., & Maire, P. (2003a). Altered myogenesis in Six1-deficient mice. *Development*, *130*(10), 2239–2252. https://doi.org/10.1242/dev.00440

Laclef, C., Hamard, G., Demignon, J., Souil, E., Houbron, C., & Maire, P. (2003b). Altered myogenesis in Six1-deficient mice. *Development*, *130*(10), 2239–2252. https://doi.org/10.1242/dev.00440

Laclef, C., Souil, E., Demignon, J., & Maire, P. (2003). Thymus, kidney and craniofacial abnormalities in Six 1 deficient mice. *Mechanisms of Development*, *120*(6), 669–679. https://doi.org/10.1016/s0925-4773(03)00065-0

Landfeldt, E., Thompson, R., Sejersen, T., McMillan, H. J., Kirschner, J., & Lochmüller, H. (2020). Life expectancy at birth in Duchenne muscular dystrophy: A systematic review and meta-analysis. *European Journal of Epidemiology*. https://doi.org/10.1007/s10654-020-00613-8

Lasko, L. M., Jakob, C. G., Edalji, R. P., Qiu, W., Montgomery, D., Digiammarino, E. L., Hansen, T. M., Risi, R. M., Frey, R., Manaves, V., Shaw, B., Algire, M., Hessler, P., Lam, L. T., Uziel, T., Faivre, E., Ferguson, D., Buchanan, F. G., Martin, R. L., … Bromberg, K. D. (2017). Discovery of a potent catalytic p300/CBP inhibitor that targets lineage-specific tumors. *Nature*, *550*(7674), 128–132. https://doi.org/10.1038/nature24028

Lassar, A. B., Buskin, J. N., Lockshon, D., Davis, R. L., Apone, S., Hauschka, S. D., & Weintraub, H. (1989). MyoD is a sequence-specific DNA binding protein requiring a region of myc homology to bind to the muscle creatine kinase enhancer. *Cell*, *58*(5), 823–831. https://doi.org/10.1016/0092-8674(89)90935-5

Lassar, A. B., Paterson, B. M., & Weintraub, H. (1986). Transfection of a DNA locus that mediates the conversion of 10T1 2 fibroblasts to myoblasts. *Cell*, *47*(5), 649–656. https://doi.org/10.1016/0092-8674(86)90507-6

Lau, O. D., Kundu, T. K., Soccio, R. E., Ait-Si-Ali, S., Khalil, E. M., Vassilev, A., Wolffe, A. P., Nakatani, Y., Roeder, R. G., & Cole, P. A. (2000). HATs off: Selective Synthetic Inhibitors of the Histone Acetyltransferases p300 and PCAF. *Molecular Cell*, *5*(3), 589–595. https://doi.org/10.1016/S1097-2765(00)80452-9

Le Grand, F., Grifone, R., Mourikis, P., Houbron, C., Gigaud, C., Pujol, J., Maillet, M., Pagès, G., Rudnicki, M., Tajbakhsh, S., & Maire, P. (2012). Six1 regulates stem cell repair potential and self-renewal during skeletal muscle regeneration. *The Journal of Cell Biology*, *198*(5), 815–832. https://doi.org/10.1083/jcb.201201050

Le Grand, F., Jones, A. E., Seale, V., Scimè, A., & Rudnicki, M. A. (2009). Wnt7a activates the planar cell polarity pathway to drive the symmetric expansion of satellite stem cells. *Cell Stem Cell*, *4*(6), 535–547. https://doi.org/10.1016/j.stem.2009.03.013

Lee, D. Y., Hayes, J. J., Pruss, D., & Wolffe, A. P. (1993). A positive role for histone acetylation in transcription factor access to nucleosomal DNA. *Cell*, *72*(1), 73–84. https://doi.org/10.1016/0092-8674(93)90051-q

Lee, J.-E., Park, Y.-K., Park, S., Jang, Y., Waring, N., Dey, A., Ozato, K., Lai, B., Peng, W., & Ge, K. (2017). Brd4 binds to active enhancers to control cell identity gene induction in adipogenesis and myogenesis. *Nature Communications*, *8*(1), 2217. https://doi.org/10.1038/s41467-017-02403-5

Lemma, R. B., Ledsaak, M., Fuglerud, B. M., Sandve, G. K., Eskeland, R., & Gabrielsen, O. S. (2021). Chromatin occupancy and target genes of the haematopoietic master transcription factor MYB. *Scientific Reports*, *11*(1), 9008. https://doi.org/10.1038/s41598-021-88516-w

Li, C., & Samulski, R. J. (2020). Engineering adeno-associated virus vectors for gene therapy. *Nature Reviews Genetics*, *21*(4), 255–272. https://doi.org/10.1038/s41576-019-0205-4

Li, G., Levitus, M., Bustamante, C., & Widom, J. (2005). Rapid spontaneous accessibility of nucleosomal DNA. *Nature Structural & Molecular Biology*, *12*(1), 46–53. https://doi.org/10.1038/nsmb869

Li, H., Handsaker, B., Wysoker, A., Fennell, T., Ruan, J., Homer, N., Marth, G., Abecasis, G., Durbin, R., & 1000 Genome Project Data Processing Subgroup. (2009). The Sequence Alignment/Map format and SAMtools. *Bioinformatics*, *25*(16), 2078–2079. https://doi.org/10.1093/bioinformatics/btp352

Li, X., Oghi, K. A., Zhang, J., Krones, A., Bush, K. T., Glass, C. K., Nigam, S. K., Aggarwal, A. K., Maas, R., Rose, D. W., & Rosenfeld, M. G. (2003). Eya protein phosphatase activity regulates Six1-Dach-Eya transcriptional effects in mammalian organogenesis. *Nature*, *426*(6964), 247–254. https://doi.org/10.1038/nature02083

Li, X., Perissi, V., Liu, F., Rose, D. W., & Rosenfeld, M. G. (2002). Tissue-Specific Regulation of Retinal and Pituitary Precursor Cell Proliferation. *Science*, *297*(5584), 1180–1183. https://doi.org/10.1126/science.1073263

Li, Z., Tian, T., Lv, F., Chang, Y., Wang, X., Zhang, L., Li, X., Li, L., Ma, W., Wu, J., & Zhang, M. (2013). Six1 Promotes Proliferation of Pancreatic Cancer Cells via Upregulation of Cyclin D1 Expression. *PLOS ONE*, *8*(3), e59203. https://doi.org/10.1371/journal.pone.0059203

Liao, Y., Smyth, G. K., & Shi, W. (2014). featureCounts: An efficient general purpose program for assigning sequence reads to genomic features. *Bioinformatics*, *30*(7), 923–930. https://doi.org/10.1093/bioinformatics/btt656

Lilja, K. C., Zhang, N., Magli, A., Gunduz, V., Bowman, C. J., Arpke, R. W., Darabi, R., Kyba, M., Perlingeiro, R., & Dynlacht, B. D. (2017). Pax7 remodels the chromatin landscape in skeletal muscle stem cells. *PLoS ONE*, *12*(4), e0176190. https://doi.org/10.1371/journal.pone.0176190

Linker, C., Lesbros, C., Gros, J., Burrus, L. W., Rawls, A., & Marcelle, C. (2005). β-Catenin-dependent Wnt signalling controls the epithelial organisation of somites through the activation of *paraxis*. *Development*, *132*(17), 3895–3905. https://doi.org/10.1242/dev.01961

Liu, Q., Li, A., Tian, Y., Liu, Y., Li, T., Zhang, C., Wu, J. D., Han, X., & Wu, K. (2016). The expression profile and clinic significance of the SIX family in non-small cell lung cancer. *Journal of Hematology & Oncology*, *9*(1), 119. https://doi.org/10.1186/s13045-016-0339-1

Liu, Y. (2017). *The Role of Six1 in Transcriptional Regulation during Myogenesis*. https://ruor.uottawa.ca/handle/10393/35952

Liu, Y., Chakroun, I., Yang, D., Horner, E., Liang, J., Aziz, A., Chu, A., De Repentigny, Y., Dilworth, F. J., Kothary, R., & Blais, A. (2013). Six1 Regulates MyoD Expression in Adult Muscle Progenitor Cells. *PLoS ONE*, *8*(6). https://doi.org/10.1371/journal.pone.0067762

Liu, Y., Chu, A., Chakroun, I., Islam, U., & Blais, A. (2010). Cooperation between myogenic regulatory factors and SIX family transcription factors is important for

myoblast differentiation. *Nucleic Acids Research*, *38*(20), 6857–6871. https://doi.org/10.1093/nar/gkq585

Liu, Y., Nandi, S., Martel, A., Antoun, A., Ioshikhes, I., & Blais, A. (2012). Discovery, optimization and validation of an optimal DNA-binding sequence for the Six1 homeodomain transcription factor. *Nucleic Acids Research*, *40*(17), 8227–8239. https://doi.org/10.1093/nar/gks587

Lock, M., Alvira, M., Vandenberghe, L. H., Samanta, A., Toelen, J., Debyser, Z., & Wilson, J. M. (2010). Rapid, Simple, and Versatile Manufacturing of Recombinant Adeno-Associated Viral Vectors at Scale. *Human Gene Therapy*, *21*(10), 1259–1271. https://doi.org/10.1089/hum.2010.055

Long, C., Amoasii, L., Mireault, A. A., McAnally, J. R., Li, H., Sanchez-Ortiz, E., Bhattacharyya, S., Shelton, J. M., Bassel-Duby, R., & Olson, E. N. (2016). Postnatal genome editing partially restores dystrophin expression in a mouse model of muscular dystrophy. *Science (New York, N.Y.)*, *351*(6271), 400–403. https://doi.org/10.1126/science.aad5725

Loosli, F., Köster, R. W., Carl, M., Krone, A., & Wittbrodt, J. (1998). Six3, a medaka homologue of the Drosophila homeobox gene sine oculis is expressed in the anterior embryonic shield and the developing eye. *Mechanisms of Development*, *74*(1), 159–164. https://doi.org/10.1016/S0925-4773(98)00055-0

Lyons, G. E., Ontell, M., Cox, R., Sassoon, D., & Buckingham, M. (1990). The expression of myosin genes in developing skeletal muscle in the mouse embryo. *Journal of Cell Biology*, *111*(4), 1465–1476. https://doi.org/10.1083/jcb.111.4.1465

Magnani, L., Eeckhoute, J., & Lupien, M. (2011). Pioneer factors: Directing transcriptional regulators within the chromatin environment. *Trends in Genetics*, *27*(11), 465–474. https://doi.org/10.1016/j.tig.2011.07.002

Mah, J. K., Korngut, L., Dykeman, J., Day, L., Pringsheim, T., & Jette, N. (2014). A systematic review and meta-analysis on the epidemiology of Duchenne and Becker muscular dystrophy. *Neuromuscular Disorders*, *24*(6), 482–491. https://doi.org/10.1016/j.nmd.2014.03.008

Maire, P., Dos Santos, M., Madani, R., Sakakibara, I., Viaut, C., & Wurmser, M. (2020). Myogenesis control by SIX transcriptional complexes. *Seminars in Cell & Developmental Biology*, *104*, 51–64. https://doi.org/10.1016/j.semcdb.2020.03.003

Mal, A., Sturniolo, M., Schiltz, R. L., Ghosh, M. K., & Harter, M. L. (2001). A role for histone deacetylase HDAC1 in modulating the transcriptional activity of MyoD: Inhibition of the myogenic program. *The EMBO Journal*, *20*(7), 1739–1753. https://doi.org/10.1093/emboj/20.7.1739

Malhotra, S. B., Hart, K. A., Klamut, H. J., Thomas, N. S. T., Bodrug, S. E., Burghes, A. H. M., Bobrow, M., Harper, P. S., Thompson, M. W., Ray, P. N., & Worton, R. G. (1988). Frame-Shift Deletions in Patients with Duchenne and Becker Muscular Dystrophy. *Science*, *242*(4879), 755–759. https://doi.org/10.1126/science.3055295

Manning, E. T., Ikehara, T., Ito, T., Kadonaga, J. T., & Kraus, W. L. (2001). p300 forms a stable, template-committed complex with chromatin: Role for the bromodomain.

Molecular and Cellular Biology, *21*(12), 3876–3887. https://doi.org/10.1128/MCB.21.12.3876-3887.2001

Maroto, M., Reshef, R., Münsterberg, A. E., Koester, S., Goulding, M., & Lassar, A. B. (1997). Ectopic Pax-3 Activates MyoD and Myf-5 Expression in Embryonic Mesoderm and Neural Tissue. *Cell*, *89*(1), 139–148. https://doi.org/10.1016/S0092-8674(00)80190-7

Marsden, I., Jin, C., & Liao, X. (1998). Structural changes in the region directly adjacent to the DNA-binding helix highlight a possible mechanism to explain the observed changes in the sequence-specific binding of winged helix proteins11Edited by P. E. Wright. *Journal of Molecular Biology*, *278*(2), 293–299. https://doi.org/10.1006/jmbi.1998.1703

Martire, S., Nguyen, J., Sundaresan, A., & Banaszynski, L. A. (2020). Differential contribution of p300 and CBP to regulatory element acetylation in mESCs. *BMC Molecular and Cell Biology*, *21*, 55. https://doi.org/10.1186/s12860-020-00296-9

Mauro, A. (1961). Satellite cell of skeletal muscle fibers. *The Journal of Biophysical and Biochemical Cytology*, *9*, 493–495. https://doi.org/10.1083/jcb.9.2.493

Maves, L., Waskiewicz, A. J., Paul, B., Cao, Y., Tyler, A., Moens, C. B., & Tapscott, S. J. (2007). Pbx homeodomain proteins direct Myod activity to promote fast-muscle differentiation. *Development (Cambridge, England)*, *134*(18), 3371–3382. https://doi.org/10.1242/dev.003905

McShane, E., Sin, C., Zauber, H., Wells, J. N., Donnelly, N., Wang, X., Hou, J., Chen, W., Storchova, Z., Marsh, J. A., Valleriani, A., & Selbach, M. (2016). Kinetic

Analysis of Protein Stability Reveals Age-Dependent Degradation. *Cell*, *167*(3), 803-815.e21. https://doi.org/10.1016/j.cell.2016.09.015

Megeney, L. A., Kablar, B., Garrett, K., Anderson, J. E., & Rudnicki, M. A. (1996). MyoD is required for myogenic stem cell function in adult skeletal muscle. *Genes & Development*, *10*(10), 1173–1183. https://doi.org/10.1101/gad.10.10.1173

Mersfelder, E. L., & Parthun, M. R. (2006). The tale beyond the tail: Histone core domain modifications and the regulation of chromatin structure. *Nucleic Acids Research*, *34*(9), 2653–2662. https://doi.org/10.1093/nar/gkl338

Mi, H., Ebert, D., Muruganujan, A., Mills, C., Albou, L.-P., Mushayamaha, T., & Thomas, P. D. (2021). PANTHER version 16: A revised family classification, tree-based classification tool, enhancer regions and extensive API. *Nucleic Acids Research*, *49*(D1), D394–D403. https://doi.org/10.1093/nar/gkaa1106

Mi, H., Muruganujan, A., Casagrande, J. T., & Thomas, P. D. (2013). Large-scale gene function analysis with the PANTHER classification system. *Nature Protocols*, *8*(8), 1551–1566. https://doi.org/10.1038/nprot.2013.092

Miller, R. g., Sharma, K. r., Pavlath, G. k., Gussoni, E., Mynhier, M., Yu, P., Lanctot, A. m., Greco, C. m., Steinman, L., & Blau, H. m. (1997). Myoblast implantation in Duchenne muscular dystrophy: The San Francisco study. *Muscle & Nerve*, *20*(4), 469–478. https://doi.org/10.1002/(SICI)1097-4598(199704)20:4<469::AID-MUS10>3.0.CO;2-U

Mizzen, C. A., & Allis, C. D. (1998). Linking histone acetylation to transcriptional regulation. *Cellular and Molecular Life Sciences (CMLS)*, *54*(1), 6–20. https://doi.org/10.1007/s000180050121

Modis, Y., & Wierenga, R. (1998). Two crystal structures of N-acetyltransferases reveal a new fold for CoA-dependent enzymes. *Structure (London, England: 1993)*, *6*(11), 1345–1350. https://doi.org/10.1016/s0969-2126(98)00134-8

Molina-Serrano, D., & Kirmizis, A. (2013). Beyond the histone tail. *Nucleus*, *4*(5), 343–348. https://doi.org/10.4161/nucl.26051

Molkentin, J. D., Black, B. L., Martin, J. F., & Olson, E. N. (1995). Cooperative activation of muscle gene expression by MEF2 and myogenic bHLH proteins. *Cell*, *83*(7), 1125–1136. https://doi.org/10.1016/0092-8674(95)90139-6

Mourikis, P., & Tajbakhsh, S. (2014). Distinct contextual roles for Notch signalling in skeletal muscle stem cells. *BMC Developmental Biology*, *14*(1), 2. https://doi.org/10.1186/1471-213X-14-2

Muir, L. A., & Chamberlain, J. S. (2009). Emerging strategies for cell and gene therapy of the muscular dystrophies. *Expert Reviews in Molecular Medicine*, *11*, e18. https://doi.org/10.1017/S1462399409001100

Mujtaba, S., He, Y., Zeng, L., Yan, S., Plotnikova, O., Sachchidanand, null, Sanchez, R., Zeleznik-Le, N. J., Ronai, Z., & Zhou, M.-M. (2004). Structural mechanism of the bromodomain of the coactivator CBP in p53 transcriptional activation. *Molecular Cell*, *13*(2), 251–263. https://doi.org/10.1016/s1097-2765(03)00528-8

Narita, T., Ito, S., Higashijima, Y., Chu, W. K., Neumann, K., Walter, J., Satpathy, S., Liebner, T., Hamilton, W. B., Maskey, E., Prus, G., Shibata, M., Iesmantavicius, V., Brickman, J. M., Anastassiadis, K., Koseki, H., & Choudhary, C. (2021). Enhancers are activated by p300/CBP activity-dependent PIC assembly, RNAPII

recruitment, and pause release. *Molecular Cell*, S1097276521001763. https://doi.org/10.1016/j.molcel.2021.03.008

Nelson, C. E., Hakim, C. H., Ousterout, D. G., Thakore, P. I., Moreb, E. A., Rivera, R. M. C., Madhavan, S., Pan, X., Ran, F. A., Yan, W. X., Asokan, A., Zhang, F., Duan, D., & Gersbach, C. A. (2016). In vivo genome editing improves muscle function in a mouse model of Duchenne muscular dystrophy. *Science*, *351*(6271), 403–407. https://doi.org/10.1126/science.aad5143

Nelson, C. E., Wu, Y., Gemberling, M. P., Oliver, M. L., Waller, M. A., Bohning, J. D., Robinson-Hamm, J. N., Bulaklak, K., Castellanos Rivera, R. M., Collier, J. H., Asokan, A., & Gersbach, C. A. (2019). Long-term evaluation of AAV-CRISPR genome editing for Duchenne muscular dystrophy. *Nature Medicine*, *25*(3), 427–432. https://doi.org/10.1038/s41591-019-0344-3

Nicolas, A., Raguénès-Nicol, C., Ben Yaou, R., Ameziane-Le Hir, S., Chéron, A., Vié, V., Claustres, M., Leturcq, F., Delalande, O., Hubert, J.-F., Tuffery-Giraud, S., Giudice, E., Le Rumeur, E., & the French Network of Clinical Reference Centres for Neuromuscular Diseases (CORNEMUS). (2015). Becker muscular dystrophy severity is linked to the structure of dystrophin. *Human Molecular Genetics*, *24*(5), 1267–1279. https://doi.org/10.1093/hmg/ddu537

Nigro, G., Comi, L. I., Politano, L., & Bain, R. J. I. (1990). The incidence and evolution of cardiomyopathy in Duchenne muscular dystrophy. *International Journal of Cardiology*, *26*(3), 271–277. https://doi.org/10.1016/0167-5273(90)90082-G

Ogryzko, V. V., Schiltz, R. L., Russanova, V., Howard, B. H., & Nakatani, Y. (1996). The Transcriptional Coactivators p300 and CBP Are Histone Acetyltransferases. *Cell*, *87*(5), 953–959. https://doi.org/10.1016/S0092-8674(00)82001-2

Ohkawa, Y., Marfella, C. G., & Imbalzano, A. N. (2006). Skeletal muscle specification by myogenin and Mef2D via the SWI/SNF ATPase Brg1. *The EMBO Journal*, *25*(3), 490–501. https://doi.org/10.1038/sj.emboj.7600943

Olguin, Yang, Tapscott, & Olwin. (2007). *Reciprocal inhibition between Pax7 and muscle regulatory factors modulates myogenic cell fate determination | Journal of Cell Biology | Rockefeller University Press*. https://rupress.org/jcb/article/177/5/769/44848/Reciprocal-inhibition-between-Pax7-and-muscle

Oliver, G., Mailhos, A., Wehr, R., Copeland, N. G., Jenkins, N. A., & Gruss, P. (1995). Six3, a murine homologue of the sine oculis gene, demarcates the most anterior border of the developing neural plate and is expressed during eye development. *Development*, *121*(12), 4045–4055. https://doi.org/10.1242/dev.121.12.4045

Olson, E. N. (2021). Toward the correction of muscular dystrophy by gene editing. *Proceedings of the National Academy of Sciences*, *118*(22), e2004840117. https://doi.org/10.1073/pnas.2004840117

Ozaki, H., Watanabe, Y., Takahashi, K., Kitamura, K., Tanaka, A., Urase, K., Momoi, T., Sudo, K., Sakagami, J., Asano, M., Iwakura, Y., & Kawakami, K. (2001). Six4, a Putative myogeninGene Regulator, Is Not Essential for Mouse Embryonal Development. *Molecular and Cellular Biology*. https://doi.org/10.1128/MCB.21.10.3343-3350.2001

Pandolfi, E. C., Tonsfeldt, K. J., Hoffmann, H. M., & Mellon, P. L. (2019). Deletion of the Homeodomain Protein Six6 From GnRH Neurons Decreases GnRH Gene Expression, Resulting in Infertility. *Endocrinology*, *160*(9), 2151–2164. https://doi.org/10.1210/en.2019-00113

Pasini, D., Malatesta, M., Jung, H. R., Walfridsson, J., Willer, A., Olsson, L., Skotte, J., Wutz, A., Porse, B., Jensen, O. N., & Helin, K. (2010). Characterization of an antagonistic switch between histone H3 lysine 27 methylation and acetylation in the transcriptional regulation of Polycomb group target genes. *Nucleic Acids Research*, *38*(15), 4958–4969. https://doi.org/10.1093/nar/gkq244

Patrick, A. N., Cabrera, J. H., Smith, A. L., Chen, X. S., Ford, H. L., & Zhao, R. (2013). Structure-function analyses of the human SIX1–EYA2 complex reveal insights into metastasis and BOR syndrome. *Nature Structural & Molecular Biology*, *20*(4), 447–453. https://doi.org/10.1038/nsmb.2505

Peng, J., Li, J., Huang, J., Xu, P., Huang, H., Liu, Y., Yu, L., Yang, Y., Zhou, B., Jiang, H., Chen, K., Dang, Y., Zhang, Y., Luo, C., & Li, G. (2019). P300/CBP inhibitor A-485 alleviates acute liver injury by regulating macrophage activation and polarization. *Theranostics*, *9*(26), 8344–8361. https://doi.org/10.7150/thno.30707

Pengelly, A. R., Copur, Ö., Jäckle, H., Herzig, A., & Müller, J. (2013). A histone mutant reproduces the phenotype caused by loss of histone-modifying factor Polycomb. *Science (New York, N.Y.)*, *339*(6120), 698–699. https://doi.org/10.1126/science.1231382

Petrof, B. J., Shrager, J. B., Stedman, H. H., Kelly, A. M., & Sweeney, H. L. (1993). Dystrophin protects the sarcolemma from stresses developed during muscle

contraction. *Proceedings of the National Academy of Sciences*, *90*(8), 3710–3714. https://doi.org/10.1073/pnas.90.8.3710

Picard Tools—By Broad Institute. (n.d.). Retrieved January 6, 2022, from http://broadinstitute.github.io/picard/

Pradeepa, M. M. (2016). Causal role of histone acetylations in enhancer function. *Transcription*, *8*(1), 40–47. https://doi.org/10.1080/21541264.2016.1253529

Pradeepa, M. M., Grimes, G. R., Kumar, Y., Olley, G., Taylor, G. C. A., Schneider, R., & Bickmore, W. A. (2016). Histone H3 globular domain acetylation identifies a new class of enhancers. *Nature Genetics*, *48*(6), 681–686. https://doi.org/10.1038/ng.3550

Price, F. D., Kuroda, K., & Rudnicki, M. A. (2007). Stem cell based therapies to treat muscular dystrophy. *Biochimica et Biophysica Acta (BBA) - Molecular Basis of Disease*, *1772*(2), 272–283. https://doi.org/10.1016/j.bbadis.2006.08.011

Puri, P. L., Avantaggiati, M. L., Balsano, C., Sang, N., Graessmann, A., Giordano, A., & Levrero, M. (1997). P300 is required for MyoD-dependent cell cycle arrest and muscle-specific gene transcription. *The EMBO Journal*, *16*(2), 369–383. https://doi.org/10.1093/emboj/16.2.369

Puri, P. L., Iezzi, S., Stiegler, P., Chen, T. T., Schiltz, R. L., Muscat, G. E., Giordano, A., Kedes, L., Wang, J. Y., & Sartorelli, V. (2001). Class I histone deacetylases sequentially interact with MyoD and pRb during skeletal myogenesis. *Molecular Cell*, *8*(4), 885–897. https://doi.org/10.1016/s1097-2765(01)00373-2

Puri, P. L., Sartorelli, V., Yang, X.-J., Hamamori, Y., Ogryzko, V. V., Howard, B. H., Kedes, L., Wang, J. Y. J., Graessmann, A., Nakatani, Y., & Levrero, M. (1997).

Differential Roles of p300 and PCAF Acetyltransferases in Muscle Differentiation. *Molecular Cell*, *1*(1), 35–45. https://doi.org/10.1016/S1097-2765(00)80005-2

Quinlan, A. R., & Hall, I. M. (2010). BEDTools: A flexible suite of utilities for comparing genomic features. *Bioinformatics (Oxford, England)*, *26*(6), 841–842. https://doi.org/10.1093/bioinformatics/btq033

Ragvin, A., Valvatne, H., Erdal, S., Arskog, V., Tufteland, K. R., Breen, K., ØYan, A. M., Eberharter, A., Gibson, T. J., Becker, P. B., & Aasland, R. (2004). Nucleosome binding by the bromodomain and PHD finger of the transcriptional cofactor p300. *Journal of Molecular Biology*, *337*(4), 773–788. https://doi.org/10.1016/j.jmb.2004.01.051

Rahnamoun, H., Lee, J., Sun, Z., Lu, H., Ramsey, K. M., Komives, E. A., & Lauberth, S. M. (2018). RNAs interact with BRD4 to promote enhanced chromatin engagement and transcription activation. *Nature Structural & Molecular Biology*, *25*(8), 687–697. https://doi.org/10.1038/s41594-018-0102-0

Raisner, R., Kharbanda, S., Jin, L., Jeng, E., Chan, E., Merchant, M., Haverty, P. M., Bainer, R., Cheung, T., Arnott, D., Flynn, E. M., Romero, F. A., Magnuson, S., & Gascoigne, K. E. (2018). Enhancer Activity Requires CBP/P300 Bromodomain-Dependent Histone H3K27 Acetylation. *Cell Reports*, *24*(7), 1722–1729. https://doi.org/10.1016/j.celrep.2018.07.041

Ramírez, F., Ryan, D. P., Grüning, B., Bhardwaj, V., Kilpert, F., Richter, A. S., Heyne, S., Dündar, F., & Manke, T. (2016). deepTools2: A next generation web server for deep-sequencing data analysis. *Nucleic Acids Research*, *44*(W1), W160–W165. https://doi.org/10.1093/nar/gkw257

Rayagiri, S. S., Ranaldi, D., Raven, A., Mohamad Azhar, N. I. F., Lefebvre, O., Zammit, P. S., & Borycki, A.-G. (2018). Basal lamina remodeling at the skeletal muscle stem cell niche mediates stem cell self-renewal. *Nature Communications*, *9*(1), 1075. https://doi.org/10.1038/s41467-018-03425-3

Relaix, F., Demignon, J., Laclef, C., Pujol, J., Santolini, M., Niro, C., Lagha, M., Rocancourt, D., Buckingham, M., & Maire, P. (2013). Six Homeoproteins Directly Activate Myod Expression in the Gene Regulatory Networks That Control Early Myogenesis. *PLOS Genetics*, *9*(4), e1003425. https://doi.org/10.1371/journal.pgen.1003425

Risso, D., Ngai, J., Speed, T. P., & Dudoit, S. (2014). Normalization of RNA-seq data using factor analysis of control genes or samples. *Nature Biotechnology*, *32*(9), 896–902. https://doi.org/10.1038/nbt.2931

Risson, V., Mazelin, L., Roceri, M., Sanchez, H., Moncollin, V., Corneloup, C., Richard-Bulteau, H., Vignaud, A., Baas, D., Defour, A., Freyssenet, D., Tanti, J.-F., Le-Marchand-Brustel, Y., Ferrier, B., Conjard-Duplany, A., Romanino, K., Bauché, S., Hantaï, D., Mueller, M., … Gangloff, Y.-G. (2009). Muscle inactivation of mTOR causes metabolic and dystrophin defects leading to severe myopathy. *Journal of Cell Biology*, *187*(6), 859–874. https://doi.org/10.1083/jcb.200903131

Roberts, T. C., Etxaniz, U., Dall'Agnese, A., Wu, S.-Y., Chiang, C.-M., Brennan, P. E., Wood, M. J. A., & Puri, P. L. (2017). BRD3 and BRD4 BET Bromodomain Proteins Differentially Regulate Skeletal Myogenesis. *Scientific Reports*, *7*(1), 6153. https://doi.org/10.1038/s41598-017-06483-7

Robinson, M. D., McCarthy, D. J., & Smyth, G. K. (2010). edgeR: A Bioconductor package for differential expression analysis of digital gene expression data. *Bioinformatics*, *26*(1), 139–140. https://doi.org/10.1093/bioinformatics/btp616

Rosenberg, I. H. (1997). *Sarcopenia: Origins and Clinical Relevance*. https://academic-oup-com.proxy.bib.uottawa.ca/jn/article/127/5/990S/4724144

Roth, J.-F., Shikama, N., Henzen, C., Desbaillets, I., Lutz, W., Marino, S., Wittwer, J., Schorle, H., Gassmann, M., & Eckner, R. (2003). Differential role of p300 and CBP acetyltransferase during myogenesis: P300 acts upstream of MyoD and Myf5. *The EMBO Journal*, *22*(19), 5186–5196. https://doi.org/10.1093/emboj/cdg473

Rudnicki, M. A., Braun, T., Hinuma, S., & Jaenisch, R. (1992). Inactivation of MyoD in mice leads to up-regulation of the myogenic HLH gene Myf-5 and results in apparently normal muscle development. *Cell*, *71*(3), 383–390. https://doi.org/10.1016/0092-8674(92)90508-a

Rudnicki, M. A., Schnegelsberg, P. N. J., Stead, R. H., Braun, T., Arnold, H.-H., & Jaenisch, R. (1993). MyoD or Myf-5 is required for the formation of skeletal muscle. *Cell*, *75*(7), 1351–1359. https://doi.org/10.1016/0092-8674(93)90621-V

Ruijter, A. J. M. de, GENNIP, A. H. van, CARON, H. N., KEMP, S., & KUILENBURG, A. B. P. van. (2003). Histone deacetylases (HDACs): Characterization of the classical HDAC family. *Biochemical Journal*, *370*(3), 737–749. https://doi.org/10.1042/bj20021321

Sassoon, D., Lyons, G., Wright, W. E., Lin, V., Lassar, A., Weintraub, H., & Buckingham, M. (1989). Expression of two myogenic regulatory factors myogenin

and MyoDl during mouse embryogenesis. *Nature*, *341*(6240), 303–307. https://doi.org/10.1038/341303a0

Scadden, D. T. (2006). The stem-cell niche as an entity of action. *Nature*, *441*(7097), 1075–1079. https://doi.org/10.1038/nature04957

Schiaffino, S., & Reggiani, C. (2011). Fiber Types in Mammalian Skeletal Muscles. *Physiological Reviews*, *91*(4), 1447–1531. https://doi.org/10.1152/physrev.00031.2010

Schiltz, R. L., Mizzen, C. A., Vassilev, A., Cook, R. G., Allis, C. D., & Nakatani, Y. (1999). Overlapping but Distinct Patterns of Histone Acetylation by the Human Coactivators p300 and PCAF within Nucleosomal Substrates *. *Journal of Biological Chemistry*, *274*(3), 1189–1192. https://doi.org/10.1074/jbc.274.3.1189

Seale, P., Asakura, A., & Rudnicki, M. A. (2001). The Potential of Muscle Stem Cells. *Developmental Cell*, *1*(3), 333–342. https://doi.org/10.1016/S1534-5807(01)00049-1

Seenundun, S., Rampalli, S., Liu, Q.-C., Aziz, A., Palii, C., Hong, S., Blais, A., Brand, M., Ge, K., & Dilworth, F. J. (2010). UTX mediates demethylation of H3K27me3 at muscle-specific genes during myogenesis. *The EMBO Journal*, *29*(8), 1401–1411. https://doi.org/10.1038/emboj.2010.37

Serikaku, M. A., & O'Tousa, J. E. (1994). Sine oculis is a homeobox gene required for Drosophila visual system development. *Genetics*, *138*(4), 1137–1150. https://doi.org/10.1093/genetics/138.4.1137

Shahbazian, M. D., & Grunstein, M. (2007). Functions of Site-Specific Histone Acetylation and Deacetylation. *Annual Review of Biochemistry*, *76*(1), 75–100. https://doi.org/10.1146/annurev.biochem.76.052705.162114

Singh, K., Cassano, M., Planet, E., Sebastian, S., Jang, S. M., Sohi, G., Faralli, H., Choi, J., Youn, H.-D., Dilworth, F. J., & Trono, D. (2015). A KAP1 phosphorylation switch controls MyoD function during skeletal muscle differentiation. *Genes & Development*, *29*(5), 513–525. https://doi.org/10.1101/gad.254532.114

Siriett, V., Platt, L., Salerno, M. S., Ling, N., Kambadur, R., & Sharma, M. (2006). Prolonged absence of myostatin reduces sarcopenia. *Journal of Cellular Physiology*, *209*(3), 866–873. https://doi.org/10.1002/jcp.20778

Smale, S. T. (2010). Pioneer factors in embryonic stem cells and differentiation. *Current Opinion in Genetics & Development*, *20*(5), 519–526. https://doi.org/10.1016/j.gde.2010.06.010

Spitz, F., Demignon, J., Porteu, A., Kahn, A., Concordet, J.-P., Daegelen, D., & Maire, P. (1998). Expression of myogenin during embryogenesis is controlled by Six/sine oculis homeoproteins through a conserved MEF3 binding site. *Proceedings of the National Academy of Sciences*, *95*(24), 14220–14225. https://doi.org/10.1073/pnas.95.24.14220

Starkey, J. D., Yamamoto, M., Yamamoto, S., & Goldhamer, D. J. (2011). Skeletal Muscle Satellite Cells Are Committed to Myogenesis and Do Not Spontaneously Adopt Nonmyogenic Fates. *Journal of Histochemistry & Cytochemistry*, *59*(1), 33–46. https://doi.org/10.1369/jhc.2010.956995

Sternglanz, R., & Schindelin, H. (1999). Structure and mechanism of action of the histone acetyltransferase Gcn5 and similarity to other N-acetyltransferases. *Proceedings of the National Academy of Sciences of the United States of America*, *96*(16), 8807–8808. https://doi.org/10.1073/pnas.96.16.8807

Sun, H., Yang, X., Zhu, J., Lv, T., Chen, Y., Chen, G., Zhong, L., Li, Y., Huang, X., Huang, G., & Tian, J. (2010). Inhibition of p300-HAT results in a reduced histone acetylation and down-regulation of gene expression in cardiac myocytes. *Life Sciences*, *87*(23), 707–714. https://doi.org/10.1016/j.lfs.2010.10.009

Supek, F., Bošnjak, M., Škunca, N., & Šmuc, T. (2011). REVIGO Summarizes and Visualizes Long Lists of Gene Ontology Terms. *PLOS ONE*, *6*(7), e21800. https://doi.org/10.1371/journal.pone.0021800

Tabebordbar, M., Lagerborg, K. A., Stanton, A., King, E. M., Ye, S., Tellez, L., Krunnfusz, A., Tavakoli, S., Widrick, J. J., Messemer, K. A., Troiano, E. C., Moghadaszadeh, B., Peacker, B. L., Leacock, K. A., Horwitz, N., Beggs, A. H., Wagers, A. J., & Sabeti, P. C. (2021). Directed evolution of a family of AAV capsid variants enabling potent muscle-directed gene delivery across species. *Cell*, *184*(19), 4919-4938.e22. https://doi.org/10.1016/j.cell.2021.08.028

Tamkun, J. W., Deuring, R., Scott, M. P., Kissinger, M., Pattatucci, A. M., Kaufman, T. C., & Kennison, J. A. (1992). brahma: A regulator of Drosophila homeotic genes structurally related to the yeast transcriptional activator SNF2SWI2. *Cell*, *68*(3), 561–572. https://doi.org/10.1016/0092-8674(92)90191-E

Tamura, I., Maekawa, R., Jozaki, K., Ohkawa, Y., Takagi, H., Doi-Tanaka, Y., Shirafuta, Y., Mihara, Y., Taketani, T., Sato, S., Tamura, H., & Sugino, N. (2021).

Transcription factor C/EBPβ induces genome-wide H3K27ac and upregulates gene expression during decidualization of human endometrial stromal cells. *Molecular and Cellular Endocrinology*, *520*, 111085. https://doi.org/10.1016/j.mce.2020.111085

Tapscott, S. J., Davis, R. L., Thayer, M. J., Cheng, P. F., Weintraub, H., & Lassar, A. B. (1988). MyoD1: A nuclear phosphoprotein requiring a Myc homology region to convert fibroblasts to myoblasts. *Science (New York, N.Y.)*, *242*(4877), 405–411. https://doi.org/10.1126/science.3175662

Tercero, J. C., Riles, L. E., & Wickner, R. B. (1992). Localized mutagenesis and evidence for post-transcriptional regulation of MAK3. A putative N-acetyltransferase required for double-stranded RNA virus propagation in Saccharomyces cerevisiae. *The Journal of Biological Chemistry*, *267*(28), 20270–20276.

Terranova, R., Sauer, S., Merkenschlager, M., & Fisher, A. G. (2005). The reorganisation of constitutive heterochromatin in differentiating muscle requires HDAC activity. *Experimental Cell Research*, *310*(2), 344–356. https://doi.org/10.1016/j.yexcr.2005.07.031

Thayer, M. J., Tapscott, S. J., Davis, R. L., Wright, W. E., Lassar, A. B., & Weintraub, H. (1989). Positive autoregulation of the myogenic determination gene MyoD1. *Cell*, *58*(2), 241–248. https://doi.org/10.1016/0092-8674(89)90838-6

Thompson, P. R., Wang, D., Wang, L., Fulco, M., Pediconi, N., Zhang, D., An, W., Ge, Q., Roeder, R. G., Wong, J., Levrero, M., Sartorelli, V., Cotter, R. J., & Cole, P.

A. (2004). Regulation of the p300 HAT domain via a novel activation loop. *Nature Structural & Molecular Biology*, *11*(4), 308–315. https://doi.org/10.1038/nsmb740

Tie, F., Banerjee, R., Stratton, C. A., Prasad-Sinha, J., Stepanik, V., Zlobin, A., Diaz, M. O., Scacheri, P. C., & Harte, P. J. (2009). CBP-mediated acetylation of histone H3 lysine 27 antagonizes Drosophila Polycomb silencing. *Development (Cambridge, England)*, *136*(18), 3131–3141. https://doi.org/10.1242/dev.037127

Torrente, Y., Belicchi, M., Sampaolesi, M., Pisati, F., Meregalli, M., D'Antona, G., Tonlorenzi, R., Porretti, L., Gavina, M., Mamchaoui, K., Pellegrino, M. A., Furling, D., Mouly, V., Butler-Browne, G. S., Bottinelli, R., Cossu, G., & Bresolin, N. (2004, July 15). *Human circulating AC133+ stem cells restore dystrophin expression and ameliorate function in dystrophic skeletal muscle*. American Society for Clinical Investigation. https://doi.org/10.1172/JCI20325

Torrente, Y., Tremblay, J.-P., Pisati, F., Belicchi, M., Rossi, B., Sironi, M., Fortunato, F., El Fahime, M., D'Angelo, M. G., Caron, N. J., Constantin, G., Paulin, D., Scarlato, G., & Bresolin, N. (2001). Intraarterial Injection of Muscle-Derived Cd34+Sca-1+ Stem Cells Restores Dystrophin in mdx Mice. *Journal of Cell Biology*, *152*(2), 335–348. https://doi.org/10.1083/jcb.152.2.335

Tropberger, P., Pott, S., Keller, C., Kamieniarz-Gdula, K., Caron, M., Richter, F., Li, G., Mittler, G., Liu, E. T., Bühler, M., Margueron, R., & Schneider, R. (2013). Regulation of transcription through acetylation of H3K122 on the lateral surface of the histone octamer. *Cell*, *152*(4), 859–872. https://doi.org/10.1016/j.cell.2013.01.032

Tsuda, M., Takahashi, S., Takahashi, Y., & Asahara, H. (2003). Transcriptional Co-activators CREB-binding Protein and p300 Regulate Chondrocyte-specific Gene Expression via Association with Sox9 *. *Journal of Biological Chemistry*, *278*(29), 27224–27229. https://doi.org/10.1074/jbc.M303471200

Umansky, K. B., Gruenbaum-Cohen, Y., Tsoory, M., Feldmesser, E., Goldenberg, D., Brenner, O., & Groner, Y. (2015). Runx1 Transcription Factor Is Required for Myoblasts Proliferation during Muscle Regeneration. *PLOS Genetics*, *11*(8), e1005457. https://doi.org/10.1371/journal.pgen.1005457

van Genderen, C., Okamura, R. M., Fariñas, I., Quo, R. G., Parslow, T. G., Bruhn, L., & Grosschedl, R. (1994). Development of several organs that require inductive epithelial-mesenchymal interactions is impaired in LEF-1-deficient mice. *Genes & Development*, *8*(22), 2691–2703. https://doi.org/10.1101/gad.8.22.2691

Vaquero, A., Scher, M., Lee, D., Erdjument-Bromage, H., Tempst, P., & Reinberg, D. (2004). Human SirT1 Interacts with Histone H1 and Promotes Formation of Facultative Heterochromatin. *Molecular Cell*, *16*(1), 93–105. https://doi.org/10.1016/j.molcel.2004.08.031

Vincek, A. S., Patel, J., Jaganathan, A., Green, A., Pierre-Louis, V., Arora, V., Rehmann, J., Mezei, M., Zhou, M.-M., Ohlmeyer, M., & Mujtaba, S. (2018). Inhibitor of CBP Histone Acetyltransferase Downregulates p53 Activation and Facilitates Methylation at Lysine 27 on Histone H3. *Molecules*, *23*(8), 1930. https://doi.org/10.3390/molecules23081930

Wade, P. A. (2001). Transcriptional control at regulatory checkpoints by histone deacetylases: Molecular connections between cancer and chromatin. *Human Molecular Genetics*, *10*(7), 693–698. https://doi.org/10.1093/hmg/10.7.693

Wagner, K. R., McPherron, A. C., Winik, N., & Lee, S.-J. (2002). Loss of myostatin attenuates severity of muscular dystrophy in mdx mice. *Annals of Neurology*, *52*(6), 832–836. https://doi.org/10.1002/ana.10385

Wang, R., He, Y., Robinson, V., Yang, Z., Hessler, P., Lasko, L. M., Lu, X., Bhathena, A., Lai, A., Uziel, T., & Lam, L. T. (2018). Targeting Lineage-specific MITF Pathway in Human Melanoma Cell Lines by A-485, the Selective Small-molecule Inhibitor of p300/CBP. *Molecular Cancer Therapeutics*, *17*(12), 2543–2550. https://doi.org/10.1158/1535-7163.MCT-18-0511

Wang, S.-P., Tang, Z., Chen, C.-W., Shimada, M., Koche, R. P., Wang, L.-H., Nakadai, T., Chramiec, A., Krivtsov, A. V., Armstrong, S. A., & Roeder, R. G. (2017). A UTX-MLL4-p300 Transcriptional Regulatory Network Coordinately Shapes Active Enhancer Landscapes for Eliciting Transcription. *Molecular Cell*, *67*(2), 308-321.e6. https://doi.org/10.1016/j.molcel.2017.06.028

Wang, W., Xue, Y., Zhou, S., Kuo, A., Cairns, B. R., & Crabtree, G. R. (1996). Diversity and specialization of mammalian SWI/SNF complexes. *Genes & Development*, *10*(17), 2117–2130. https://doi.org/10.1101/gad.10.17.2117

Weinert, B. T., Narita, T., Satpathy, S., Srinivasan, B., Hansen, B. K., Schölz, C., Hamilton, W. B., Zucconi, B. E., Wang, W. W., Liu, W. R., Brickman, J. M., Kesicki, E. A., Lai, A., Bromberg, K. D., Cole, P. A., & Choudhary, C. (2018). Time-Resolved Analysis Reveals Rapid Dynamics and Broad Scope of the

CBP/p300 Acetylome. *Cell*, *174*(1), 231-244.e12. https://doi.org/10.1016/j.cell.2018.04.033

Weintraub, H., Davis, R., Tapscott, S., Thayer, M., Krause, M., Benezra, R., Blackwell, T. K., Turner, D., Rupp, R., Hollenberg, S., Zhuang, Y., & Lassar, A. (1991). The myoD Gene Family: Nodal Point During Specification of the Muscle Cell Lineage. *Science*, *251*(4995), 761–766.

Xu, J., Li, J., Zhang, T., Jiang, H., Ramakrishnan, A., Fritzsch, B., Shen, L., & Xu, P.-X. (2021). Chromatin remodelers and lineage-specific factors interact to target enhancers to establish proneurosensory fate within otic ectoderm. *Proceedings of the National Academy of Sciences of the United States of America*, *118*(12), e2025196118. https://doi.org/10.1073/pnas.2025196118

Yang, X. M., Vogan, K., Gros, P., & Park, M. (1996). Expression of the met receptor tyrosine kinase in muscle progenitor cells in somites and limbs is absent in Splotch mice. *Development*, *122*(7), 2163–2171. https://doi.org/10.1242/dev.122.7.2163

Yang, Z., Yik, J. H. N., Chen, R., He, N., Jang, M. K., Ozato, K., & Zhou, Q. (2005). Recruitment of P-TEFb for Stimulation of Transcriptional Elongation by the Bromodomain Protein Brd4. *Molecular Cell*, *19*(4), 535–545. https://doi.org/10.1016/j.molcel.2005.06.029

Yanowitz, J. L., Shakir, M. A., Hedgecock, E., Hutter, H., Fire, A. Z., & Lundquist, E. A. (2004). UNC-39, the C. elegans homolog of the human myotonic dystrophy-associated homeodomain protein Six5, regulates cell motility and differentiation.

Developmental Biology, *272*(2), 389–402. https://doi.org/10.1016/j.ydbio.2004.05.010

Yao, T.-P., Oh, S. P., Fuchs, M., Zhou, N.-D., Ch'ng, L.-E., Newsome, D., Bronson, R. T., Li, E., Livingston, D. M., & Eckner, R. (1998). Gene Dosage–Dependent Embryonic Development and Proliferation Defects in Mice Lacking the Transcriptional Integrator p300. *Cell*, *93*(3), 361–372. https://doi.org/10.1016/S0092-8674(00)81165-4

Yoshimura, M., Sakamoto, M., Ikemoto, M., Mochizuki, Y., Yuasa, K., Miyagoe-Suzuki, Y., & Takeda, S. (2004). AAV vector-mediated microdystrophin expression in a relatively small percentage of mdx myofibers improved the mdx phenotype. *Molecular Therapy*, *10*(5), 821–828. https://doi.org/10.1016/j.ymthe.2004.07.025

Young, C. S., Hicks, M. R., Ermolova, N. V., Nakano, H., Jan, M., Younesi, S., Karumbayaram, S., Kumagai-Cresse, C., Wang, D., Zack, J. A., Kohn, D. B., Nakano, A., Nelson, S. F., Miceli, M. C., Spencer, M. J., & Pyle, A. D. (2016). A Single CRISPR-Cas9 Deletion Strategy that Targets the Majority of DMD Patients Restores Dystrophin Function in hiPSC-Derived Muscle Cells. *Cell Stem Cell*, *18*(4), 533–540. https://doi.org/10.1016/j.stem.2016.01.021

Zammit, P. S., Relaix, F., Nagata, Y., Ruiz, A. P., Collins, C. A., Partridge, T. A., & Beauchamp, J. R. (2006). Pax7 and myogenic progression in skeletal muscle satellite cells. *Journal of Cell Science*, *119*(9), 1824–1832. https://doi.org/10.1242/jcs.02908

Zaret, K. S., & Carroll, J. S. (2011). Pioneer transcription factors: Establishing competence for gene expression. *Genes & Development*, *25*(21), 2227–2241. https://doi.org/10.1101/gad.176826.111

Zeng, L., & Zhou, M.-M. (2002). Bromodomain: An acetyl-lysine binding domain. *FEBS Letters*, *513*(1), 124–128. https://doi.org/10.1016/S0014-5793(01)03309-9

Zhang, T., Zhang, Z., Dong, Q., Xiong, J., & Zhu, B. (2020). Histone H3K27 acetylation is dispensable for enhancer activity in mouse embryonic stem cells. *Genome Biology*, *21*(1), 45. https://doi.org/10.1186/s13059-020-01957-w

Zhang, X., Bailey, S. D., & Lupien, M. (2014). Laying a solid foundation for Manhattan 'Setting the functional basis for the post-GWAS era.' *Trends in Genetics : TIG*, *30*(4), 140–149. https://doi.org/10.1016/j.tig.2014.02.006

Zhang, Y., Liu, T., Meyer, C. A., Eeckhoute, J., Johnson, D. S., Bernstein, B. E., Nusbaum, C., Myers, R. M., Brown, M., Li, W., & Liu, X. S. (2008). Model-based Analysis of ChIP-Seq (MACS). *Genome Biology*, *9*(9), R137. https://doi.org/10.1186/gb-2008-9-9-r137

Zhang, Y., Xue, Y., Shi, J., Ahn, J., Mi, W., Ali, M., Wang, X., Klein, B. J., Wen, H., Li, W., Shi, X., & Kutateladze, T. G. (2018). The ZZ domain of p300 mediates specificity of the adjacent HAT domain for histone H3. *Nature Structural & Molecular Biology*, *25*(9), 841–849. https://doi.org/10.1038/s41594-018-0114-9

Zhou, J., So, K. K., Li, Y., Li, Y., Yuan, J., Ding, Y., Chen, F., Huang, Y., Liu, J., Lee, W., Li, G., Ju, Z., Sun, H., & Wang, H. (2019). Elevated H3K27ac in aged skeletal muscle leads to increase in extracellular matrix and fibrogenic

conversion of muscle satellite cells. *Aging Cell*, *18*(5), e12996. https://doi.org/10.1111/acel.12996

Zhu, L. J., Gazin, C., Lawson, N. D., Pagès, H., Lin, S. M., Lapointe, D. S., & Green, M. R. (2010). ChIPpeakAnno: A Bioconductor package to annotate ChIP-seq and ChIP-chip data. *BMC Bioinformatics*, *11*(1), 237. https://doi.org/10.1186/1471-2105-11-237